THE STUDY ON THE CRASHWORTHINESS BEHAVIOR OF HYBRID AL/GFRP TUBES SUBJECTED TO IMPACT LOAD

VISIT JUNCHUAN

A THESIS SUBMITTED IN PARTIAL FULFILLMENT OF THE REQUIREMENTS FOR THE DEGREE OF DOCTOR OF PHILOSOPHY
MAJOR IN MECHANICAL ENGINEERING
FACULTY OF ENGINEERING
UBON RATCHATHANI UNIVERSITY
ACADEMIC YEAR 2019

UBON RATCHATHANI UNIVERSITY

THESIS APPROVAL

DOCTOR OF PHILOSOPHY

IN MECHANICAL ENGINEERING FACULTY OF ENGINEERING

TITLE THE STUDY ON THE CRASHWORTHINESS BEHAVIOR OF HYBRID AL/GFRP TUBES SUBJECTED TO IMPACT LOAD

AUTHOR MR. VISIT JUNCHUAN

EXAMINATION COMMITTEE

PROF. DR. SUJIN BUREERAT	CHAIRPERSON
ASSOC. PROF. DR. CHAWALIT THINVONGPITUK	MEMBER
ASSOC. PROF. DR. SOMYA POONAYA	MEMBER

ADVISOR

....

(ASSOC. PROF. DR. CHAWALIT THINVONGPITUK)

....

(ASST. PROF. DR. MONGKOL PUSAYATANONT)

DEAN, FACULTY OF ENGINEERING

....

(ASSOC. PROF. DR. ARIYAPORN PONGRAT)

VICE PRESIDENT FOR ACADEMIC AFFAIRS

ACADEMIC YEAR 2019

ACKNOWLEDGEMENTS

The thesis was well accomplished with the great help of Associate Professor Dr. Chawalit Thinvongpitak, thesis advisor. The author has received suggestions, valuable opinions and support as well as helping to correct defects of the work throughout his study period. Thank you to Associate Professor Lieutenant Dr. Somyaya Phunaya, the committee for the thesis examination, who gave suggestions for more complete thesis and recommendations for research throughout the study. Thank you, Department of Mechanical Engineering, Faculty of Engineering, Ubon Ratchathani University For supporting research funds and experimental equipment.

Thanks to my parents for their continued support and encouragement. Thanks to my friends, brothers and sisters, from the Department of Mechanical Engineering for their continued support and encouragement.

Visit junchuan
Researcher

บทคัดย่อ

เรื่อง : การศึกษาพฤติกรรมการตอบสนองของท่อโครงสร้างร่วมระหว่าง AL/GFRP ภายใต้แรงกระแทก

ผู้วิจัย : วิศิษฐ์ จันทร์ชื่น

ชื่อปริญญา : ปรัชญาดุษฎีบัณฑิต

สาขาวิชา : วิศวกรรมเครื่องกล

อาจารย์ที่ปรึกษา : รองศาสตราจารย์ ดร.ชวลิต ถิ่นวงศ์พิทักษ์

คำสำคัญ : ท่อไฮบริด, การป้องกันโครงสร้างห้องผู้โดยสารภายใต้แรงกระแทก, การชน, ไฟไนต์เอลิเมนต์, พลาสติกเสริมเส้นใยแก้ว

งานวิจัยนี้มีวัตถุประสงค์เพื่อศึกษาพฤติกรรมของท่อโครงสร้างร่วมระหว่าง AL/GFRP ภายใต้แรงกระแทกในแนวแกน อิทธิพลของจำนวนชั้นของเส้นใยแก้ว มุมของเส้นใยแก้วและลำดับ การเรียงทับซ้อนของเส้นใยแก้วต่อพฤติกรรมการเสียหายของโครงสร้างเป็นเป้าหมายหลัก ในการศึกษาชิ้นงานที่ใช้สร้างมาจากท่ออลูมิเนียมทรงกระบอกขนาดเส้นผ่าศูนย์กลาง 25.39, 30.48, 38.10 และ 45.72 mm หนา 1.20 mm และยาว 100.00 mm หุ้มด้วยพลาสติกเสริมเส้นใยแก้ว (GFRP) จำนวน 1, 2, 3 และ 4 ชั้น ชิ้นงานถูกทดสอบด้วยเครื่องทดสอบแรงกระแทก โดยใช้น้ำหนักของ หัวค้อนตกกระแทก 30 kg จากความสูง 2.43 m ผลการทดลองแสดงให้เห็นว่า ท่อไฮบริด AL/GFRP สามารถต้านทานแรงกระแทกได้มากกว่าท่ออลูมิเนียมเปล่าในทุกกรณี เมื่อพิจารณาค่าภาระสูงสุดและค่าภาระเฉลี่ยของ พบว่าค่าของภาระมีแนวโน้มเพิ่มสูงขึ้นตามจำนวนชั้นของเส้นใย โดยเฉพาะอย่างยิ่งเมื่อจำนวนชั้นมีจำนวน 3 และ 4 ชั้น ในส่วนของอิทธิพลของมุม พบว่าการวางมุมของเส้นใย 45 องศามีผลกระทบต่อค่าภาระน้อยมาก ในขณะที่การจัดวางมุมแบบ 0 และ 90 องศา ให้ผลที่ดีกว่า นอกจากนี้ยังพบว่าการลำดับเรียงตัวของมุมเส้นใยมีผลกระทบต่อรูปแบบการเสียหายและความสามารถในการรับแรงกระแทก ดังนั้นความสามารถโครงสร้างจึงอาจยกระดับได้ด้วยการเรียงลำดับมุมของเส้นใยอย่างเหมาะสม การศึกษานี้พบว่าการวางมุมของเส้นใยที่เหมาะสมที่สุดคือมุม [0/0/90], [0/90/90] และ [0/0/90/90]

ABSTRACT

TITLE : THE STUDY ON THE CRASHWORTHINESS BEHAVIOR OF HYBRID AL/GFRP TUBES SUBJECTED TO IMPACT LOAD

AUTHOR : VISIT JUNCHUAN

DEGREE : DOCTOR OF PHILOSOPHY

MAJOR : MECHANICAL ENGINEERING

ADVISOR : ASSOC.PROF. CHAWALIT THINVONGPITUK, Ph.D.

KEYWORDS : HYBRID TUBE, CRASHWORTHINESS, IMPACT LOAD, FINITE ELEMENT, GFRP

The objective of this research is to investigate the behavior of hybrid AL/GFRP tube due to an axial impact loading. The effect of the number of GFRP layers, fiber angles and stacking sequence on collapse behavior of structure was focused. The specimens were made from cylindrical aluminum tube with the diameters of 25.39, 30.48, 38.10 and 45.72 mm, and the thickness of 1.20 mm and 100.00 mm long. They were wrapped with 1-, 2-, 3-, and 4-layer of GFRP to form hybrid tubes. The specimens were tested under the impact load using a vertical impact testing machine by dropping a 30 kg hammer at 2.43 m high. The result revealed that AL/GFRP tube could resist more impact load than that of naked AL tube for every case. The maximum load and the mean load of hybrid tubes increased when the number of layers increased, especially for the 3- and 4-layer tubes. For the effect of fiber angle, it was found that the 45 degree fiber did not have a significant effect to structure crashworthy. The 0 and 90 degree fibers were found to be able to significantly promote the crashworthiness capacity of the structure. The stacking sequence of the fiber angle was also found to have an effect on the collapse behavior of the structure as well as on its crashworthiness parameters. Therefore, the crashworthy of specimen may be improved by proper sequence of fiber angles. According to this study, the recommended pattern of AL/GFRP tubes are [0/0/90], [0/90/90] and [0/0/90/90].

CONTENTS

	PAGE
ACKNOWLEDGEMENTS	**I**
THAI ABSTRACT	**II**
ENGLISH ABSTRACT	**III**
CONTENTS	**IV**
LIST OF TABELS	**VI**
LIST OF FIGURES	**VII**
CHAPTER 1 INTRODUCTION	
1.1 Background	1
1.2 Objectives	2
1.3 Scope	2
CHAPTER 2 LITERATURE REVIEW	
2.1 Composite materials	5
2.2 The matrix and reinforcement materials	6
2.3 Crashworthiness parameters	10
2.4 Finite element analysis	12
2.5 Literature review	13
CHAPTER 3 RESEARCH METHODOLOGY	
3.1 Research conceptual framework	27
3.2 Experimental process	28
3.3 Material properties of Aluminum and GFRP	33
3.4 FEA model	36
CHAPTER 4 RESULTS AND DISCUSSION	
4.1 Mode of collapse	38
4.2 Observation results of hybrid tube with diameter of 25.39 mm	39
4.3 Observation results of hybrid tube with diameter of 30.48 mm	49

CONTENTS (CONTINUED)

PAGE

4.4 Observation results of hybrid tube with diameter of 38.10 mm 57

4.5 Observation results of hybrid tube with diameter of 45.72 mm 65

CHAPTER 5 CONCLUSIONS AND RECOMMENDATIONS

5.1 Conclusions 73

5.2 Recommendations 74

REFERENCES 75

APPENDIX 81

VITAE 88

LIST OF TABLES

TABLE		PAGE
1.1	The dimensions of aluminum tubes	3
1.2	Orientation angle of the fiber and the number of fiber layers	3
3.1	Material properties of aluminum tube	35
3.2	Yield stress and plastic strain of aluminum tube	35
3.3	Material properties of E-glass fiber/polyester lamina	35
3.4	Strength of E-glass fiber/polyester lamina	35
3.5	Fracture energy of E-glass fiber/polyester lamina	36
3.6	Traction separation of delamination	36

LIST OF FIGURES

FIGURE		PAGE
2.1	The load-displacement curve under the axial crushing load	10
2.2	FEA model with fiber angles $[0_3/90_3]_s$	14
2.3	FEA model	15
2.4	The FEA model	15
2.5	FEA model	17
2.6	Front part of a racing car	18
2.7	Semicircle specimen	19
2.8	The specimen of open hat	19
2.9	Characteristics of the specimen on the test machine	20
2.10	Experimental tubes and models	21
2.11	Braided fiber model with angles of 15, 30 and 45 degrees	22
2.12	Comparison of experimental results and models at pressure of 0.2 and 0.4 MPa	22
2.13	Experimental	23
2.14	The composition of the model that consists of thin-walled structures	23
2.15	Top element size of 7.0 mm, bottom element of 4.0 mm and coefficient of friction 0.1, 0.2 and 0.3 from left to right	23
2.16	Pultruded composite tubes	24
2.17	Model FEA	24
2.18	The characteristics of the bumper structure	25
2.19	Model of thick elements and the bonding area of the elements	25
2.20	Semi-hexagonal section	26
3.1	Conceptual framework of this study	27
3.2	Experiment setup	28
3.3	The geometry of specimens and ply angle of each layer	29
3.4	Diagram of aluminum tube was wrapped with E glass mats, release film, peel ply, infusion net, and bagging film	30

LIST OF FIGURES (CONTINUED)

FIGURE		PAGE
3.5	aluminum tube was wrapped with E glass mats and the specimen was contained in sealed vacuum bag	31
3.6	vacuum infusion process	32
3.7	The finished specimens those are ready to be tested	32
3.8	Universal Testing Machine	33
3.9	Delamination testing of GFRP specimen	34
3.10	FEA model of specimen	37
4.1	Terminal mode of collapse of aluminum tubes	39
4.2	Mode of collapse of hybrid tubes	39
4.3	Load-time curves of naked AL tube and hybrid tubes of D=25.39 mm, with GFRP of 1, 2, 3 and 4 layers under impact	40
4.4	Failure mode of 25.39 mm diameter hybrid tube with 1 layer of GFRP	42
4.5	Failure mode of 25.39 mm diameter hybrid tube with 2 layers of GFRP	43
4.6	Failure mode of 25.39 mm diameter hybrid tube with 3 layers of GFRP	44
4.7	Failure mode of 25.39 mm diameter hybrid tube with 4 layers of GFRP	45
4.8	Mean and maximum loads of AL and hybrid tubes of D=25.39 mm	47
4.9	Load-time curves of naked AL tube and hybrid tubes of D=30.48 mm, with GFRP of 1, 2, 3 and 4 layers under impact	50
4.10	Failure mode of 30.48 mm diameter hybrid tube with 1 layer of GFRP	51
4.11	Failure mode of 30.48 mm diameter hybrid tube with 2 layers of GFRP	52
4.12	Failure mode of 30.48 mm diameter hybrid tube with 3 layers of GFRP	53
4.13	Failure mode of 30.48 mm diameter hybrid tube with 4 layers of GFRP	54
4.14	Mean and maximum loads of AL and hybrid tubes of D=30.48 mm	56
4.15	Load-time curves of naked AL tube and hybrid tubes of D=38.10 mm, with GFRP of 1, 2, 3 and 4 layers under impact	58
4.16	Failure mode of 38.10 mm diameter hybrid tube with 1 layer of GFRP	59
4.17	Failure mode of 38.10 mm diameter hybrid tube with 2 layers of GFRP	60
4.18	Failure mode of 38.10 mm diameter hybrid tube with 3 layers of GFRP	61

LIST OF FIGURES (CONTINUED)

FIGURE **PAGE**

4.19 Failure mode of 38.10 mm diameter hybrid tube with 4 layers of GFRP 62

4.20 Mean and maximum loads of AL and hybrid tubes of D=38.10 mm 64

4.21 Load-time curves of naked AL tube and hybrid tubes of D=45.72 mm, with GFRP of 1, 2, 3 and 4 layers under impact 65

4.22 Failure mode of 45.72 mm diameter hybrid tube with 1 layer of GFRP 67

4.23 Failure mode of 45.72 mm diameter hybrid tube with 2 layers of GFRP 68

4.24 Failure mode of 45.72 mm diameter hybrid tube with 3 layers of GFRP 69

4.25 Failure mode of 45.72 mm diameter hybrid tube with 4 layers of GFRP 70

4.26 Mean and maximum loads of AL and hybrid tubes of D=45.72 mm 71

CHAPTER 1
INTRODUCTION

1.1 Background

Glass Fiber Reinforced Plastic, (GFRP) is a high potential alternative material. It has been widely used in many industries such as spacecraft and automobile. This is because its strength per weight is high which is very useful for transportation. In addition, the property of composite material can be improved according to direction of load. In general, the automobile cockpit is generally made of metal, because metal is prominent in absorbing impact. However, metal is low strength per weight, fatigue and corrosive. Therefore, composite can be alternative for metal and preferably used in many parts of automotive. However, using composite alone as a main structure may be not efficient since its overall strength is not high enough for impact. Therefore, the combination of composite and metal, generally called hybrid structure, has gained attention from many researchers. Kil-Sung Lee et al., [1] – [2] carried out studies on the crush characteristics of square CFRP/AL hybrid tubes compared to CFRP tubes and AL tubes alone. They concluded that the hybrid tubes provide highest energy absorption compared to other two. M. Costas et al. [3] aimed to applied hybrid tube for car frontal impact absorber. The GFRP conglomerates combined with cold-form steel polygonal tubes were used and tested under quasi-static and dynamic loads. The hybrid structure was found to provide higher specific energy absorption. Some researchers studied hybrid structures of different geometries such as aluminum conical frusta wrapped with E-glass/epoxy [4], hybrid sinusoidal plate [5], rectangular and circular hybrid tubes [6] under axial impact. Other modes of load on hybrid tubes were also investigated by H.C. Kim et al. [7], D.K. Shin et al. [8] and Q. Liu et al. [9]. Similar finding from those studies is the hybrid structure provides higher crashworthiness capacity, no matter what the geometric cross sections or types of load are. Nowadays, the influence of fiber orientation, number of fiber layers and stacking sequence are also focused. S. Solaimurugan et al. [10] investigated the effect of number of fiber glass layers on energy absorption capacity of cylindrical tube. They concluded that the increasing of number of layers can increase energy absorption of specimens. The study on influence of fiber orientation on circular and rectangular hybrid tube was also performed by M.M. Shokrieh et al. [11] as well as by D. Hu et al. [12]. In addition, the influence of fiber stacking sequence was investigated by S. Solaimurugan et al. [10] and by M. Mirzaei et al. [13]. Those studies found that fiber orientations and stacking sequence affect to the crashworthiness capacity of specimens significantly. However, the detail on energy absorption mechanism of hybrid specimens is still uncleared and further study needs to be carried out in order to gain clear picture and understand how the fiber orientation and stacking sequence affect to the specimens crashworthy.

This research was aimed to carried out a detailed study on the influence of fiber orientation and stacking sequence on the crashworthiness behavior of hybrid tubes. The specimens were tested under axial impact load. Both experiment and finite element simulation techniques were used. Detailed investigation on mode of collapse, collapse progressive and failure mechanism linked to some crashworthiness parameters are performed.

1.2 Objective

1.2.1 To study the behavior of impact response and crashworthiness capacity of hybrid tube.

1.2.2 To study the influence of the stacking sequence and orientation angles of fiber on the behavior of hybrid tube under axial impact.

1.3 Scope

1.3.1 Specimens

The study focuses on studying the crashworthiness and behavior of aluminum tubes wrapped with composite materials under impact. The specimens were made of Aluminum tubes wrapped with GFRP. Experimental and FEA approaches were used. Dimension of AL tubes were showed in Table 1.1. while orientation angles of fiber used in this study were listed in Table 1.2 according to number of fiber layers.

Table 1.1 The dimensions of aluminum tubes

No.	Diameter (mm)	Thickness (mm)	The rate of diameter per thickness (D/t)
1	25.39	1.2	21.16
2	30.48	1.2	25.40
3	38.10	1.2	31.75
4	45.72	1.2	38.10

Table 1.2 Orientation angle of the fiber and the number of fiber layers

Layers	Orientation angle of the fiber (degree)						
1	[0]	[90]	[45]				
2	$[0]_2$	$[90]_2$	$[-45]_2$	[0/90]	[90/0]	[+45/-45]	
3	$[0]_3$	$[90]_3$	$[0_2/90]$	$[0/90_2]$	$[90_2/0]$	$[90/0_2]$	$[+45/-45_2]$
4	$[0]_4$	$[90]_4$	$[0_2/90_2]$	$[90_2/0_2]$	$[+45_2/-45_2]$	[0/+45/90/-45]	

1.3.2 Controlled variables

1.3.2.1 Specimens were with a length of 100 mm and the diameter per thickness (D/t) ratio of the aluminum tubes as showed Table 1.1.

1.3.2.2 Orientation angles of fiber were 0, 45 and 90 degree. They were used to wrap the tube with some combination making a number of sequences as showed in Table 1.2.

1.3.2.3 The experiment was conducted by impact testing machine with a dropped hammer of 30 kg from 2.43 m height.

1.3.2.4 Finite element analysis (FEA) were applied using ABAQUS/Explicit commercial code.

1.3.2.5 The FEA model consists of 4 parts as follows.

1) Aluminum tube (Deformable)

2) Composite tube (Deformable)

3) Plate impact (Rigid body)

4) Plate support (Rigid body)

1.3.1.6 Modeling of composite materials layers were separated from each other and each layer adherence (Cohesive) with defined properties of contact layer.

1.3.3 The dependent variable

1.3.3.1 The reaction force from the experiment was recorded by a load cell.

1.3.3.2 Mode of collapse and progressive collapse of specimens were recorded by high speed camera.

1.3.3.3 Crashworthiness parameter focused in this study are maximum load and mean load.

CHAPTER 2
LITERATURE REVIEW

2.1 Composite materials

Fiber reinforced polymers are classified as one of an engineering materials. It provides good mechanical properties and is also benefited from property of polymers such as being light in weight, excellent resistance to chemical corrosion and good thermal insulation. Its strength is a result of reinforcement with various fibers, such as glass fibers, carbon fiber etc. Fiber reinforced polymers provide better property than conventional materials such as steel or other types of metals. The composite material has high strength when compared to density. It also has a high specific modulus. Therefore, composite materials are light but good mechanical properties. In addition, composite is easy to manufactured, there for many shapes are able to be formed and suitable for any purposes [14].

Nowadays, the use of polymers as a matrix has been improved and developed in order to obtain higher mechanical properties and efficiency. Some example developments are fiber development in various forms, strength, structure and adhesion ability with the matrix.

The diversity of fibers results in greater usability and greater suitability for demand, but also increases the price of the material. Therefore, when producing or forming, apart from considering the required properties, the cost and the product design process must be considered. This is in order to be effective in choosing the best materials and the most worthwhile.

2.1.1 Raw materials for polymer composite materials

The composite material consists of two major components

2.1.1.1 The matrix is to prevent damage to the reinforcement due to friction from the environment, moisture, and also helps to transfer the force to the reinforcement.

2.1.1.2 The reinforcement is an important part of the composite material because it performs strength to the material. The reinforcements are the main supporting parts of the composites.

2.2 The matrix and reinforcement materials

2.2.1 The matrix

The Matrix is a material or component of composite materials that has continuous phase. In general, for composite materials, It is more in volume than the reinforcements. The matrix serves to protect and secure the reinforcement, as well as to transfer the external load to the reinforcement.

Some example of matrix materials are polymers, metals, ceramics and carbon etc. In case polymer, many choices can be made for making matrix such as thermosets, thermoplastic and rubbers. There are variety of materials in each group, such as for thermoset, one may use epoxy, polyesters, polyamide and phenolics etc.

Polymer matrix is commonly used in composite materials, including thermosetting. Because it is a low molecular weight substrate with low viscosity, it can mix and insert well into the reinforcements. In the process of making the set, the binder is used to help create the bond between the molecules of the polymer until finally obtaining a three-dimensional mesh structure. In which the resulting polymer is strong and good resistance to temperature and also chemicals. There are many types of thermosetting matrices as follows.

2.2.1.1 Polyester resin is widely used in composite materials because it is cheap, easy to find and good mechanical properties. The disadvantage of polyester resin is a lot of contraction between the structural linkage process and low resistant to the environment compared to epoxy resin.

1) Ortho resin can be prepared from phthalic anhydride and maleic anhydride or formic acid to be Orth phthalic. It is considered to be the first polyester resin that is still popular in use today. This resin is cheap, easy to find and there are many types to choose depending on the manufacturer and the need of users. However, orthopedic resins have limitations in thermal stability, chemical stability and very high shrinkage.

2) Iso resin can be prepared from isophthalic acid and malic anhydride or fumaric acid to be isophthalic. It is considered a better resin than orthophthalic resins in terms of resistance to heat, chemicals and mechanical properties because of its linear structure and high molecular weight.

3) Vinyl ester is prepared from unsaturated acids, such as acrylic acid and bisphenol epoxides, to form a vinyl ester chain that has double bonds at the ends, allowing for reaction. The linking agents commonly used are styrene monomer or vinyl monomer, which are sensitive to external reactions and ripening, as can be done with polyester. Therefore, vinyl esters can be used like other types of polyester, which are expensive but with good resistance to chemicals, heat and provides good mechanical property.

4) Epoxy Resin is available in many types and various physical properties, good mechanical properties, capable of being compatible with all types of fibers and can be molded in many processes, such as by hand molding etc. Therefore, epoxy resin is the most popular choice. Chemical structure of epoxy, the curing agent, and types of modifying reactants determine the toughness, chemical resistance, chemical property, mechanical property, flexibility, strength, resistance to creep and fatigue etc. In addition, the epoxy is outstanding for adhesion with fibers, excellent resistance to heat and electrical properties. During the linking reaction it does not create a co-by-product and low shrinkage. The major disadvantage of epoxy is highly hygroscopic and brittle, easily broken.

2.2.2 The reinforcement

In the reinforcement of the composite material, the most important component is fiber because the fibers are the parts that support and strengthen the structure. There are many types of fibers used in composite materials, but each type has different properties. The types of fibers can be classified as follows.

(1) Natural fibers

(2) Mineral fibers

(3) Synthetic fibers

(3.1) Synthetic organic fibers

(3.1.1) Aramid fibers

(3.1.2) PET fibers

(3.1.3) Polyethylene inorganic fibers

(3.2) Synthetic inorganic fibers

(3.2.1) Glass fibers

(3.2.2) Carbon and graphite fibers

(3.2.3) Alumina fibers

(3.2.4) Boron fibers

(3.2.5) Silicon fibers

Fiber normally plays main role in strengthen of the composite. Some factors that affect the strengthen of composite are:

(1) the mechanical properties of the fibers.

(2) the surface contact between the fiber and the matrix.

(3) the amount of fiber.

(4) the arrangement of the fibers.

Fibers those normally used to make composite are:

2.2.2.1 Aramid fiber or Kevlar is fibers that have high strength, resistant to tear, high thermal stability, outstanding strength, high toughness compared to other fibers, withstand impact, light weight and excellent fatigue resistance. However, the usage is still limited due to low compressive strength, poor UV resistance, moisture absorption and poor adhesion to the matrix.

2.2.2.2 Carbon fiber is fibers that are wildly used. because its highest specific stiffness. It has high strength in both tensile and compression directions, good resistance to corrosion, fatigue and creep. In general, the fibers produced are about 5-7 microns in diameter and have outstanding properties in other areas such as excellent chemical resistance, very low thermal expansion, excellent friction properties, a high electrical conductivity and excellent heat conductivity. The disadvantage of this type of fiber is fragile and low impact resistance or low toughness.

2.2.2.3 Alumina fiber has outstanding properties, which is able to maintain mechanical properties both strength and modulus. It can withstand temperature up to 100 degrees, allowing it to be used at high temperatures.

2.2.2.4 Boron fiber is classified as the first high performance fiber commercially produced. Currently, this type of fiber is commonly used to reinforce epoxy in the spacecraft and sports equipment. The use of this type of fiber is limited by price.

In addition, its large diameter allows the fiber to withstand strong pressure. Due to its outstanding mechanical properties such as tensile, compression, bending and high temperature resistance, this type of fiber is mainly used in military applications. It is also high impact resistance, since the fibers have a tungsten core, which makes the fibers dense. It has medium specific properties. However, the large size of fibers makes it difficult to mold.

2.2.2.5 Silicon fiber has properties and processes similar to boron fibers. It is able to withstand great pressure. It can be used at high temperature because the bond in the structure is covalent, so the fiber is strong and highly modulus, like other high-performance fiber. Silicon fiber is used in plane, construction of bridge and sport equipment. However, this type of fiber is not very popular because of the cost.

2.2.2.6 Glass fiber is inexpensive and widely used when compared to other fibers. In addition, It has outstanding property of high tensile strength, impact resistance and high chemical resistance. However, it is low modulus, not resistant to abrasion and a low adhesion ability to the matrix.

Glass fiber is a material that have a mixture of glass. The fiber is bright, hard and chemical resistant. It has glass inertia and has high strength, flexibility and light weight. Glass fibers can be divided into different types which provide different mechanical properties. The commonly used fiber glass are;

(1) E-glass: (Electrical grade) is most commonly used because of its high strength. good electrical properties, inexpensive and easy to find.

(2) ECR-glass: (Electrical-chemical grade) is stronger than E-glass. It is high chemical resistance, good electrical properties but high price.

(3) C-glass: (Chemical grade) has excellent chemical resistance. It has low strength and commonly used as a surface that directly touches chemicals.

(4) S-glass: (Strength grade) is a fiber with high modulus and temperature resistance, 30% stronger than E-glass but 7 times more expensive. It is commonly used in military and spacecraft.

2.3 Crashworthiness parameters

Structural crashworthiness is a term that refers to the performance of a structure under an impact loading. It defines the quality of response of a structure when it is involved in or undergoes an impact. It is necessary to understand the impact deformation of a structure under various conditions first, before learning how to improve its crashworthiness. The crashworthiness parameters consist of various kinds interested to evaluate the performance of the energy absorption device. Consider the typical uniaxial compression, load-displacement curve of a collapse structural given in Figure 2.1.

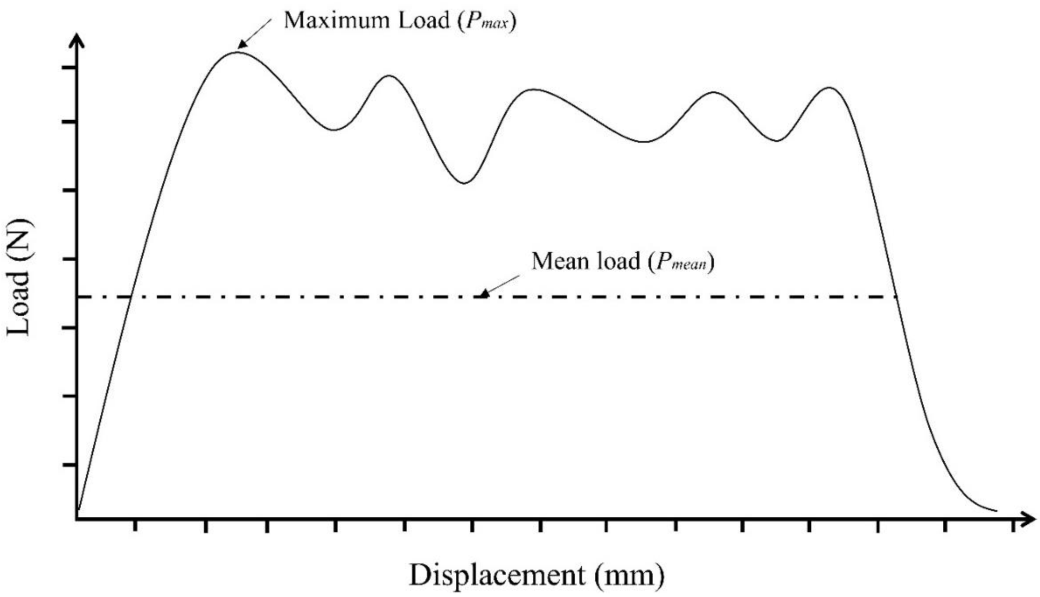

Figure 2.1 The load-displacement curve under the axial crushing load

The crashworthiness parameter can be considered from the load-displacement curve of structure under collapse. Initially, the tube deforms elastically until it reaches a peak load. Then, the structure plastically collapses as the folds formed progressively and the load values increase sharply in this region. Then, the curve is created in wavy shape corresponding to the form of progressive folding or mode of collapse until terminating the test. From the curve, the energy absorption is measured by the area under the load-displacement curve. For all specimens under axial crush, the collapse process is terminated when the structure is fully collapsed. By overloading a specimen after full collapse, the load will be, of course, raised sharply. However, the energy absorber in the region after full collapse is unrelated to the usefulness of the structure. Therefore, the energy absorption based on only the load before a complete collapse is considered. Fundamentally, the load-displacement response of energy absorbing devices can primarily measure their energy absorption performance [15].

2.3.1 Energy absorption

In any crushing event of structure, the energy absorption (E_a) of a structure is defined as an integration of area under the load-displacement curve from Figure 2.1 as follows on Eq. (2.1), where P and S_{max} is an instantaneous crushing force and the maximum crush distance, respectively.

$$E_a = \int_0^{S_{max}} PdS \approx P_{mean}.S \tag{2.1}$$

2.3.2 Mean crushing load

The mean crushing load (P_{mean}) can be determined using the Eq. (2.2). The mean crushing load is indicated that the energy absorption capacity of a structure when compared to the collapse displacement. Generally, high mean crushing load is required in order to achieve high energy absorption. However, the body tolerance should be considered because too high a value of mean crushing load may lead to high deceleration. The characteristics of an ideal energy absorber under axial loading can then simply be calculated as the average area under the load-displacement curve. The corresponding mean crushing load is calculated by dividing the absorbed energy by the displacement.

$$P_{mean} = \frac{1}{S}\int_0^{S_{max}} P(S)dS \tag{2.2}$$

2.3.3 Specific energy absorption

The important characteristic of energy absorbers is the specific energy absorption (E_s) capacity. The specific energy absorption is defined by energy absorption per unit mass and *mass* is the original undeformed mass of the specimen. The specific energy absorption is usually used as an indicator of the weight efficiency of energy absorption. For a given absorbed energy, a higher value of E_s indicates a more efficient crash absorber in terms of its weight. The specific energy absorption per unit mass is calculated using Eq. (2.3), where *mass* is the original undeformed mass.

$$E_s = \frac{E_a}{mass} \tag{2.3}$$

2.4 Finite element analysis

The crushing behavior of thin walled tubes has been studied for over 50 years. For the last decade, the studies were also extended to simulation by using finite element analysis. The numerical tools are helpful to predict the crushing behavior of tubes with different geometrical parameters, which may greatly reduce the number and the cost of experimentation. Finite element analysis has become an integral part of the design process for most structural or thermal applications. This tool can be used to predict the structural response of a given geometry under various loading conditions. Structural responses can be classified into two types, linear or nonlinear. A linear response means there is a linear relationship between the response of the structure and the load that is applied to that structure. A nonlinear response involves a part or assembly whose stiffness changes as a result of deformation. As all real-world structures are actually nonlinear. Two types of computational methods are used in finite element analysis, explicit and implicit. The implicit solving method is better suited for static, linear problems such as small displacements. The explicit analysis is better suited for loading cases such as high-speed dynamics, complex contact between deformable bodies, complex post buckling problems, and material degradation simulations. In order to develop a structural member for energy absorption, the commercially available package of FEA model was created and performed. To simulate the large deformation and self contact associated with axial crushing load, the mathematical calculations require the use of a powerful set of programs. In this study the FEA package, entitled, ABAQUS, is adopted for modeling and analysis. ABAQUS is a suite of finite element analysis modules that offers a wide range of elements for modeling the structure, such as solid elements, shell elements, beam elements, rigid elements, and truss elements.

It includes ABAQUS/CAE, ABAQUS/Standard, ABAQUS/Explicit, and ABAQUS/Viewer. ABAQUS is a general purpose computer code that performs static and dynamic analysis by the finite element method. For static analysis, the implicit method iterates the solution until it converges, at each deflection step of the problem. It relates forces to deflections but does not consider the acceleration of mass. For dynamic problems, the explicit method estimates forces and then applies them to the masses to calculate the accelerations in the next time step. For the shell or thin-wall structure, either shell or solid elements can be used explicit nonlinear method. The finite element analysis used in this thesis is nonlinear analysis [16].

2.4.1 The processing of the finite element analysis are as follows

2.4.1.1 Preprocessing phase

1) Geometric construction

2) Discretization

2.4.1.2 Shape function

1) Create an equation for the elements

2) Define initial conditions and boundary conditions, loading conditions with the problem.

3) Define Material properties

2.4.1.3 Solution phase is to find the answer to the equation, which is in the form of linear equations or equations, nonlinear, which answer is the displacement at the nodes.

2.4.1.4 Post processing phase is the analysis of the results. In this stage the results from calculation such as stress, deflection or energy are display. The results can be performed in graphic, contour or in data format.

2.5 Literature review

V.S. Sokolinsky et al. (2011) [17] studied the numerical model of the crushing process of corrugated sheets with composite materials. The objective of this research was to study the FEA model. The arrangement of fibers was $[0/90]_{2s}$ with a thickness of 2 mm. The bottom end of the specimen is chamfered to 45 degrees. The FEA model was carried out with Abaqus/explicit. There were 8 sheets of corrugated sheets assembled together and each sheet is created at a time. Mesh was used the SC8R element, the size of the meter is 1 mm. The speed used in the test was 0.2 m/s. The results from the experiment and the FEA model showed that from the load and time graph and the damage characteristics of the specimens are agreed well.

F. Aymerich et al. (2009) [18] studied carbon fiber sheet model under the impact, using FEA with cohesive elements on the surface between two parts. The materials used in the experiment were carbon fibers and epoxy. The test speed was between 0.7 m/s to 2.5 m/s for the composite materials with angles of $[0_3/90_3]_s$ and $[90_3/0_3]_s$, with angles 0_3 and 90_3, as shown in Figure 2.2. Solid element type of C3D8R is in the skin adhesion by using adhesion elements or Cohesive element type COH3D8. The model are accurate in predicting the energy response and separation of layers.

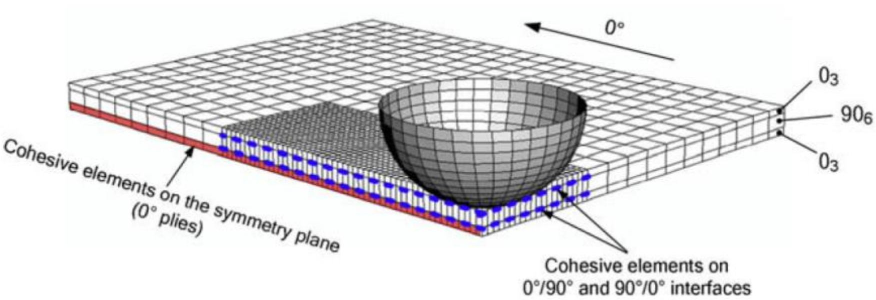

Figure 2.2 FEA model with fiber angles $[0_3/90_3]_s$ [18]

J. Zang and Xiang Zhang (2015) [19] studied the separation layers of composite materials of surface cohesive with models under quasi-static loads. The objective was to predict the damage at low speed by using the FEA model as shown in Figure 2.3, which was developed from F. Aymerich's research. The results showed that the model of surface cohesive is consistent between the models. This research showed that their technique can reduce calculation time of F.Aymerich from 8 hours to be only 2 hours.

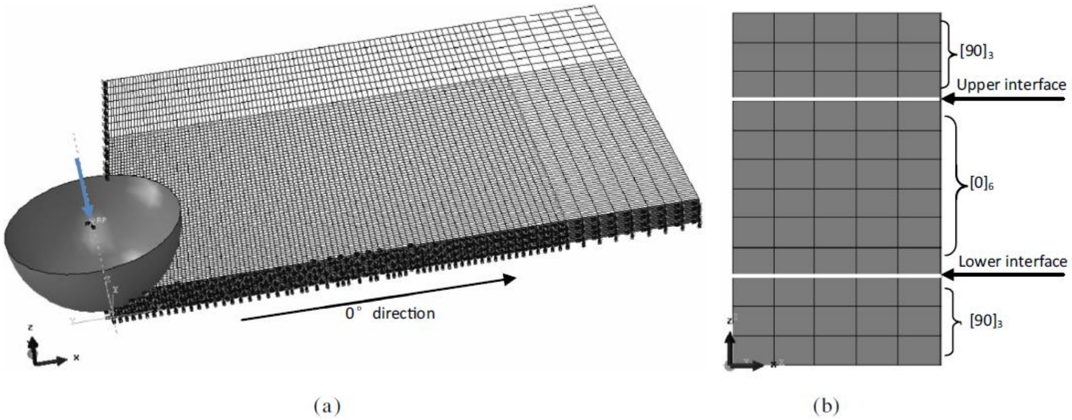

Figure 2.3 FEA model: (a) Model under load and (b) Cohesive surface [19]

S. Zhu and G. Boay Chai (2012) [20] studied the impact response and the damage model of the composite sheet with aluminum under low speed. Reinforced plastic with two different types of glass fibers: Unidirectional glass fibers and woven glass fibers the composite sheet is made of aluminum alloy 2024-T3, the thickness is 0.3 mm and prepregs glass fiber and L-530 type epoxy. The FEA model in this study was ABAQUS/Explicit. The impact head was defined as a rigid object with a diameter of 13.1 mm and a mass of 2.735 kg as shown in Figure 2.4. The surface between aluminum layer and the layer of glass fiber reinforced plastic are bonded together. Presses, composite materials and aluminum was modeled by C3D8R type 8-node element. The results of the experiment and FEA were presented and discussed.

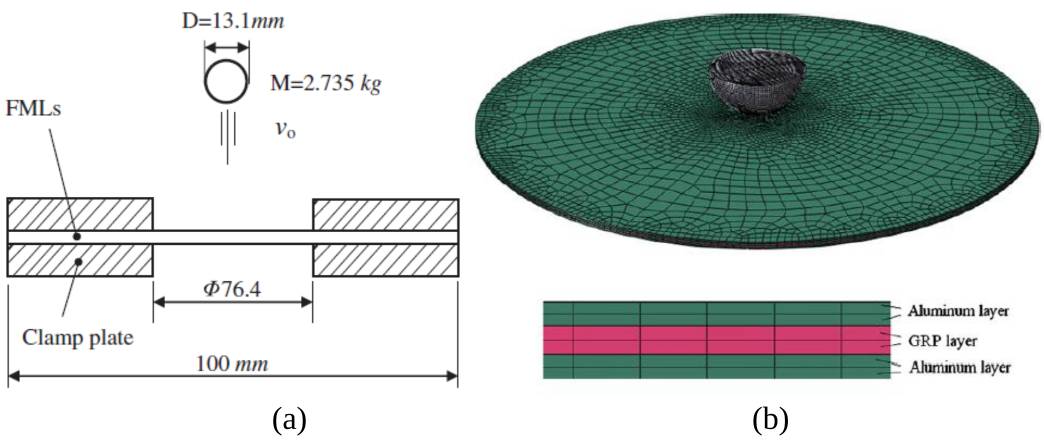

Figure 2.4 The FEA model: (a) Impact testing and (b) Layer of fiber [20]

J.H Lee et al. (2007) [21] studied the experiment of glass fiber reinforced plastic bridges under static load using ABAQUS program. There were two types of specimens which are DBT [45/90/-45] and LT [0/90]. The results of the experiment showed that the specimens of the LT were stronger than DBT. The results from comparison of experiment and FEA were agreed well.

M. Golzar et al. (2010) [22] studied the composite automobile body. The construction of composite materials for splicing structures to replace steel in car body were studied. The angles of the fiber were as follows [0/90] and [45/-45]. The result revealed that [0/90] can absorb more energy and when compared to steel or its original structure it was found to be 42% lighter.

S.M.R. Khalili et al. (2011) [23] studied the models of composite materials and thin wall cylinders under impact at low speed by using the program ABAQUS/Explicit. The element sheet is SC8R. The result showed that the thin sheet and thin shell S4R element are suitable and accurate. In the case of using SC8R element which can be used and more accurate but will increase the CPU calculation time.

C. Hua Huang et al. (2003) [24] studied carbon fiber reinforcement sheets under quasi-static load by using the ABAQUS program. The moldings were made from carbon fibers, Toho ETA 12000 and ACD 8810 Epoxy resin. The stacking orientation of fibers were $[90/0]_{4s}$ and $[45/-45]_{4s}$ respectively. The test specimen has a width of 16 cm, a length of 7 cm and a thickness of 0.228 cm. The results of study showed that the stacking orientation of fibers $[90/0]_{4s}$, has more strength than $[45/-45]_{4s}$. The comparison models and experiments was made and good agreement was achieved.

G. Belingardi et al. (2013) [25] studied the energy absorption of bumper beams made from composite materials using Pultrusion methods as in Figure 2.5. Composite material was made from E-glass/epoxy to compare with steel by using the finite element model. The test speed was 15 km/h. The results found that composite material can absorb energy better than steel and can also reduce the maximum load when a collision.

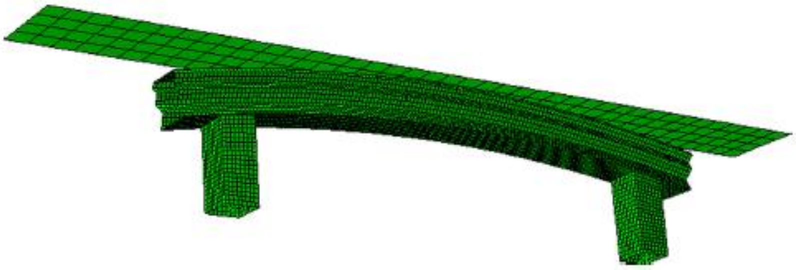

(a)

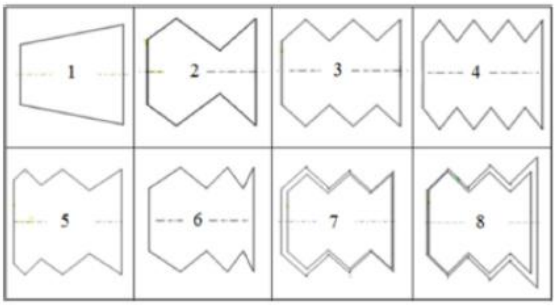

(b)

Figure 2.5 FEA model: (a) the energy absorber that is added to the bumper and (b) the cross-section of different bumper beams [25]

C. J. McGregor et al. (2007) [26] studied the model of the damage process of a braided material tube under axial impact load. The object was to study the properties of composite materials based on continuum damage mechanism using LS-DYNA program for braided tube composite materials made from carbon fibers with angles [0/+ 30/-30]. The top end of the specimen was made for 45 degrees. The thickness of the tubes were 2.3, 4.9 and 8.1 mm. The length was 360 mm. The impact head weigh is 140 kg and impact speed was 7.1 m/s. The result found that the specimen with a 3 layer angle can absorb energy and absorb specific energy more than other specimens.

D. Siromani et al. (2014) [27] studied the collapse behavior of thin-walled carbon fiber tube under axial impact using FEA model. The specimens used in the experiment was cylindrical tubes made from HEXCEL IM / 8552 carbon fiber type. The orientation of fiber were [15/-15/15/0_3/-15/15/-15]. The specimens were tested under quasi-static load at 7.6 m/s until the specimen collapsed to a distance of 50.8 mm. The FEA model used LS-DYNA 4-element type shell element. The study found that the relationship between the load and collapse distance and the damage mode of the model and experiment are similar.

J. Obradovic et al. (2012) [28] studied the energy absorption capacity of composite material from the impact in the front of the race car, as shown in Figure 2.6. The structures were made from carbon fiber with different thickness and number of layers. The quasi-static test with a speed of 0.5 mm/s and impact at 4 m/s of LS-DYNA program. The results found that the experiment the FEA model has the ability to absorb energy up to 2.59 kJ and 2.01 kJ respectively.

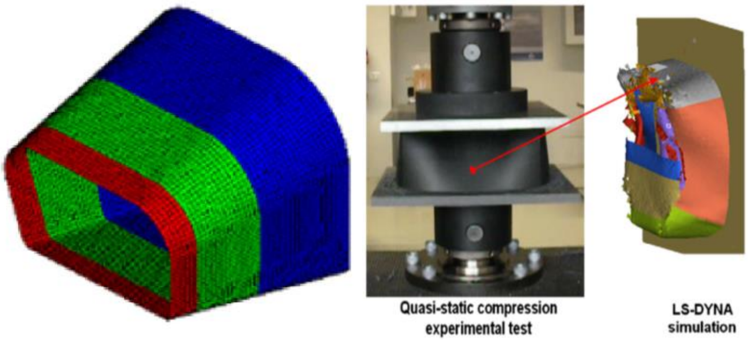

(a) (b)

Figure 2.6 Front part of a racing car: (a) Different thickness model and (b) Structure damage [28]

C. McGregor et al. (2010) [29] studied of braided composite tube under axial impact. The specimen was a square tube with 2 layers and 4 layers of stacking fibers. The length is 360 mm, the width is 55 mm and the thickness are 2.3 and 6.1 mm. The specimen was made from braided carbon fiber, with the angle of [0/+45/-45] and the Hetron 922 epoxy resin. The impactor had a mass of 535 kg and a height of 2.0 m and impact speed was 6.3 m/s. The FEA model was conducted with LS-DYNA. The results showed the graph between the load and the collapse of the specimens. The experiments and simulations have similar trend in terms of energy absorption. The specimen with 4 layers can absorb specific energy better than other specimens.

M. David and Alastair F. Johnson (2015) [30] studied the absorbed energy of composite material under axial load. The objective of this research was to study the absorbed energy under axial load by experiment and FEA model. The specimen has a semicircle and has a flange protruding in a square shape base as shown in Figure 2.7.

The specimens were made from carbon fiber and Epoxy. There were 9 layers of fibers and the angle of the fibers was 0/90. The FEA model using PAM-CRASH 2009 was adopted. The comparison of FEA model and experiment was made and good agreement was achieved. Mode of collapse and detailed study on energy absorption were discussed.

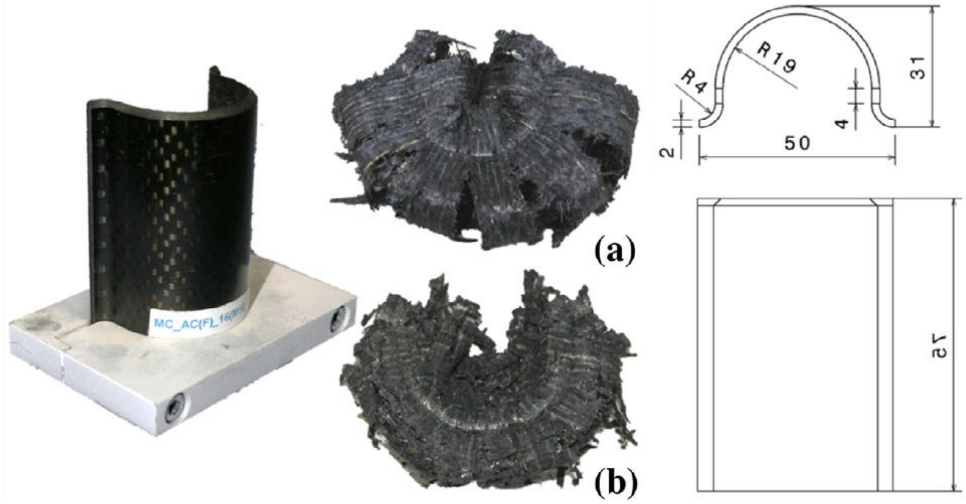

Figure 2.7 Semicircle specimen: (a) cross-section of the part and (b) Top views [30]

M.W. Joosten et al. (2011) [31] studied the ability to absorb energy under quasi-static load of open hat structure. The specimen was an open hat section, made from carbon fiber woven and epoxy resin. The orientation stacking of fibers was $[0/90]_8$. The test was conducted with Instron 3369 as shown in Figure 2.8 and 2.9. The speed was 5 mm/min. The results from compression found that the damage characteristics are similar and the graph between the load and the collapse period is likely to be the same. The average load of FEA was 19.09 kN and the experiment showed that the average load is 19.39 kN with a discrepancy of 1.57%.

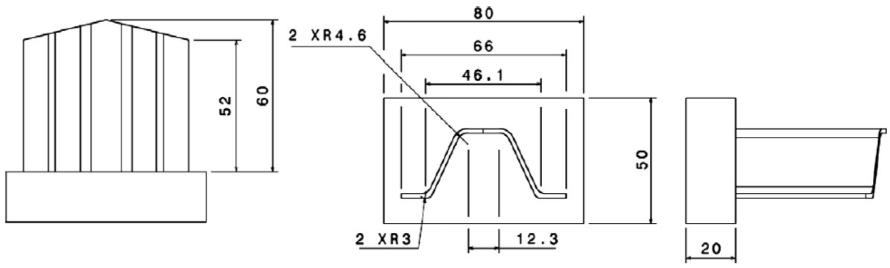

Figure 2.8 The specimen of open hat [31]

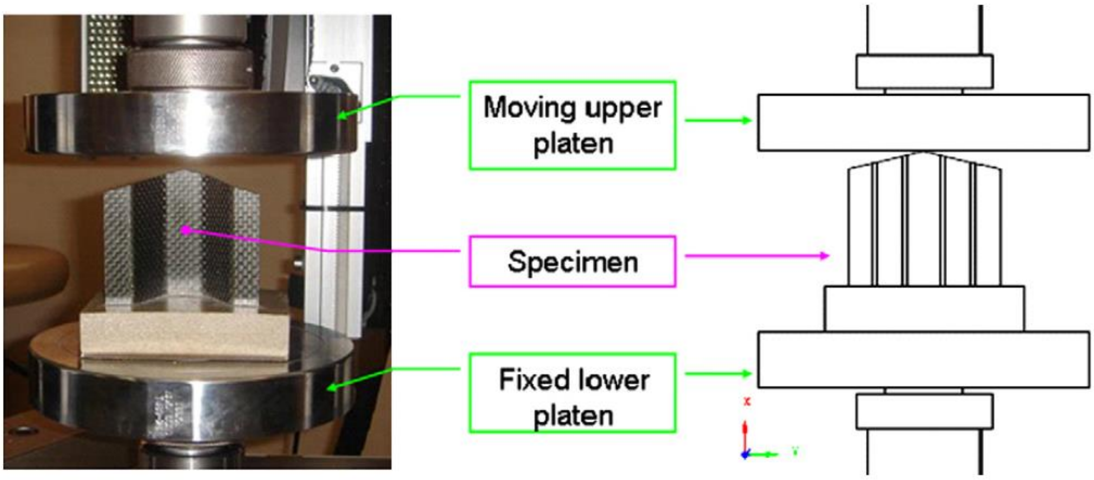

Figure 2.9 Characteristics of the specimen on the test machine [31]

P. Feraboli et al. (2009) [32] has studied the energy absorption under axial impact load of composite materials. The specimens were different in all 5 cross-sectional areas in which the specimens used are carbon fiber/epoxy prepreg. The 12 ktow woven sheets were formed by vacuum and the orientation stacking of fiber is $[0/90]_{4S}$. Thickness is 1.65 mm and tested with speed of 50.8 mm/min. The results showed that for the mixture and layup rate study, it affected the energy absorption at the corner of the specimens. While the smooth area specimen found that there is a low energy absorption percentage.

L.N.S Chiu et al. (2015) [33] studied the FEA model of composite materials under quasi-static load. Tulip-shaped tubes as shown in Figure 2.10 (a) were made from unidirectional T200/M21 carbon fibers. The orientation stacking of the fibers was $[0/90/0/90]_s$ and the thickness was 1.2 mm. The test speed was 0.5 mm/min. The program used in the study is ABAQUS/Explicit. The element size was 1 mm. The comparison results between FEA and experiment was found to be similar, both for the Load-displacement curve and the mode of collapse, as showed in Figure 2.10 (b).

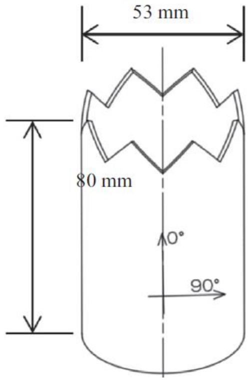

(a)

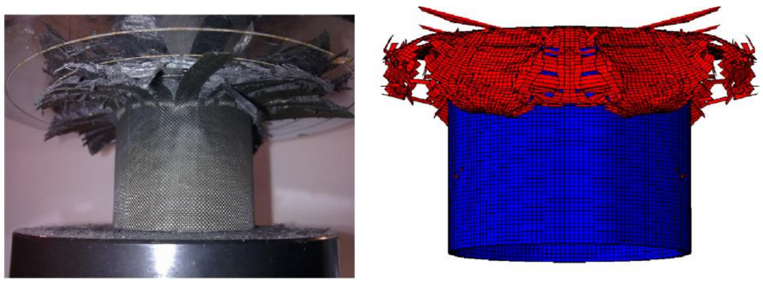

(b)

Figure 2.10 Experimental tubes and models: (a) Tulip tube and (b) Damage of tulip [33]

H. Zhou et al. (2015) [34] investigated the model of the braided composite tube. The specimens were made from T700 carbon fibers and epoxy the braided fiber. Tube laid at an angle of 15, 30 and 45 degrees. The diameter was 20.5 mm, thickness was 1.75, 2.20 and 2.65 mm respectively as shown in Figure 2.11. The impact testing was conducted with Split Hopkinson Bar (SHPB). The impact speed were 7 m/s, 12 m/s and 17 m/s respectively. Results was found that the calibration of the model from the load and collapse graph are in similar trend with experimental results. The braided fiber specimen was placed at an angle of 45 degrees at an impact pressure of 0.6 MPa. The maximum load of the model is slightly higher, as shown in Figure 2.12.

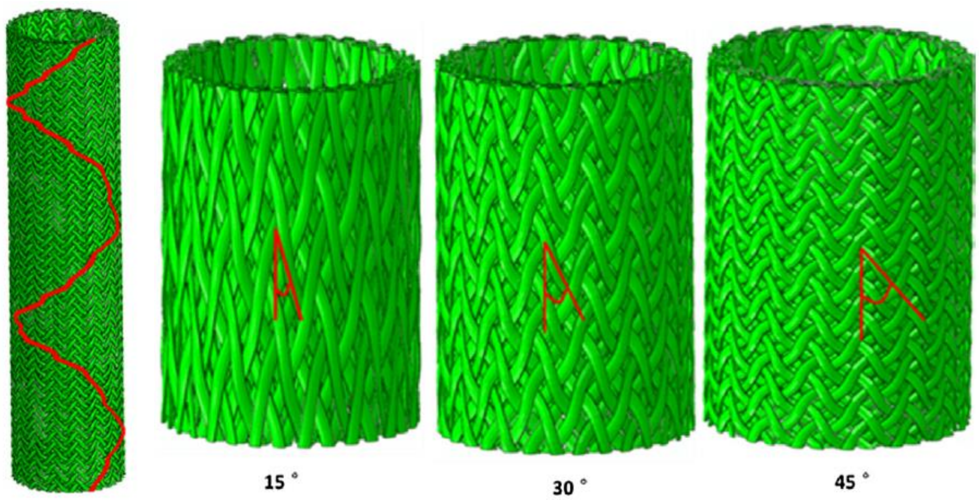

Figure 2.11 Braided fiber model with angles of 15, 30 and 45 degrees [34]

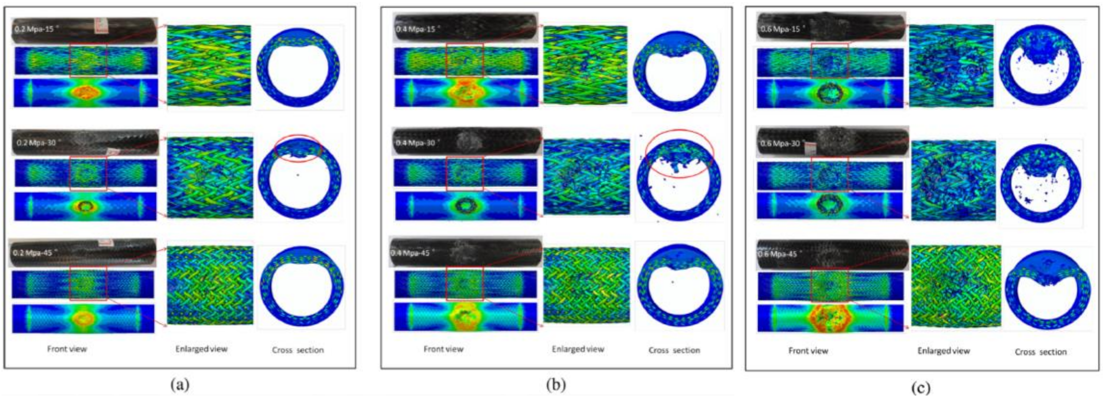

Figure 2.12 Comparison of experimental results and models at pressure of 0.2 and 0.4 MPa [34]

B.P. Bussadori et al. (2014) [35] studied the model of carbon fiber reinforced plastic tubes under impact. The tube was made with prepreg carbon fibers and epoxy. The specimens were square tube as in Figure 2.13. The internal width was 50 mm, 2.08 mm of thickness and length of 150 mm. The angle of the fibers was [45/-45/0/-45/45]. The test was carried out by using the instrument Instron 5900 capacity 250 kN. The speed was 20 mm/min. The FEA model as shown in Figure 2.14 used PAMCRASH. The study indicated that all models of the 6 specimens have similar collapse characteristics, as shown in Figure 2.15. It was also found that the increase in the number of layers dose not change the collapse of the tubes and specific energy absorption of the 4 and 5 layers tubes.

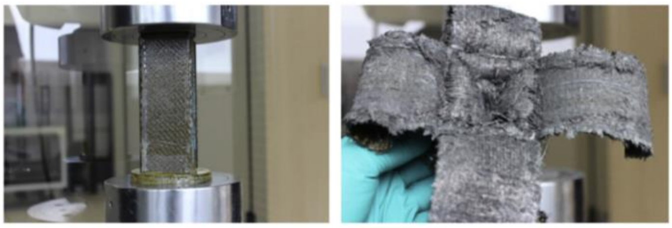

(a) (b)

Figure 2.13 Experimental: (a) square tube and (b) damage square tube [35]

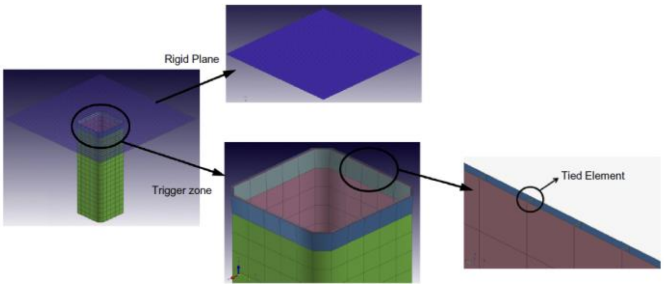

Figure 2.14 The composition of the model that consists of thin-walled structures [35]

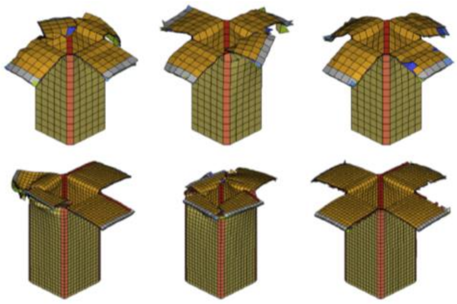

Figure 2.15 Top element size of 7.0 mm, bottom element of 4.0 mm and coefficient of friction 0.1, 0.2 and 0.3 from left to right [35]

D. Kakogiannis et al. (2013) [36] studied the response of pultruded composite material under axial impact. The cylindrical tubes, with the top end in a tulip shape, as shown in Figure 2.16, were formed from glass fibers and vinyl esters resin. Thickness was 2 mm and length was 100 mm. The blast conducted by accelerating motion with the impact mass to the specimens. The masses of land mines were 4, 5 and 6 g. The LS-DYNA program, under impact, as shown in Figure 2.17, were used. The study revealed the behavior of specimens under blasting.

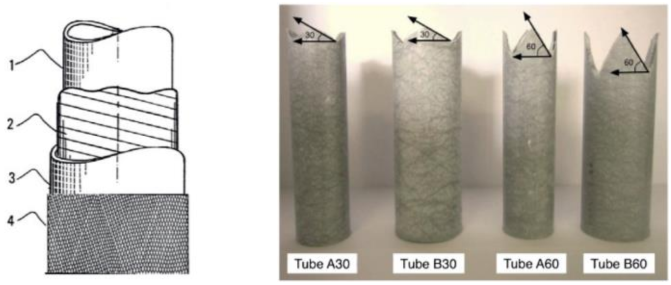

(a) (b)

Figure 2.16 Pultruded composite tubes: (a) The layer of glass fibers and (b) Tulip cylindrical specimens, the inclination angle is 30 and 60 degrees [36]

(a)

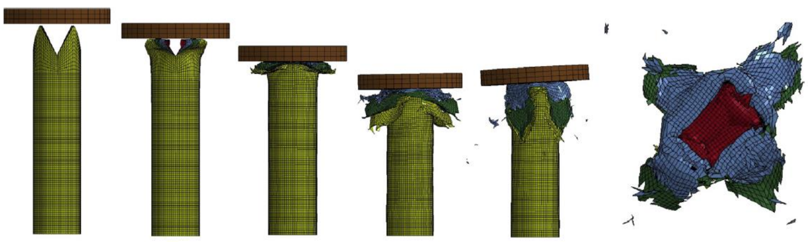

(b)

Figure 2.17 Model FEA: (a) the damage process under impact load and (b) damage process with an angle of 60 degrees [36]

S. Boria et al. (2015) [37] conducted an experiment and FEA study on bumper composite under impact as shown in Figure 2.18 using LS-DYNA. The model used two types of element, shell elements and solid elements as shown in Figure 2.19. The size of the element was 5 mm for drop testing. Mass of the impact head was 300 kg and the speed were 7 m/s. It was found that the model using thick solid elements that step by the adhesion element helps to separate the layers from each other causing the model to look divided and blossom like a fern. The damage of the front bumper found that models with a 5 mm element size and experiment tend to be similar.

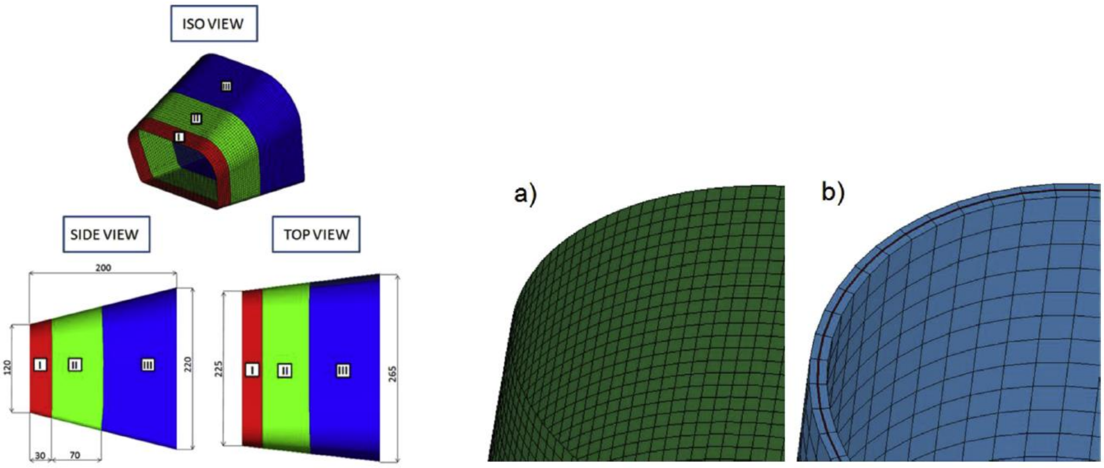

(a) (b)

Figure 2.18 The characteristics of the bumper structure: (a) FEA model bumper and (b) models of cylindrical tubes [37]

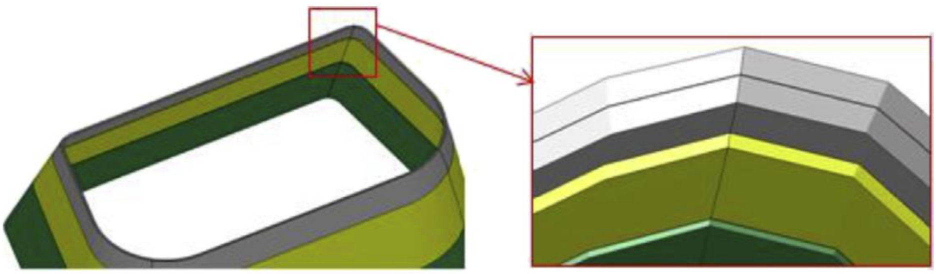

Figure 2.19 Model of thick elements and the bonding area of the elements [37]

A. Esnaola et al. (2016) [38] studied the specific energy absorption of the specimen which is having semi-hexagonal section in Figure 2.20. The specimen was made of glass fibers and polyester unidirectional fiber type 300 g/m^2, angle 0 degrees. The test was using a universal test machine Instron 4206, tested at speeds of 10 mm/min. The volume of glass fibers were varied as follows 40, 47, 55, 58 and 60 percent, with the overlapping of fibers, is 6, 7, 8, 9 and 10 layers respectively. It was found that the increase in the fiber content causes the average load to be higher. It was also found that the specimen with 47 percent fiber or 7 layers of fiber can absorb energy and absorb high specific energy. In terms of damage to the specimen, it was found that there were three parts of damage, break and splitting. The fibers were separated by collapsing into the breakage and separating the two layers between the inside and the outside of the crack.

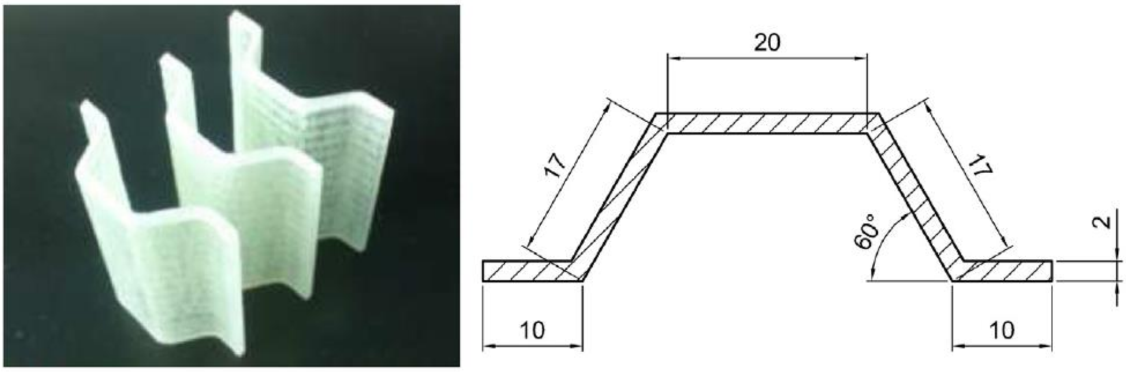

(a) (b)

Figure 2.20 Semi-hexagonal section (a) Specimens and (b) Dimension of specimens [38]

CHAPTER 3
RESEARCH METHODOLOGY

3.1 Research conceptual framework

This research was aimed to investigate the behavior of hybrid tubes under impact. The hybrid tube was made form AL tube wrapped with GFRP layers. Number of layers, fiber orientation angles and the sequence of layer were investigated to determine their effect to crush behavior of specimens. This study focused on the mode of collapse, progressive collapse, load response, mean load and maximum load of specimens. Experimental and FEA approaches were used in this study. Conceptual framework of this study is showed in Figure 3.1. Detail of experiment, specimens and FEA model are explained in the following topic.

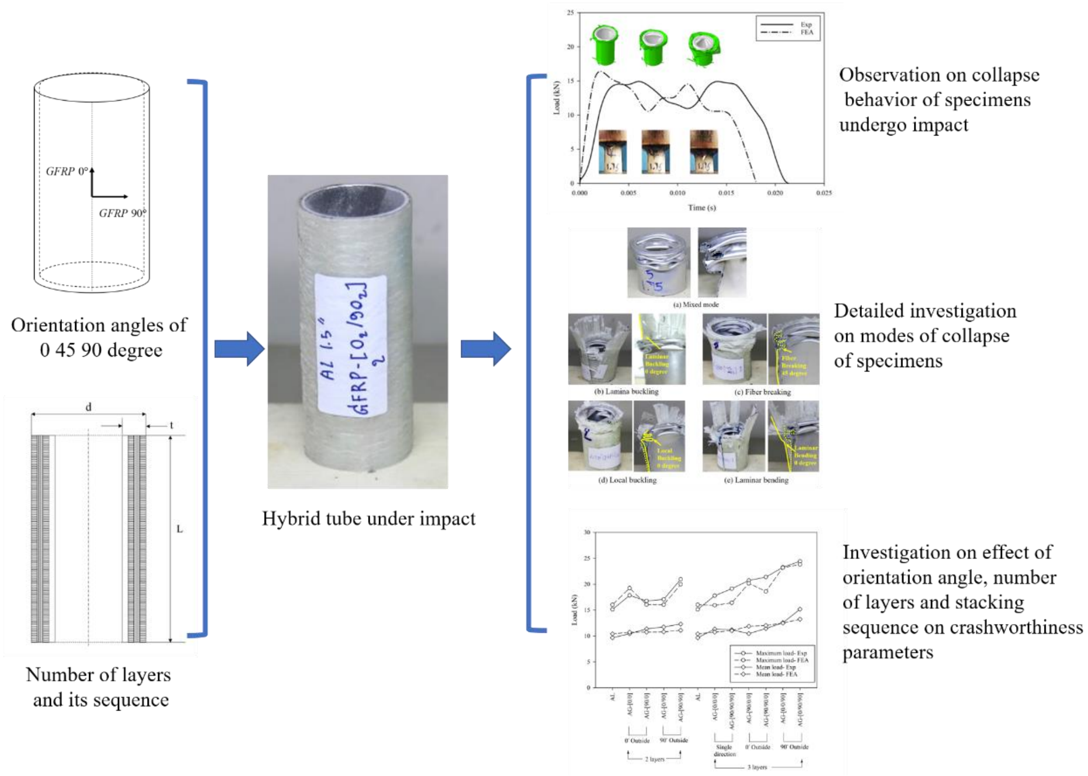

Figure 3.1 Conceptual framework of this study

3.2 Experimental process

3.2.1 Experimental setup

The impact test was carried out using vertical impact testing machine, as showed in Figure 3.2 The machine is a 3 m height tower and is consisted of a 20-60 kg hammer which can be free fallen to impact to targeted specimen. The bottom of machine is an anvil with load cell embedded. The load cell is connected to data logger to record reaction force. A specimen was placed on the anvil with simply supported. A 30 kg hammer was dropped from 2.43 m to impact to the specimen with approximated speed of 6.76 m/s, while load and time of impact were recorded then proceeded for analysis. A high speed camera was also used to record the collapse development throughout the process. 88 cases were triplicated tested, hence totally of 264 specimens were tested. The average value of each case was made and used for further analysis.

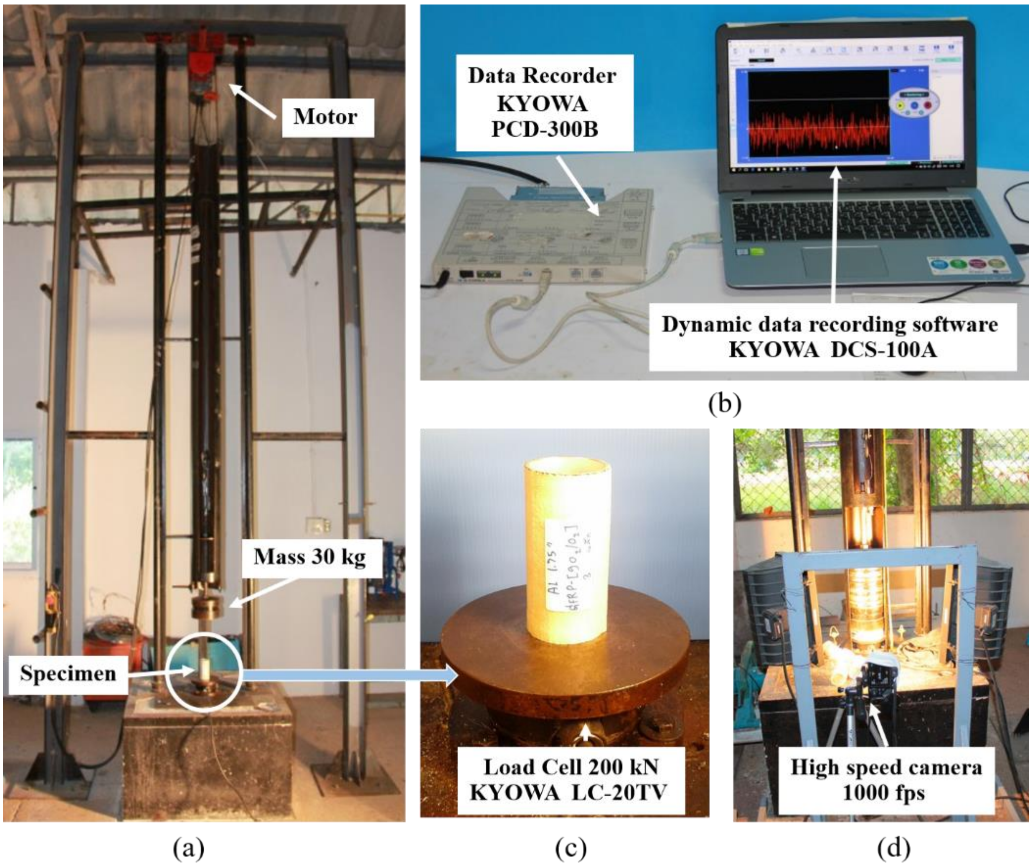

Figure 3.2 Experiment setup: (a) Vertical impact testing machine, (b) data recorder set, (c) load cell and specimen setup and (d) high speed camera setting

3.1.2 Specimens

The specimens were made from aluminum tubes wrapped with E-glass unidirectional mat and isophthalic polyester resin. They were fabricated using vacuum process in order to reduce the effect of air bubble. The geometry and fabrication process of specimens are showed in Figure 3.3 and 3.4 illustrates the designation of ply angle, 0 degree is as the fiber line along the axis while 90 degree is for the fiber that is in hoop direction. The fabrication process of specimen is showed in Figure 3.5 Aluminum tube was cleaned with acetone and wrapped with E-glass mat. The wrapped tube was then proceeded to the vacuum process by containing specimen in a sealed vacuum bag. Air was evacuated from the bag using vacuum pump and the mixture of polyester resin and hardener was pulled from a container and flowed all over the specimen. The specimen was left for 24 hours, took the mold off and cut in a desired size. Figure 3.6 shows the diagram of vacuum infusion process. Figure 3.7 shows the finished specimens those are ready to be tested.

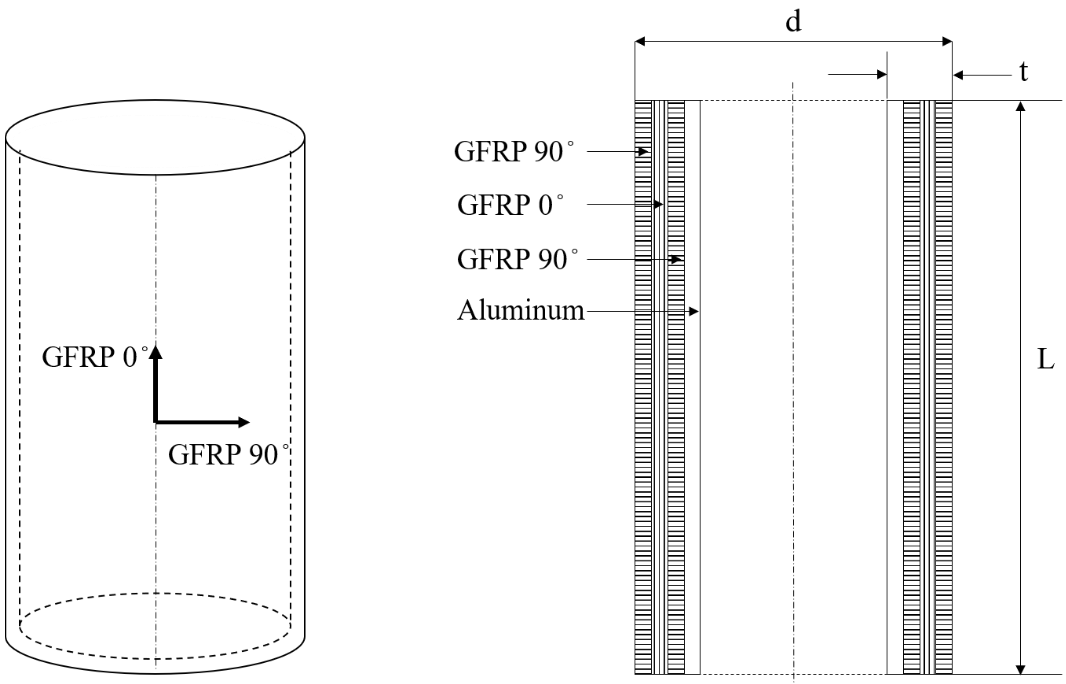

Figure 3.3 The geometry of specimens and ply angle of each layer

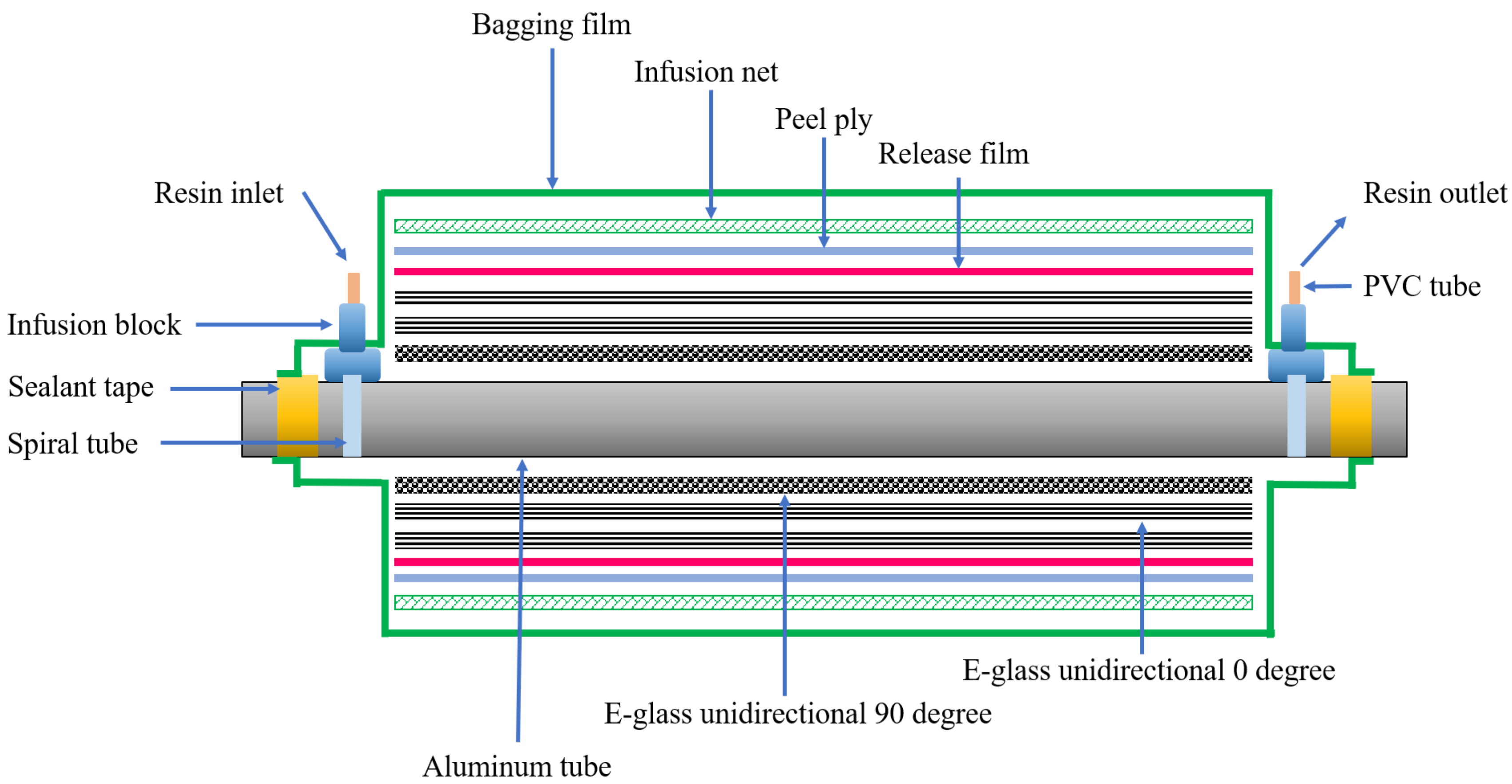

Figure 3.4 Diagram of aluminum tube was wrapped with E glass mats, release film, peel ply, infusion net, and bagging film

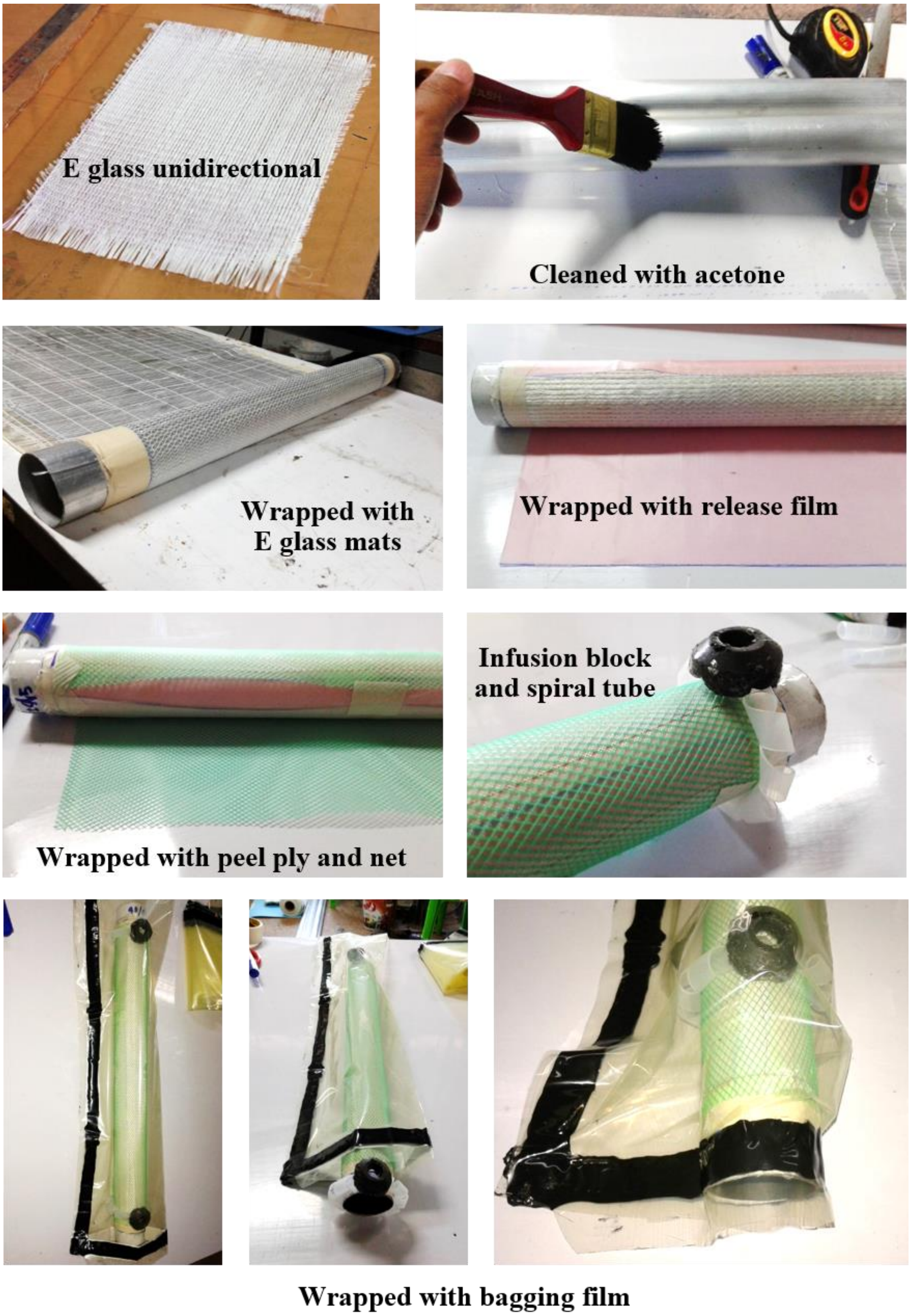

Figure 3.5 aluminum tube was wrapped with E glass mats and the specimen was contained in sealed vacuum bag

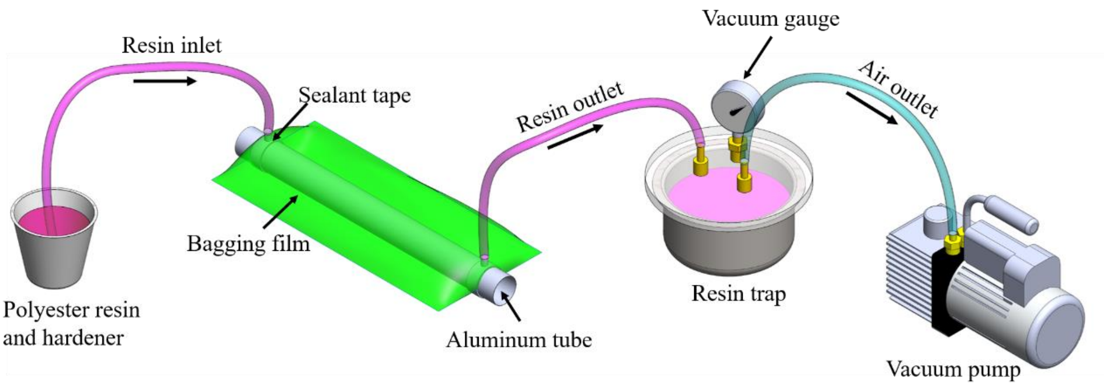

Figure 3.6 vacuum infusion process

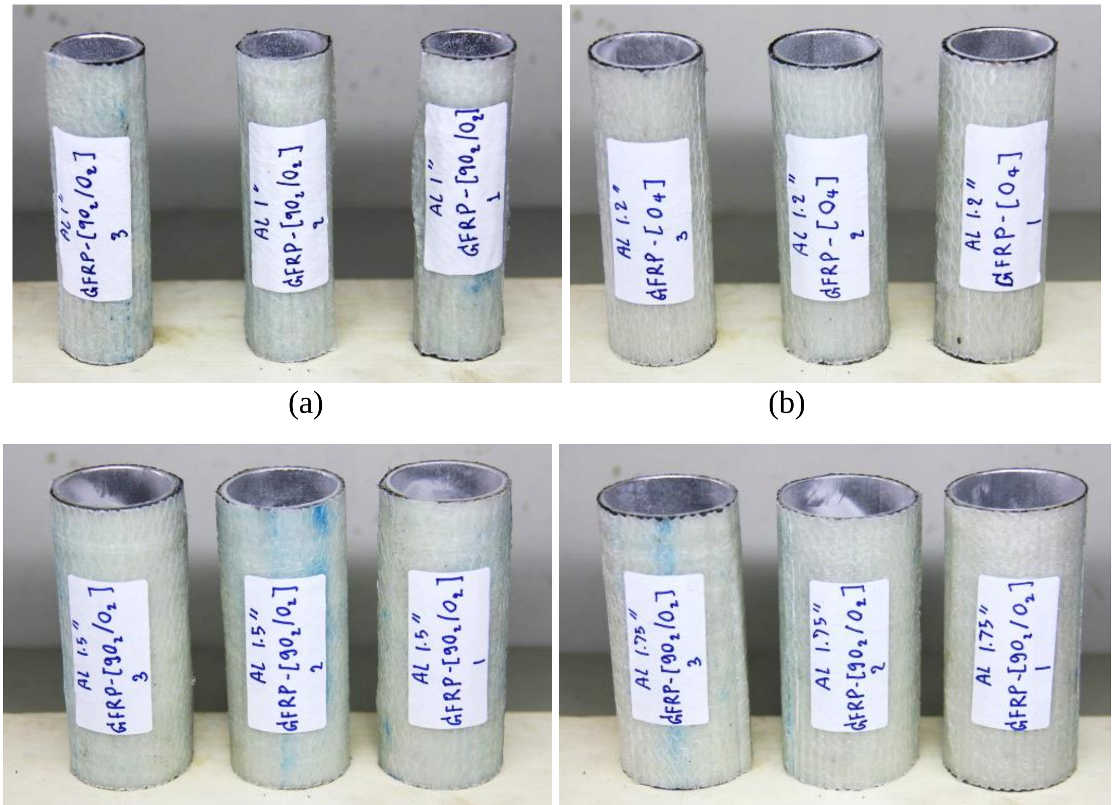

(a) (b)

(c) (d)

Figure 3.7 The finished specimens those are ready to be tested: (a) the diameter of 25.39 mm (b) diameter of 30.48 mm (c) diameter of 38.10 mm and (d) diameter of 45.72 mm

3.3 Material properties of Aluminum and GFRP

In order to determine material property, the specimens were sent to National Metal and Materials Technology Center, Thailand (MTEC) for tensile test. The material testing was carried out with Universal Testing Machine, Instron 8801 Dynamic Type. The machine capacity is 100 kN of compression and tension, as in showed in Figure 3.8 The standard tensile for test code ASTM E8 was adopted in this study.

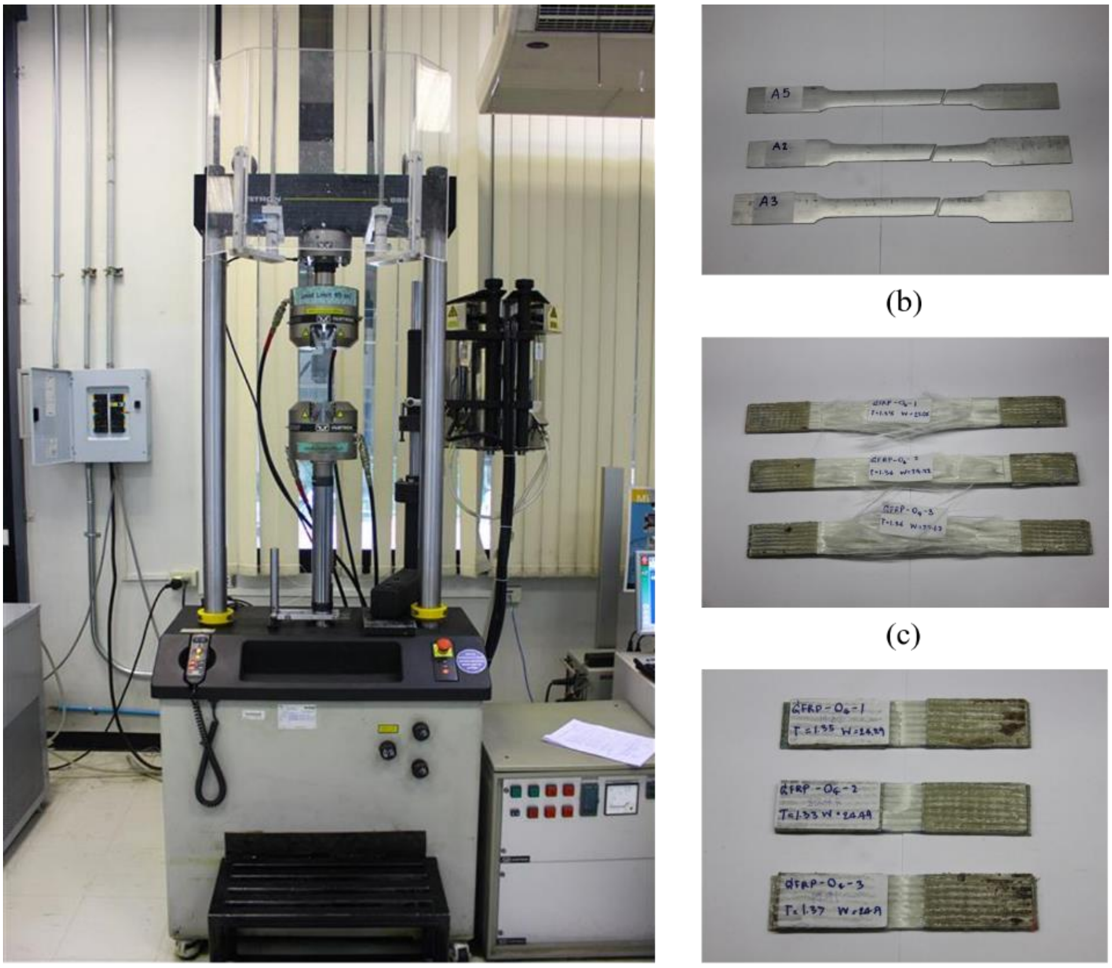

(a) (b) (c) (d)

Figure 3.8 Universal Testing Machine: (a) Instron 8801 - Dynamic Type, (b) aluminum specimens after tensile test, (c) GFRP specimens after tensile test and (d) GFRP specimens after compression test

The aluminum specimens for standard test were 1.2 mm thick, 12.5 mm wide and 250 mm long. They were tested with a quasi static tensile speed of 10 mm/min.

The results are showed in Table 3.1 and Table 3.2 The property test for GFRP was carried out using standard test code ASTM 3039. The specimens were 25 mm wide and 250 mm long. They were made of 3 different orientation angles GFRP sheets, i.e. [0/0/0/0], [90/90/90/90] and [45/45/45/45]. The tensile test was made with a 10 mm/min of speed. The GFRP specimens were also tested under compression using ASTM 3039 code. The compressive specimens were made also from 3 different orientation angle similar to the tensile test. They were 25 mm wide and 120 mm long, and tested with a compressive speed of 10 mm/min. The test result of GFRP properties are showed in Table 3.3, 3.4 and 3.5 The delamination testing of GFRP was also carried out, as showed in Figure 3.9. The specimens were 25 mm wide, 150 mm long and 100 mm of initial crack. It was found that specimen can resist maximum stress of 8.333 MPa and 0.263 mJ/m^2 of energy fracture. Detailed results of delamination test are in Table 3.6

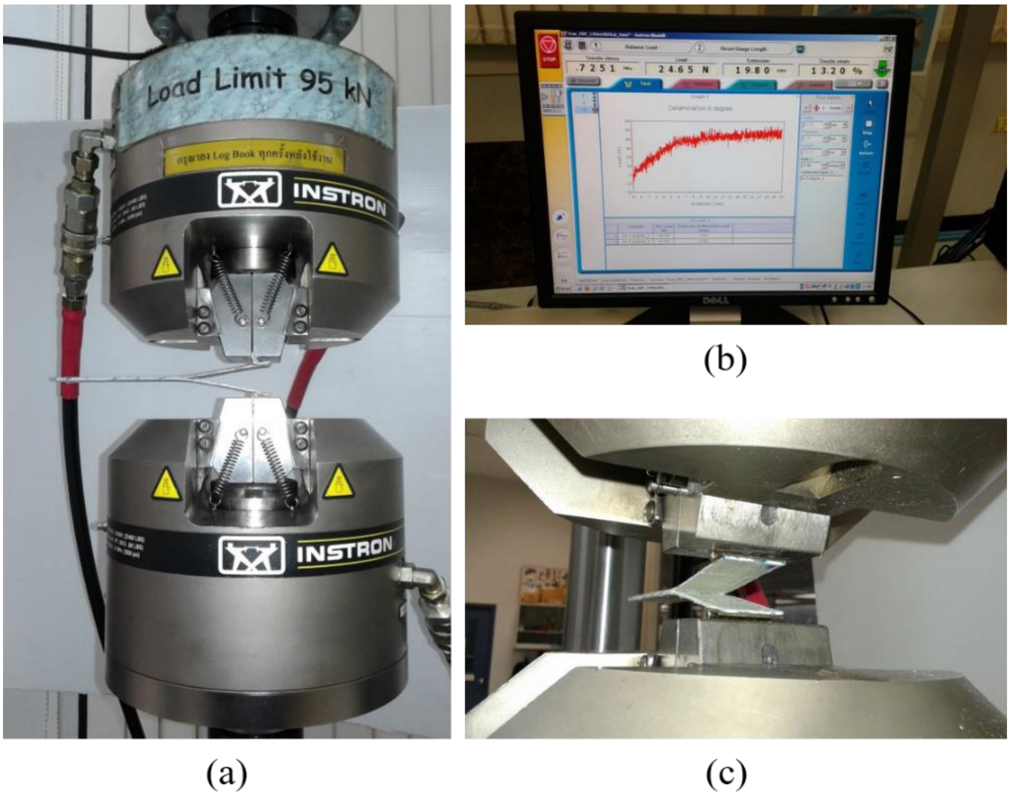

Figure 3.9 Delamination testing of GFRP specimen: (a) delamination testing setup, (b) load – displacement curve and (c) specimen at initial crack

Table 3.1 Material properties of aluminum tube

Properties	Descriptions	Value	Unit
ρ	Density	2,700	kg/m^3
E	Young's modulus	42.92	GPa
υ	Poisson's ratio	0.33	-

Table 3.2 Yield stress and plastic strain of aluminum tube

Properties	Descriptions	Value					Unit
σ_t	True stress	163.366	172.847	180.113	184.901	189.133	MPa
ε_p	Plastic strain	0.000	0.008	0.016	0.024	0.032	-

Table 3.3 Material properties of E-glass fiber/polyester lamina

Properties	Descriptions	Value	Unit
ρ	Density	1,800	kg/m^3
E_{11}	Young's modulus in longitudinal (fiber) direction	30.75	GPa
E_{22}	Young's modulus in transverse (fiber) direction	2.38	GPa
G_{12}	In-Plane shear modulus	6.37	GPa
G_{23}	Out of plane shear modulus	1.056	GPa
υ_{12}	Poisson's ratio	0.28	-
υ_{23}	Poisson's ratio	0.28	-

Table 3.4 Strength of E-glass fiber/polyester lamina

Properties	Descriptions	Value	Unit
X_t	Longitudinal tensile strength	721.55	MPa
X_c	Longitudinal compressive strength	138.11	MPa
Y_t	Transverse tensile strength	13.78	MPa
Y_c	Transverse compressive strength	24.31	MPa
S_{12}	Longitudinal shear strength	12.01	MPa
S_{23}	Transverse shear strength	24.02	MPa

Table 3.5 Fracture energy of E-glass fiber/polyester lamina

Properties	Descriptions	Value	Unit
G_t	Longitudinal tensile fracture energy	0.260	mJ/m^2
G_c	Longitudinal compressive fracture energy	0.005	mJ/m^2
G_t	Transverse tensile fracture energy	0.007	mJ/m^2
G_c	Transverse compressive fracture energy	0.001	mJ/m^2

Table 3.6 Traction separation of delamination

Properties	Descriptions	Value	Unit
ρ	Density	1,800	kg/m^3
t_n	Damage initiation	8.333	MPa
G_n	Energy Fracture	0.263	mJ/m^2

3.4 FEA model

The numerical study was also conducted in this study using finite element program called ABAQUS. This is in order to make detailed study on the response of hybrid tube. The FEA model was made in the same condition and geometry of the experiment. Detail of the FEA model is showed in Figure 3.10. As can be seen from Figure 3.10 (a), the model consists of hybrid tube which is in between top and bottom rigid plates. The two rigid plates are square with 100 mm width and 100 mm length. The element type of plates is 4-node 3-D bilinear rigid quadrilateral (R3D4) with size of 5 mm to reduce the CPU time. The bottom plate is assigned to be fixed by movement constraint in any direction. The top plate is assigned to be an impactor, so it is allowed to move in vertical direction (U2) while movement in other directions are constrained (U1, U3, UR1, UR2, and UR3 are set to 0). The top plate is set to move downward with initial velocity of 6.76 m/s and inertia mass of 30 kg.

The model of hybrid tube is consisted of two parts i.e. aluminum tube and GFRP column which are attached together. The aluminum tube model has diameter of 25.39, 30.48, 38.10 and 45.72 mm, a thickness of 1.2 mm and a length of 100 mm, these are the same dimension of experimental specimen. A 4-node doubly curved thin or thick shell (S4R) element is used for aluminum tube. Element size analysis was conducted and found that 2 mm was an optimum size for this study. The GFRP column was modelled with 1-, 2-, 3- or 4-layer respectively. The thickness of each layer is 0.5 mm and with length of 100 mm. The element type of 3-node triangular thin or thick shell (S3R) with 2 mm size was used for this part. Condition of contact model was determined by contact surface of the model. General contact determined the coefficient of friction of 0.1 by the global property assignments. Surface cohesive was assigned by defining surface based cohesive, which was defined in layer such as GFRP 1st to GFRP 2nd and GFRP 2nd to GFRP 3rd as showed in Figure 3.10 (c) using individual contact.

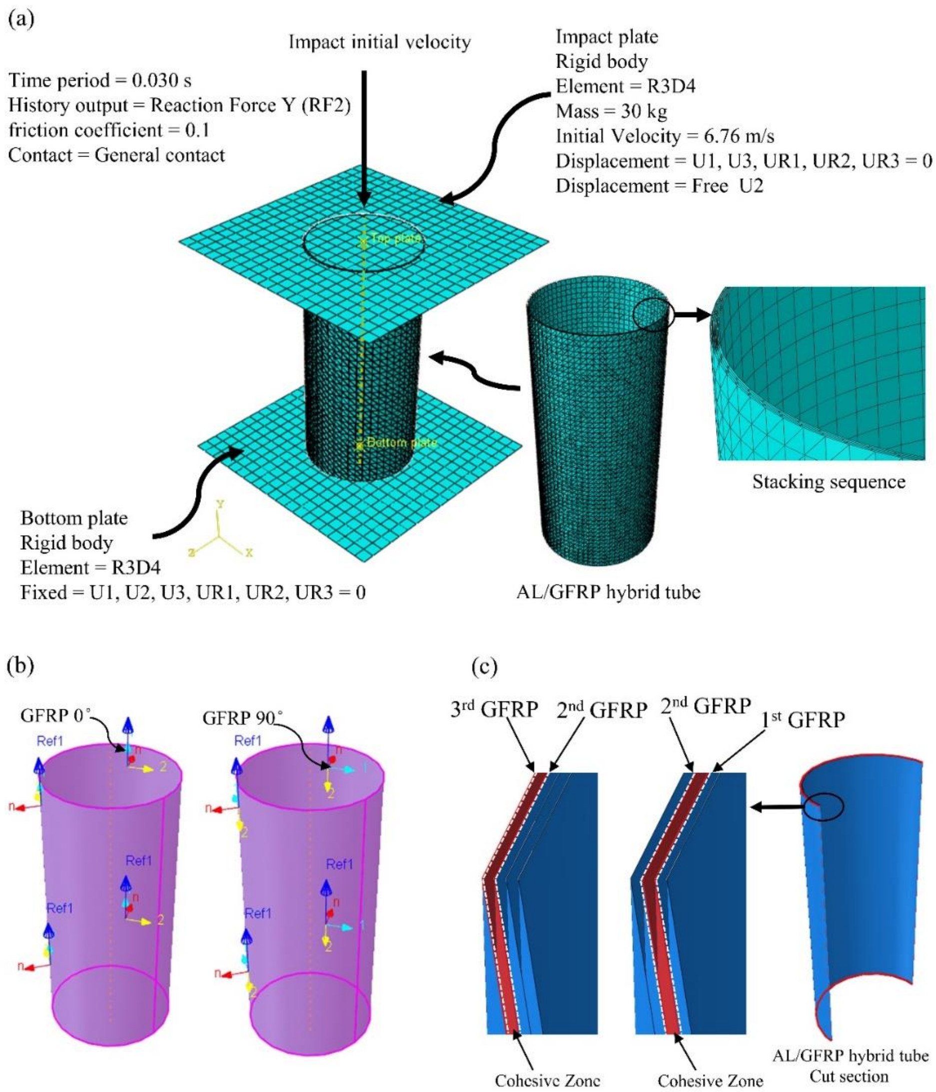

Figure 3.10 FEA model of specimen (a) AL/GFRP hybrid tube (b) The orientations of GFRP and (c) Surface-based cohesive behavior

CHAPTER 4
RESULTS AND DISCUSSION

The results from experiment and FEA as well as the discussion are presented in this chapter. Since the specimens are made of 4 different diameters i.e. 25.39, 30.48, 38.10 and 45.72 mm, the result of each will be presented and discussed one by one. Effect of number of layers, orientation angles and stacking sequence are main focused. The response of specimens to impact in terms of load-time curves, mode of collapse, maximum load and mean load are presented and discussed.

4.1 Mode of collapse

In this study, a number of mode of collapse of aluminum tubes and hybrid tubes are found. For aluminum tubes, 3 modes of collapse are observed i.e. Concertina mode, Diamond mode and Mixed mode as showed in Figure 4.1. The collapse mechanism of hybrid specimens may be examined by considering the collapse pattern of aluminum tube and collapse pattern of GFRP tube separately. For aluminum tubes, they normally failed in diamond mode with 3-4 lobes or failed in mixed mode which is the combination of concertina mode and diamond mode. Considering the GFRP, the fiber is broken in various patterns and takes some interaction with aluminum tubes. The combination of collapse mode of aluminum and breaking behavior of GFRP forms the terminal collapse mode of hybrid tubes. Types of collapse mode of hybrid tubes found in this study are showed in Figure 4.2. Considering the GFRP part, there are 4 modes of collapse found which are (1) laminar buckling (2) fiber breaking (3) local buckling and (4) laminar bending. The laminar buckling mode is showed in Figure 4.2 (a), it fails by the outer fiber is buckled, bended outward and totally separated from aluminum tube. The fiber breaking mode is showed in Figure 4.2 (b). In this mode, the fiber is broken in pieces, some are inserted between the folds of aluminum while some are torn out from the aluminum tube. The local buckling mode are showed in Figure 4.2 (c), the fiber is buckling in a limited area adjacent to the impact hammer and inserted in between the folds.

Figure 4.2 (d) shows the laminar bending mode. In this mode, fiber adjacent to the impact hammer is broken and bended outward from AL tube.

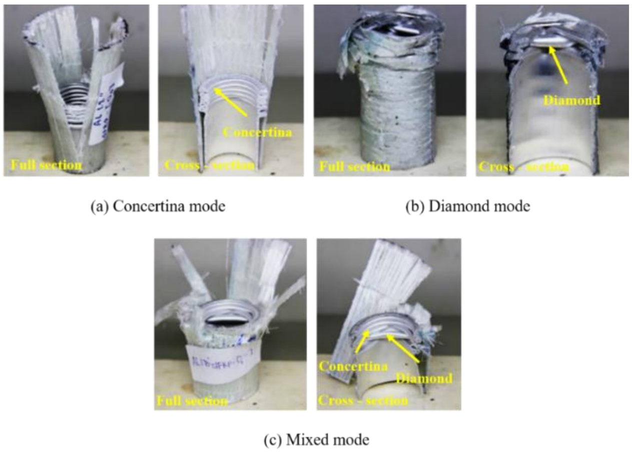

Figure 4.1 Terminal mode of collapse of aluminum tubes (a) Concertina mode (b) Diamond mode and (c) Mixed mode

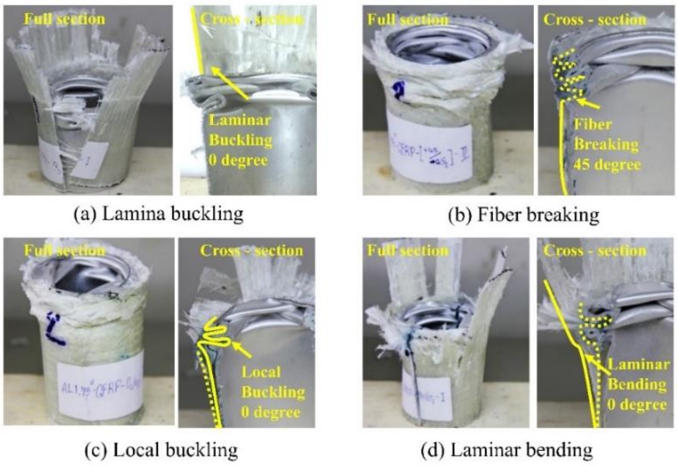

Figure 4.2 Mode of collapse of hybrid tubes (a) lamina buckling (b) fiber breaking (c) local buckling and (d) laminar bending

4.2 Observation results of hybrid tube with diameter of 25.39 mm

The specimen is aluminum tube wrapped with GFRP having diameter of 25.39 mm, thickness of 1.2 mm and 100 mm long. The GFRP is E-glass/Polyester resin with 1, 2, 3 and 4 layers wrapped with different angles and sequences as showed in Table 1.2, Chapter 1.

4.2.1 Load response of the specimen

The response of the specimens can be presented in form of load-time curves as showed in Figure 4.3. In the beginning of process, the curve is rising sharply and then fluctuating up and down in wavy shape until the end of the process. As can be seen from Figure 4.3 that the load-time curve is fluctuating in a wavy-shape, corresponding to the formation of failure lobes. It is observed that the curves of hybrid tubes are generally higher than the curve of aluminum tube. This implies that AL/GFRP hybrid tube can absorb higher energy than naked AL tube. However, the collapse process of hybrid tube is a bit shorter than that of AL tube. It is also noticed that, the fiber orientation angle and stacking sequence of fiber layers also affect to the characteristic of curves. This will be discussed more later.

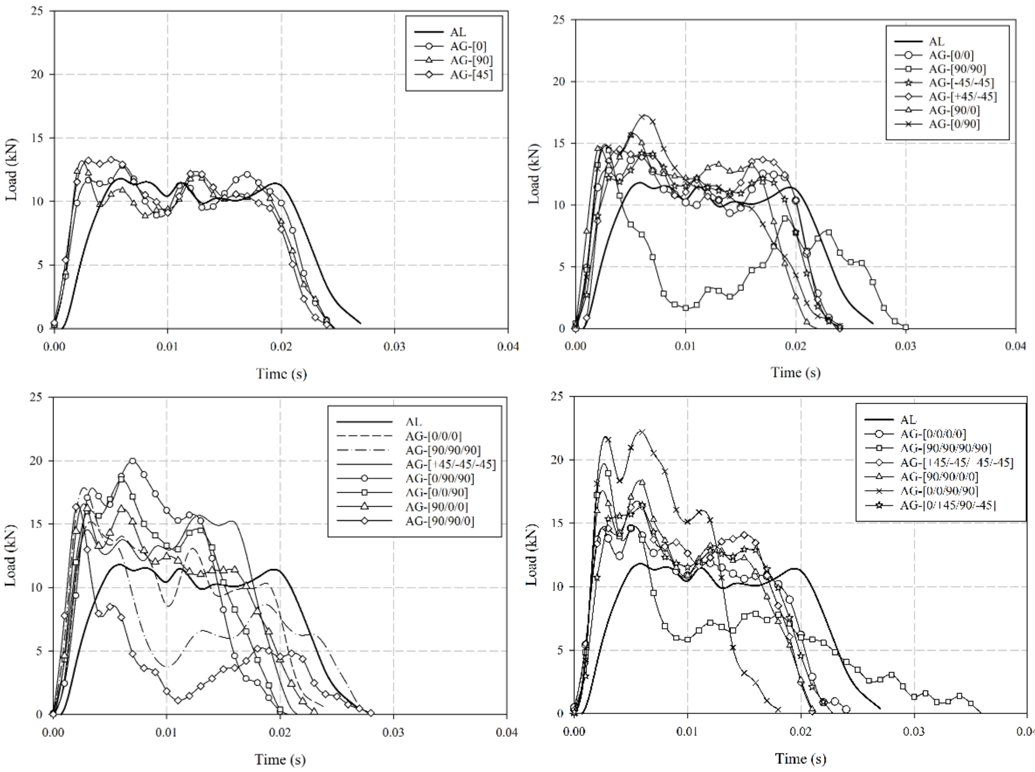

Figure 4.3 Load-time curves of naked AL tube and hybrid tubes of D=25.39 mm, with GFRP of 1, 2, 3 and 4 layers under impact

The FEA technique was used to model the behavior of those tubes under similar condition of experiment. Comparison of the result are showed in Figure 4.4 – 4.7. As can be seen from those Figure that the curves achieved from FEA are in similar pattern and magnitude. In addition, the modes of collapse of tubes from FEA and experiment are also similar. Therefore, it should be summarized that the FEA model used in this study is agreed well with the experiment.

4.2.2 Mechanism and mode of collapse of the specimen

The collapse mechanism of specimens will be investigated and explained in this section according to the FEA and experimental results showed in Figure 4.4-4.7. In case of hybrid tube with 1 layer of GFRP, please refer to Figure. 4.4, it is observed that AL tube is failed in Diamond mode with 4 lobes. This is in the same pattern for FEA and experiment. For hybrid tube with 1 layer, AL tube is failed in Mixed mode which is a combination of 2-3 rings of Concertina mode on the top and 1-2 folds of Diamonds lobes on the later layers. Considering failure mode of fiber layers, there are 2 modes found which are laminar buckling and fiber breaking mode. The laminar buckling mode normally occur with fiber angle of 0 degree. When this kind of fiber is hit by the hammer, it buckles and unbounds from AL tube. The fiber breaking is found in case of fibers with 90 or 45 degree. In this fiber format, the fiber is broken. Some of the broken fiber are inserted in between the folds while some are fall-off the AL tube. Mode of collapse of these tubes are in Figure. 4.4.

Considering on failure mode of hybrid tube with 2 GFRP layers, it is found that the AL tube is failed in Diamond and Mixed mode. The Mixed mode is found in tubes with the same fiber angles i.e. [0/0] and [+45/-45]. The collapse starts from Concertina rings on the top and follow by Diamond folds. The Dimond mode is also found for hybrid tubes with [0/90] and [90/0]. The broken fiber is found to insert in between the lobes causing asymmetric failure mode until the end of process. Considering the collapse mechanism of fiber, the Laminar buckling mode is found in 0 degree tube in which the fiber is broken, torn off and fall-off from AL core. The Fiber breaking mode is found in tube with 90 or 45 degree fiber. The Local buckling mode is found in [0/90] in which the inner layer of 0 degree is bended and buckles but still attach with the AL tube because the second layer of 90 degree fasten them together. The Laminar bending is found in case of [90/0] in which the fiber is broken and separated from each other ,then spring out from the tube. The Figure 4.5 illustrates modes of collapse of these tubes.

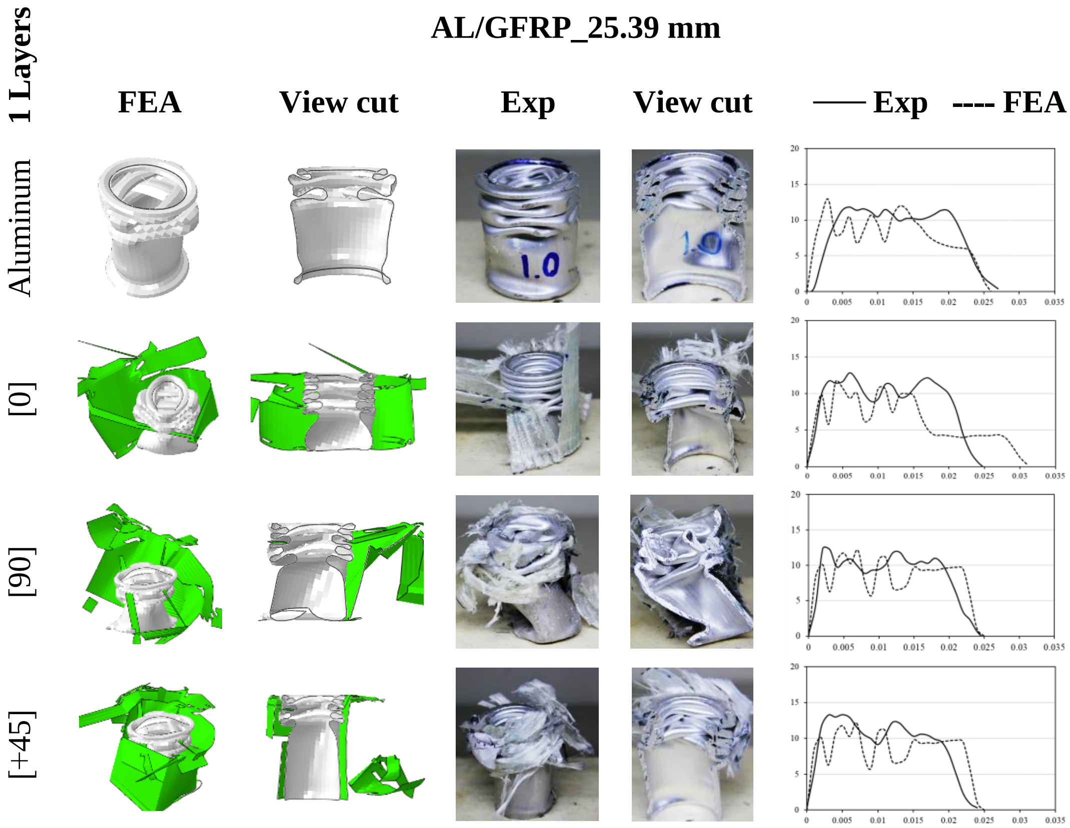

Figure 4.4 Failure mode of 25.39 mm diameter hybrid tube with 1 layer of GFRP

Failure modes of 25.39 mm diameter hybrid tube with 3 layers of GFRP are showed in Figure 4.6. In this case, the Diamond mode and Mixed mode are also found for AL tube. Mode of collapse of fiber is found in 4 modes. The Laminar buckling is found for hybrid tube with [0/0/0] in which the fiber is buckled and split from AL tube. The Fiber breaking mode is found in tube with [+45/-45/-45], the fiber is broken in pieces, some is fall-off from AL tube while some is inserted in between AL folds. The Local buckling mode is found in [0/0/90] and [0/90/90] tubes while the Laminar bending mode is found for [90/0/0] and [90/90/0] tubes.

Failure mode of 25.39 mm diameter hybrid tube with 4 layers of GFRP is showed in Figure 4.7. The AL tube is also found to failed in Diamond and Mixed modes. The Diamond mode is normally found for tube with 0 degree fiber, and the rest is failed in Mixed mode. Considering the fiber layers, the fiber of [0/0/0/0] is buckled in the top, split and spring out from the tube, this is the Laminar buckling mode. The Fiber breaking mode is found with [+45/+45/-45/-45] in which some of the broken fiber is inserted between AL lobes. For the hybrid tube of [0/0/90/90], there are 2 modes found, first mode is the Local buckling which occur in 0 degree fiber of 1-2 layers and secondly the Fiber breaking mode found in 3rd and 4th layers. The broken fiber in this mode is found to be inserted in between lobes of AL tube quite well causing higher load absorption. In case of [90/90/0/0] tube, the Fiber breaking mode and Laminar mode are found.

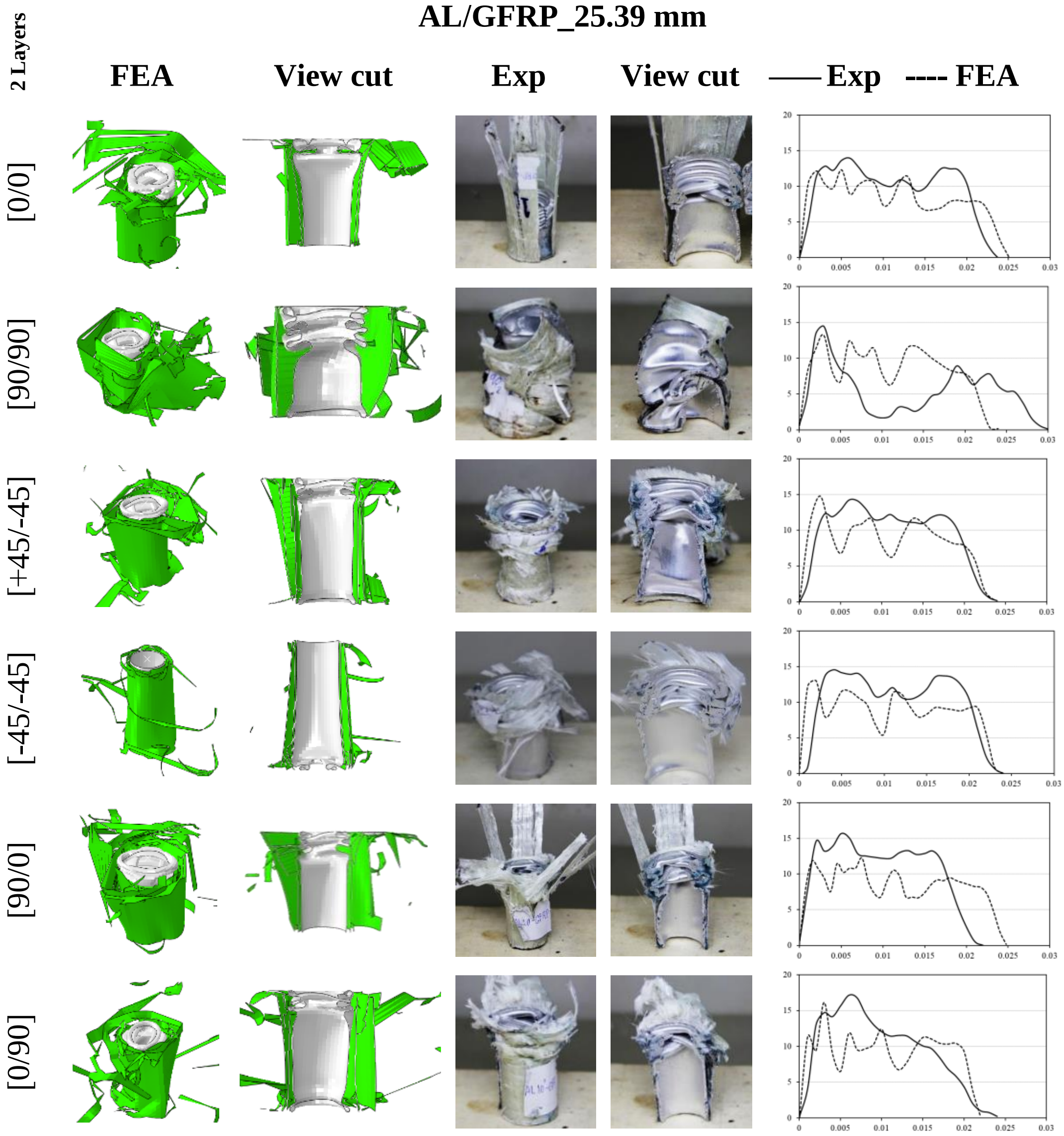

Figure 4.5 Failure mode of 25.39 mm diameter hybrid tube with 2 layers of GFRP

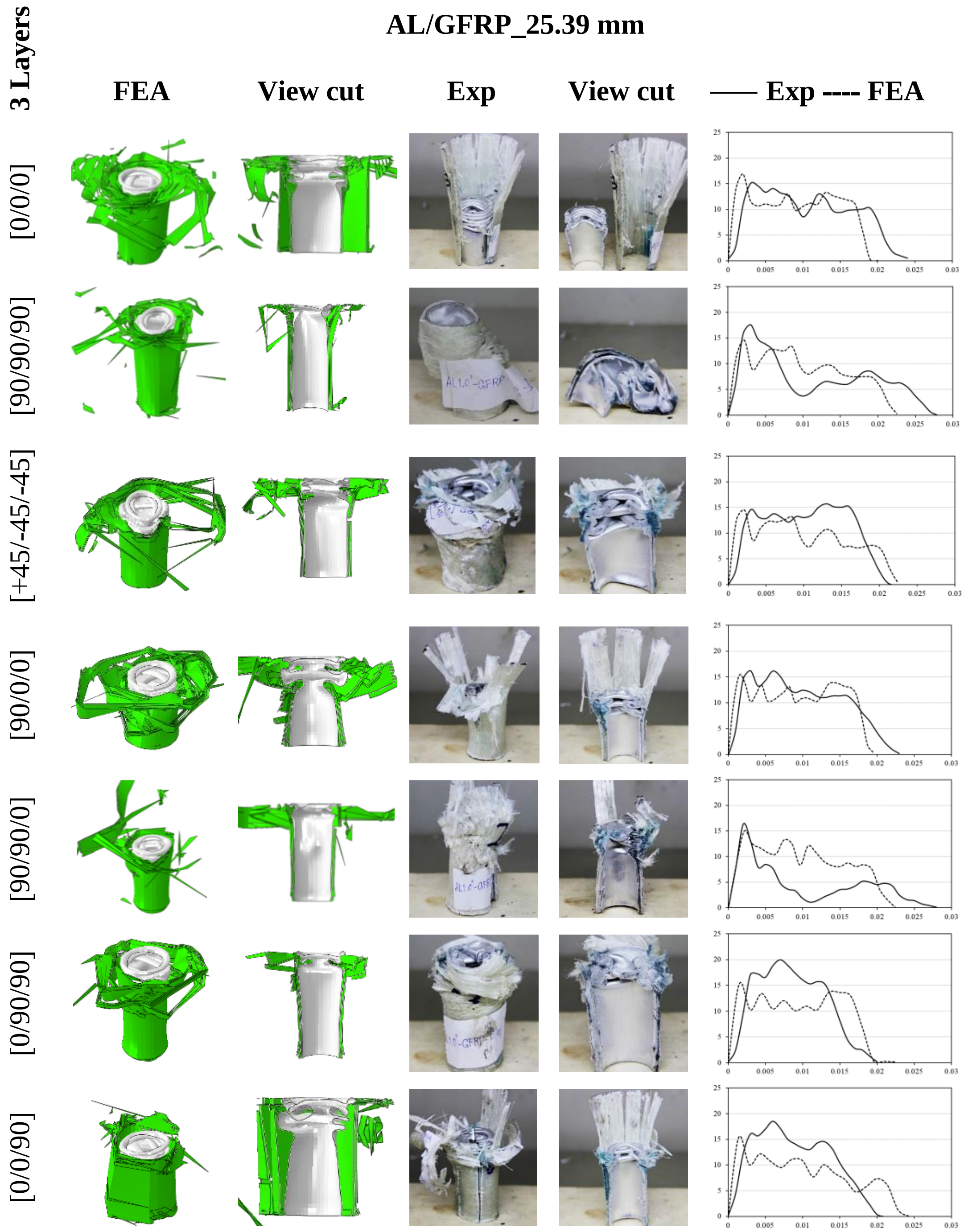

Figure 4.6 Failure mode of 25.39 mm diameter hybrid tube with 3 layers of GFRP

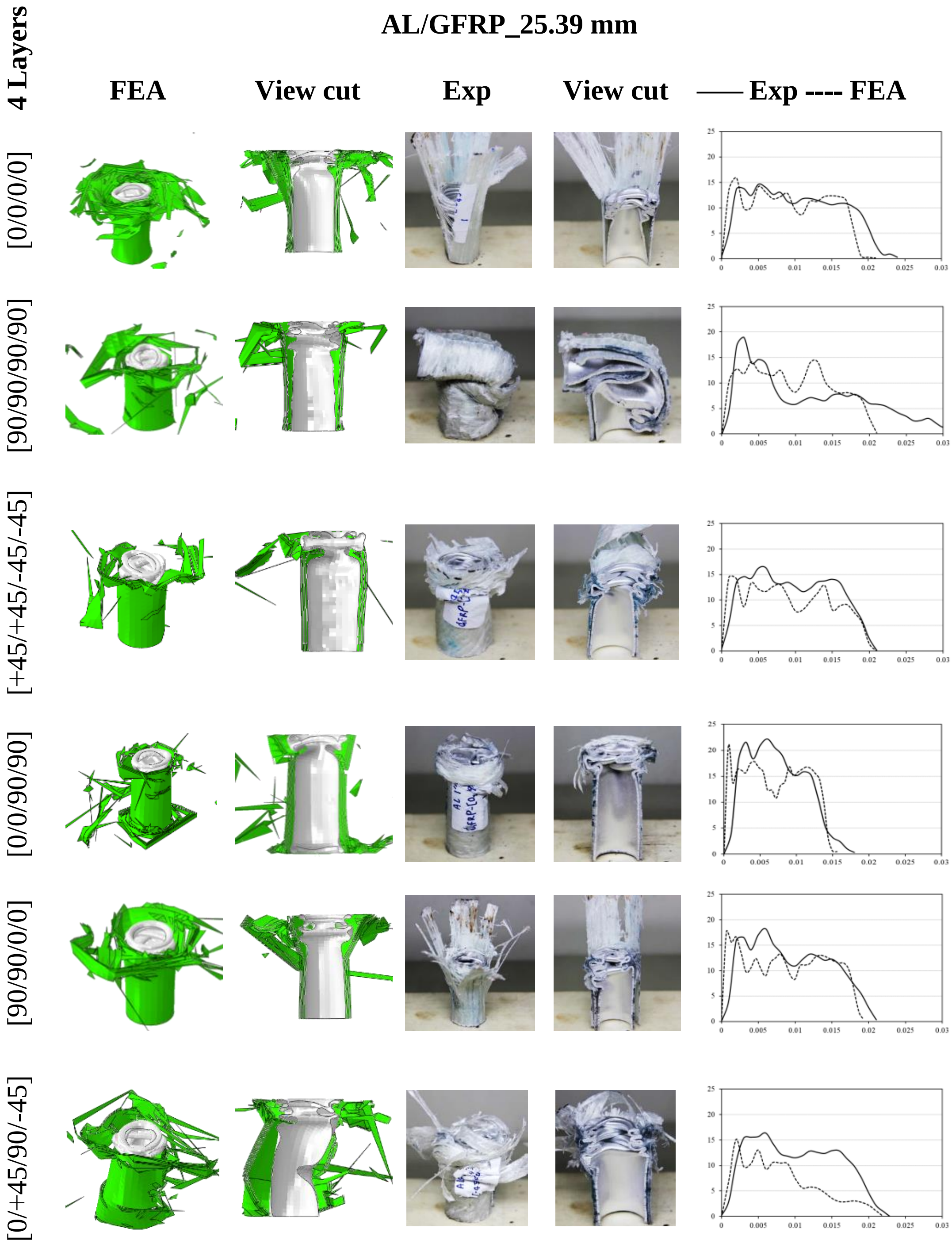

Figure 4.7 Failure mode of 25.39 mm diameter hybrid tube with 4 layers of GFRP

The Fiber breaking mode is occur for fiber with 90 degree are 1st and 2nd layers, while the Laminar bending is found in 3rd and 4th layers which are in 0 degree.

This mode, the 3rd and 4th layers are bended and spring out from AL tube. In case of tube with [0/+45/90/-45], the inner layer of 0 degree fiber fails in Local buckling. The 2nd – 4th are failed in Fiber breaking. Summary of collapse modes of these tubes are in Figure 4.7

4.2.3 Maximum load and mean load

The load response of specimens as showed in Figure 4.3 is proceeded to analyze, maximum load and mean load are extracted to be discussed and presented in Figure 4.8. Figure 4.8 (a) illustrates maximum load and mean load achieved from experiment of AL tube and hybrid tube 1, 2, 3 and 4 layers of GFRP. It is obviously seen that, as the number of layers is increasing, the value of maximum load is also increases. However, the value of maximum loads of naked AL tube and hybrid tube with 1 layer are not much different. The influence of fiber orientation in 1 layer hybrid tube is found insignificant. This may be because the volume of fiber of 1 layer is too small to play major role compared to AL volume.

Considering hybrid tubes of which 2 and 3 layers of fiber, the maximum load trends to increase significantly. The influence of fiber layers and fiber angle is quite prominent, especially for tube with fiber angle of 0 degree. However, the 0 degree fiber layers need other layer to support then with the AL tube, there for the hybrid tubes with angle of [0/90/90] and [0/0/90/90] are preferable. In those kind of tubes, the 0 degree in 1st and 2nd layers is in charge for axial impact load, while the 90 degree of fiber in 3rd and 4th layers is supporting and fasten them to AL tube, as well as push the fiber broken pieces in between AL lobes.

In case of the mean load, one can observed that the mean load is slightly increasing as number of layer increases. However, mean load of hybrid tube with 1 layer is not significantly increases no matter what fiber angle is. For hybrid tube with 2, 3 and 4 layers of fiber, their mean loads are increasing, especially for tubes with 0 degree in the inner layers and 90 degree at the outer layers. This is because the 0 degree layer help resisting axial impact load while the 90 degree layer supports them to stay with AL tube and also help to insert the broken fiber into to failure lobes. However, tube with [90/90] fiber is noticed to give lower value of mean load. This is because the whole hybrid tube is failed in local buckling and dramatically collapse. This kind of collapse mode is not preferred because it is considered as premature collapse.

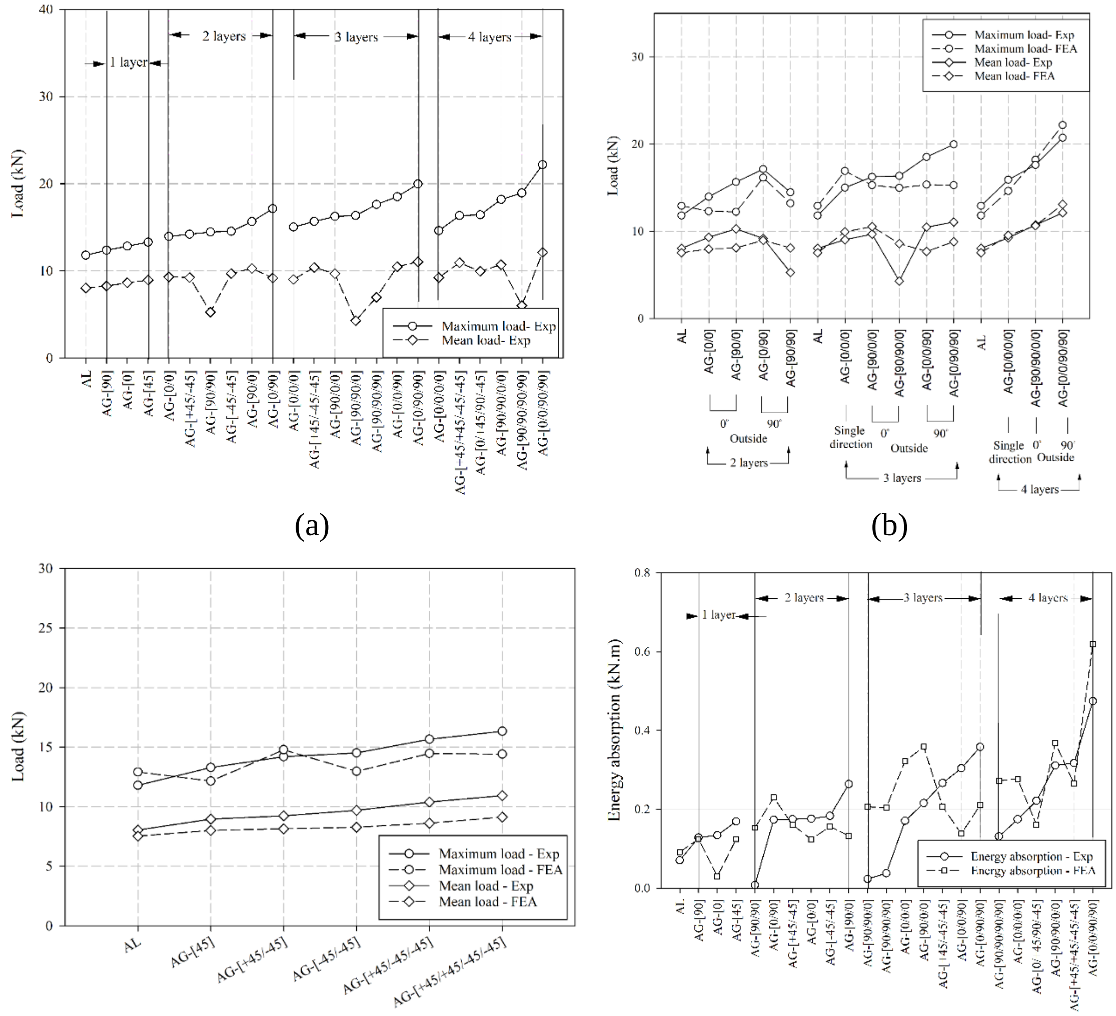

(a) (b)

(c) (d)

Figure 4.8 Mean and maximum loads of AL and hybrid tubes of D=25.39 mm, (a) results of all experimental specimens (b) results from specimens with 0 and 90 degree (c) results from specimens with 45 degree (d) energy absorption

4.2.4 Influence of stacking sequence

From Figure 4.8 (c), it can be seen that fiber angle of 45 degree does not significantly affect to P_{mean} ,no matter 1, 2, 3 or 4 layers. In case of P_{max} it seems to be slightly increasing as number of layers increases. However, the influence of 45 degree seems to offer too small increment in P_{mean} and P_{max}, especially when compared with 90 or 0 degree. Therefore, this study should manly focus on 0 and 90 degree.

Figure 4.8 (b) shows maximum load and mean load of specimens with 0 and 90 degree and their combinations. It is found that the loads trend to increases as the number of fiber layers increase. It is also noticed that, the sequence of fiber-angle layers does affect to the loads. I case of 2 layers hybrid tube, the values of P_{mean} and P_{max} are higher when put 0 degree fiber is inside and 90 degree fiber at outside. The load values are dropped when using the same fiber degree at both layers, i.e. [0/0] or [90/90]. In case of 3 layers of fiber, it is found that by putting 90 degree fiber at outside gives values of P_{mean} and P_{max} higher than those when putting 0 degree fiber at outside. For hybrid tubes with 4 layers, tube with [0/0/90/90] provides highest values of P_{max} and P_{mean}. From those results, it is noticed that by putting 90 degree fiber at outside combined with 0 degree fiber at inside can give higher values of P_{mean} and P_{max}. This because, the 0 degree fiber helps to resist axial impact load while the 90 degree fiber helps supporting the inner layer and keep them stick with AL tube. This combination pattern could improve the capacity of hybrid tube significantly.

It is interesting to make a discussion on the behavior of tubes with [90/90/0/0] and [0/0/90/90], comparatively. Those combination are preferable choice, better than the [0/0/0/0]. However, by putting 90 degree fiber in the outside layers is the most efficient pattern. This is because for [90/90/0/0], when it is under goes impacted, the two inner fiber layers (90 degree) are broken in pieces while the 2 outer layers (0 degree) are laminar bending and spring out from the tube. In this phenomenon, the fiber layers are not able to pack together and fall-off from AL tube. In contrast, the hybrid tube with [0/0/90/90] fails in different way. The two inner layers (0 degree) are in charge for resisting of axial impact while the two outer layers (90 degree) are in charge for supporting those two inner fiber layers and keep them in place and push the broken pieces to be inserted in between AL lobes. Hence, the value of loads can be promoted by this mechanism.

The comparison of results from Exp and FEA as showed in Figure 4.8 (b) are quite acceptable, they are about 1%-9% except values of specimen with [0/90/90] which the discrepancy of P_{max} and P_{mean} of are 23.43 % and 20.38% respectively.

4.2.5 Energy absorption capacity

The energy absorption capacity of the hybrid tubes are showed in Figure 4.8 (d). It must be noted that the energy absorption value in this thesis is approximated by the mean load times collapse stroke of each tube. It is noticed that the energy absorption of naked AL tube and 1-layer hybrid tube are not much different. The effect of layers is obviously noticed in 2-layer, especially in 3- and 4-layers hybrid tubes. Similar to the result and discussion about P_{mean}, the hybrid tube with 90 degree fiber in the outer layers i.e. [0/90/90] and [0/0/90/90] trend to provide higher value of energy absorption compares to other sequences. This is due to the failure mechanism as explained earlier.

4.3 Observation results of hybrid tube with diameter of 30.48 mm

The specimen is aluminum tube wrapped with GFRP having diameter of 30.48 mm, thickness of 1.2 mm and 100 mm long. The GFRP is E-glass/Polyester resin with 1, 2, 3 and 4 layers wrapped with different angles and sequences as showed in Table 1.2, Chapter 1.

4.3.1 Load response of the specimen

The response of the specimens can be presented in form of load-time curves as showed in Figure 4.9. In the beginning of process, the curve is rising sharply and then fluctuating up and down in wavy shape until the end of the process. As can be seen from Figure 4.9 that the load-time curve is fluctuating in a wavy-shape, corresponding to the formation of failure lobes. It is observed that the curves of hybrid tubes are generally higher than the curve of aluminum tube. This implies that AL/GFRP hybrid tube can absorb higher energy than naked AL tube. However, the collapse process of hybrid tube is a bit shorter than that of AL tube. It is also noticed that, the fiber orientation angle and stacking sequence of fiber layers also affect to the characteristic of curves.

The FEA technique was used to model the behavior of those tubes under similar condition of experiment. Comparison of the result are showed in Figure 4.10 – 4.13. As can be seen from those Figure that the curves achieved from FEA are in similar pattern and magnitude. In addition, the modes of collapse of tubes from FEA and experiment are also similar. Therefore, it should be summarized that the FEA model used in this study is agreed well with the experiment.

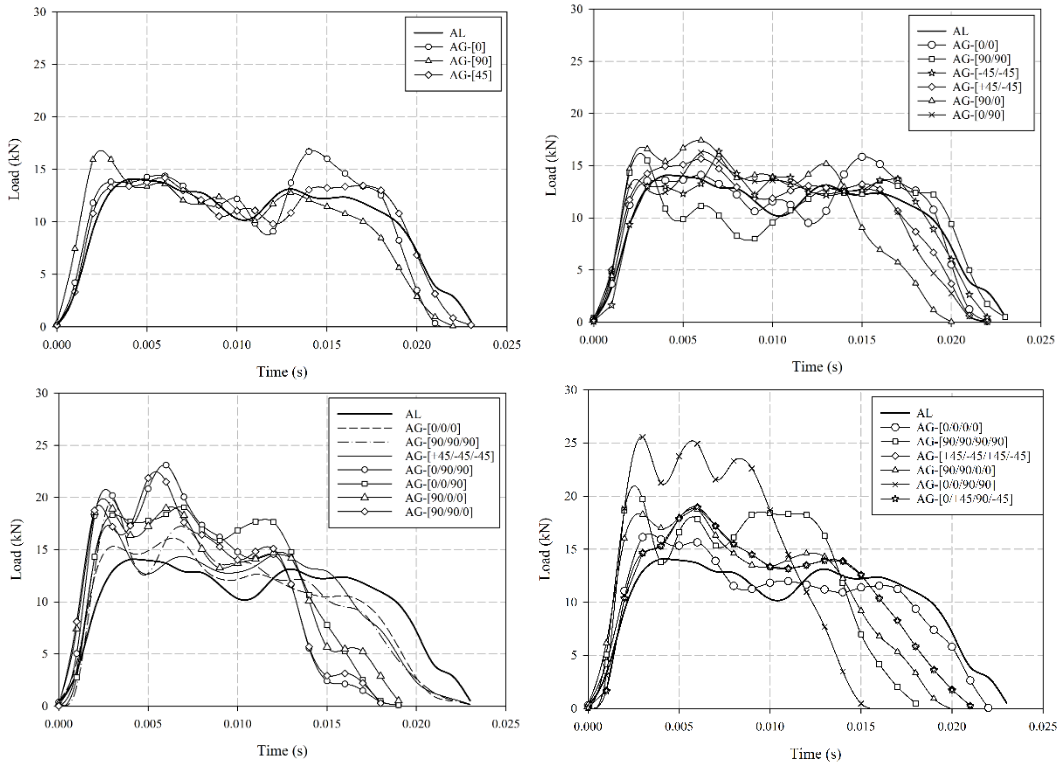

Figure 4.9 Load-time curves of naked AL tube and hybrid tubes of D=30.48 mm, with GFRP of 1, 2, 3 and 4 layers under impact

4.3.2 Mechanism and mode of collapse of the specimen

The collapse mechanism of specimens will be investigated and explained in this section according to the FEA and experimental results showed in Figure 4.10-4.13.

Considering naked AL tube, there are 4 folds of Diamond mode in the top part, but FEA model is failed in the bottom part. In case of hybrid tube with 1-layer, it is failed in Mixed mode and Concertina mode. The Concertina mode occurs in 0 degree fiber tube with 5 folds. While the Mixed mode occurs with tubes of 45 and 90 degree by consisting of 3 concertina rings and 1-2 folds of diamond folds.

The failure mode of 1-layer fiber is found to be Laminar buckling and Fiber breaking modes. The Laminar buckling is found in 0 degree fiber while the Fiber breaking is found for 90 or 45 degree fiber as showed in Figure 4.10.

The failure mode of AL of 2-layer hybrid tube is found be 3 modes, which are Concertina mode, Diamond and Mixed mode. The Concertina mode is found in [0/0] tube, the Mixed mode, which is a combination of concertina rings and 2-diamond folds, is found in [90/90], [+45/-45] and [-45/-45] tubes. The Diamond mode is found for

[0/90] and [90/0] tubes. Considering the GFRP layers, it is found that the Laminar buckling occurs with fiber of 0 degree, while the Fiber breaking is found for fiber with 90 or 45 degree. In case of Local buckling, it is found for [0/90] and Laminar bending is found for [90/0]. Those modes of collapse are showed in Figure 4.11.

For hybrid tube with 3-layer, the AL tube is failed in 3 modes i.e. Concertina, Diamond and Mixed modes. The Concertina mode is found for pure 0 degree tube. The Mixed mode is found in [+45/-45/-45] while the Diamond mode occurs with tube which has 0 degree cross between 90 degree. Considering the fiber layers, there are 4 modes of collapse. They are the Laminar buckling which occurs for [0/0/0], the Fiber breaking occurs for [+45/-45/-45], the Local buckling occurs for hybrid tubes with 0-degree fiber at the inner ([0/0/90] and [0/90/90]) and the Laminar bending happens for [90/0/0] and [90/90/0] which has 0 degree at the outer. The illustration of modes is showed in Figure 4.12.

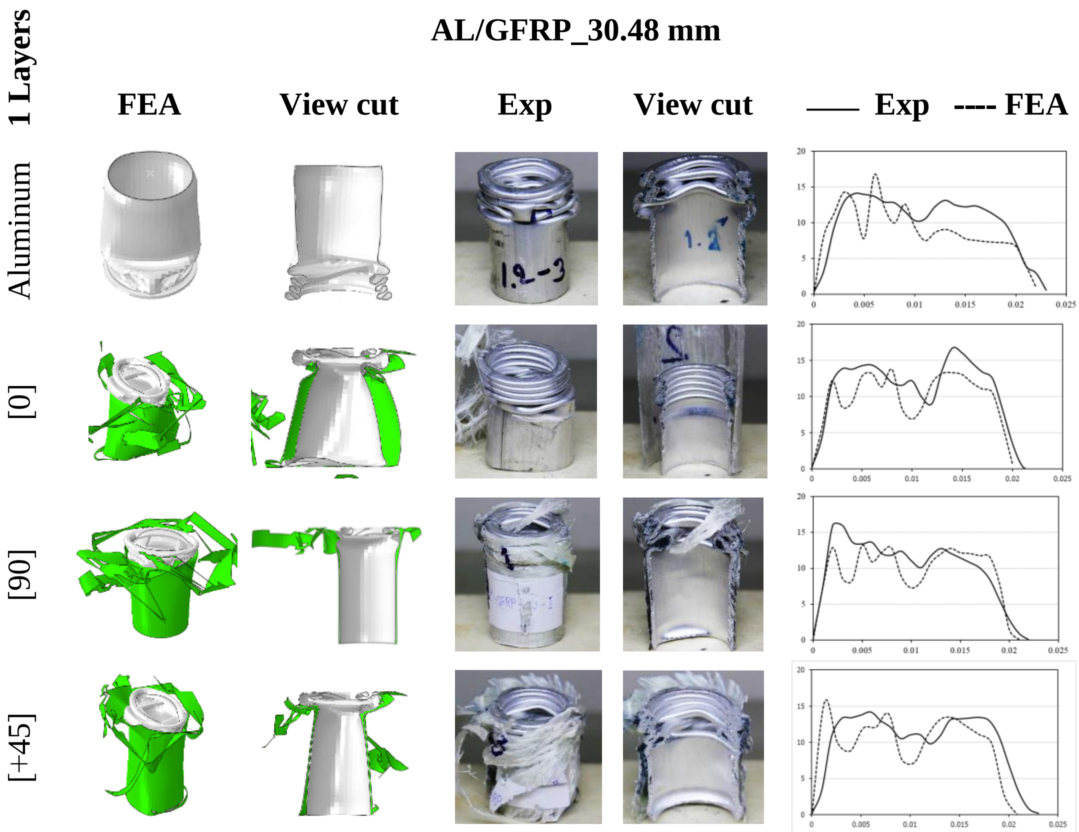

Figure 4.10 Failure mode of 30.48 mm diameter hybrid tube with 1 layer of GFRP

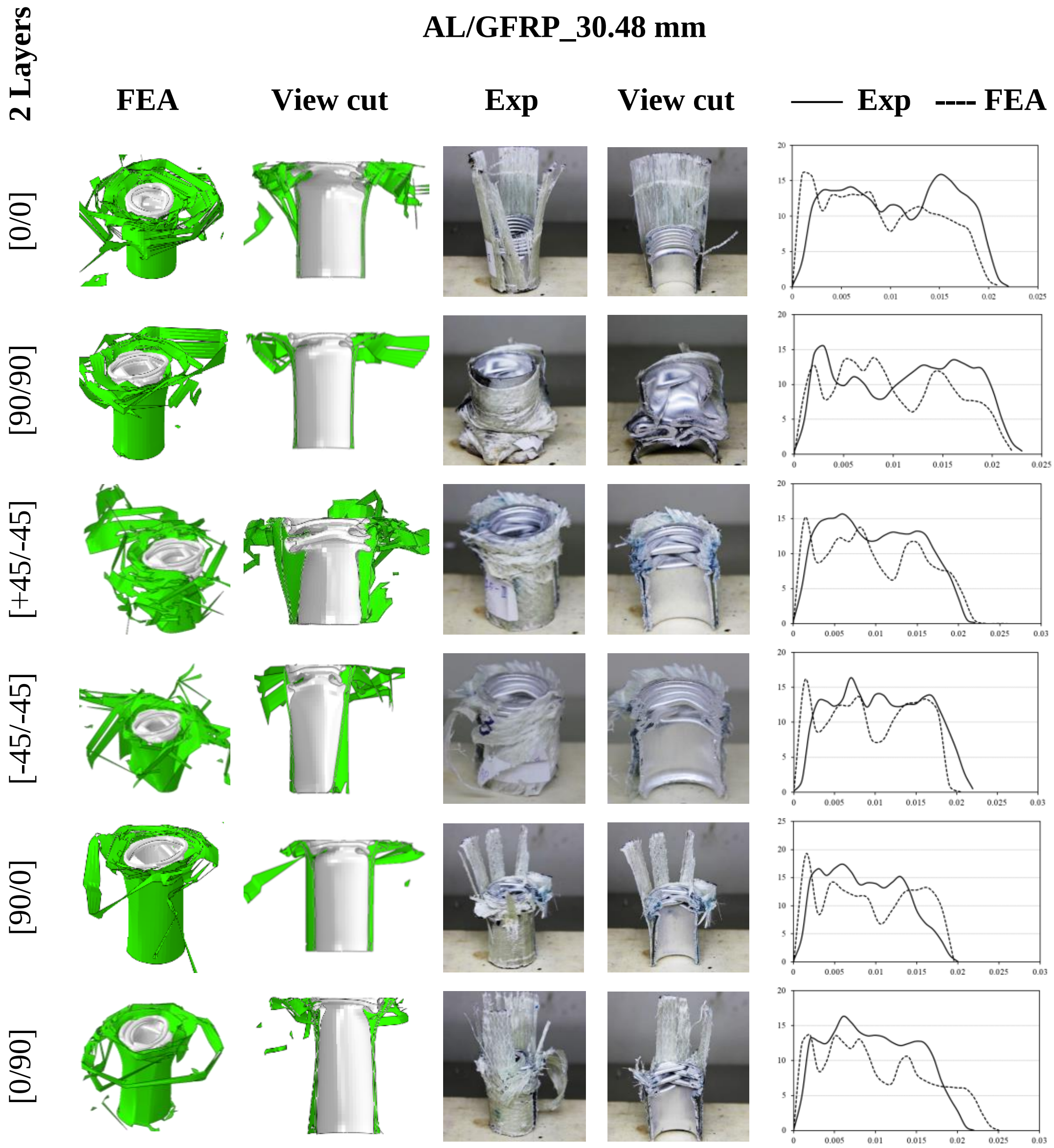

Figure 4.11 Failure mode of 30.48 mm diameter hybrid tube with 2 layers of GFRP

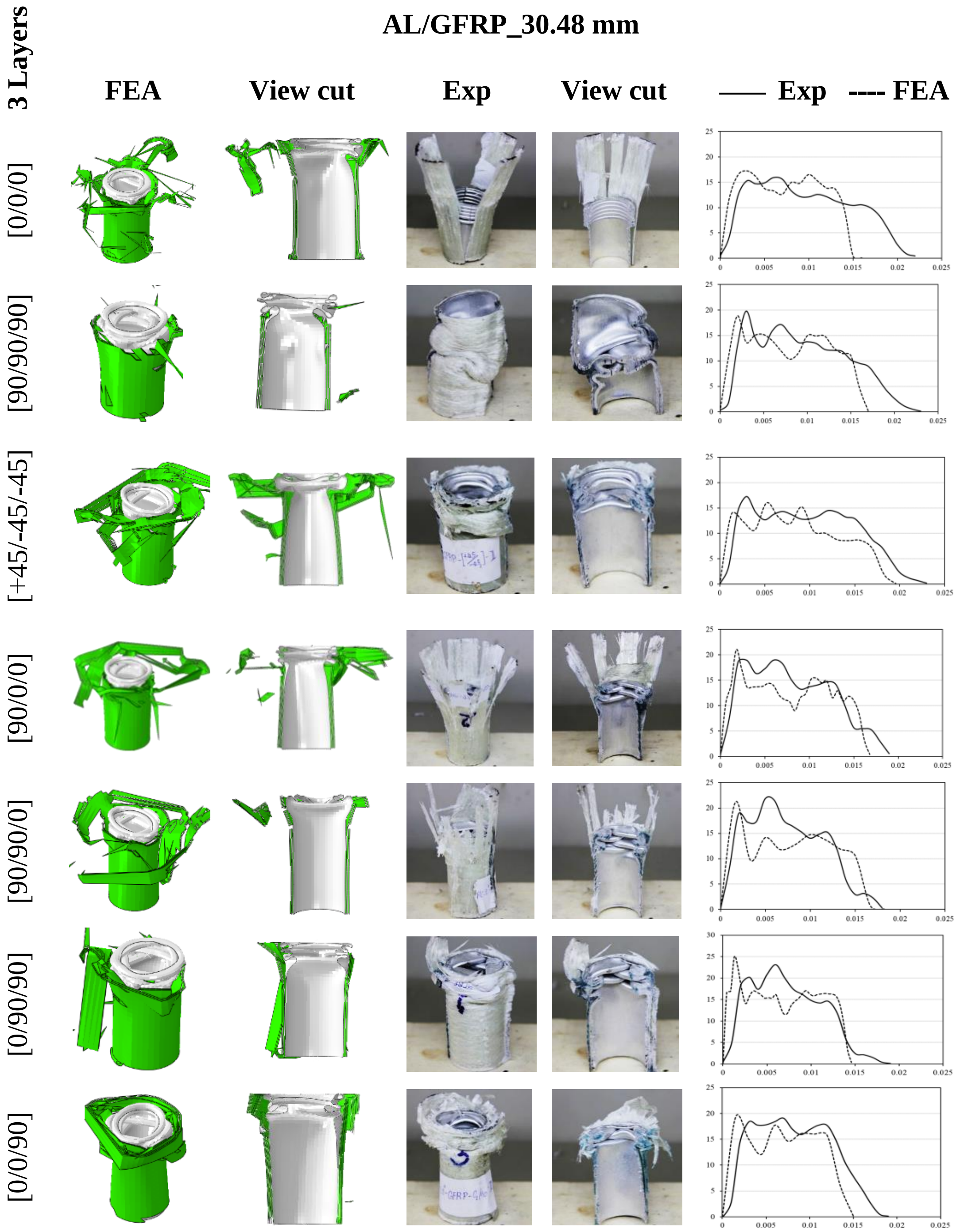

Figure 4.12 Failure mode of 30.48 mm diameter hybrid tube with 3 layers of GFRP

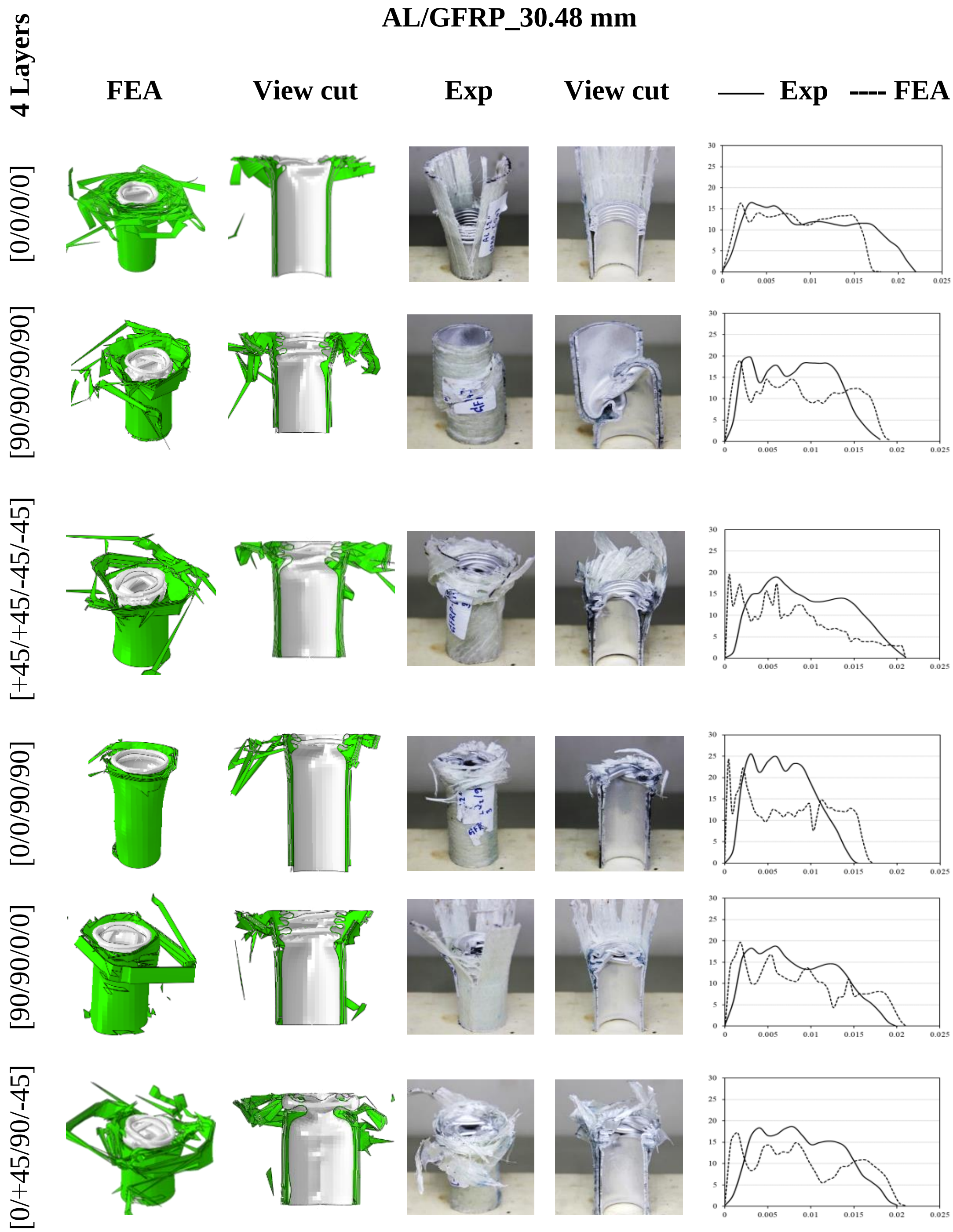

Figure 4.13 Failure mode of 30.48 mm diameter hybrid tube with 4 layers of GFRP

Considering hybrid tube with 4-layer, the AL tube is failed in Concertina, Diamond and Mixed modes. The Concertina mode of 5-ring occurs for pure 0 degree tube. The Mixed mode is found for [+45/+45/-45/-45] while the Diamond mode is found for [90/90/0/0] and [0/0/90/90]. Looking at the fiber layer, the [0/0/0/0] fiber is failed in Laminar buckling while the Fiber breaking is found for [+45/+45/-45/-45]. The [0/0/90/90] fiber is found to failed in 2 modes i.e. the Local buckling occurs for 0 degree fiber in 1st and 2nd layers followed by the Fiber breaking in the 3^{rd} and 4^{th} layer of 90 degree. In case of [90/90/0/0] fiber, it failed in Fiber breaking for 90 degree fiber and failed in Laminar bending for 0 degree fiber. Lastly, for the [0/+45/90/-45] tube, the 0 degree fiber failed in Local buckling while the rest is failed in Fiber breaking. Figure 4.13 shows mode of collapse of those tubes.

4.3.3 Maximum load and mean load

Figure 4.14 (a) shows maximum load of AL tube and hybrid tubes with 1, 2, 3 and 4 GFRP layers. It is observed that, the maximum load is increasing as number of layers increases, especially for hybrid tube with 2 and 3 layers. In general, the fiber with angle of 0 degree can efficiently resist axial impact load but it needs to have other fiber angle to support and keep them with AL tube. Therefore, tube with [0/90/90] and [0/0/90/90] trend to offer higher maximum load. This is because the interaction of those fiber orientations as explained. Considering the mean load in Figure 4.14 (a), it is observed that hybrid tubes with GFRP fiber provide higher mean load compared to naked AL tube and it is increased as number of layers is increasing. However, the 1 layer of fiber does not increase mean load much on AL tube, no matter what angle it is. In case of 2, 3 and 4 layers GFRP tubes, the mean load is significantly increased for tubes with fiber layers that are angle cross between such as [0/90] and [0/0/90/90]. In that pattern of fiber, the inner-layer 0 degree fiber is responsible for resist the impact load while the outer-layers 90 degree fiber helps supporting the inner fiber and keep them stick with AL tube as well as push the broken fiber pieces in between AL lobes. As the result of this mechanism, the mean load is enhanced. The mean load and maximum load of hybrid tube of 45 degree are plotted in Figure 4.14 (c) and is noticed that 45-degree fiber does not have significant effect to mean load, no matter how many layers there is.

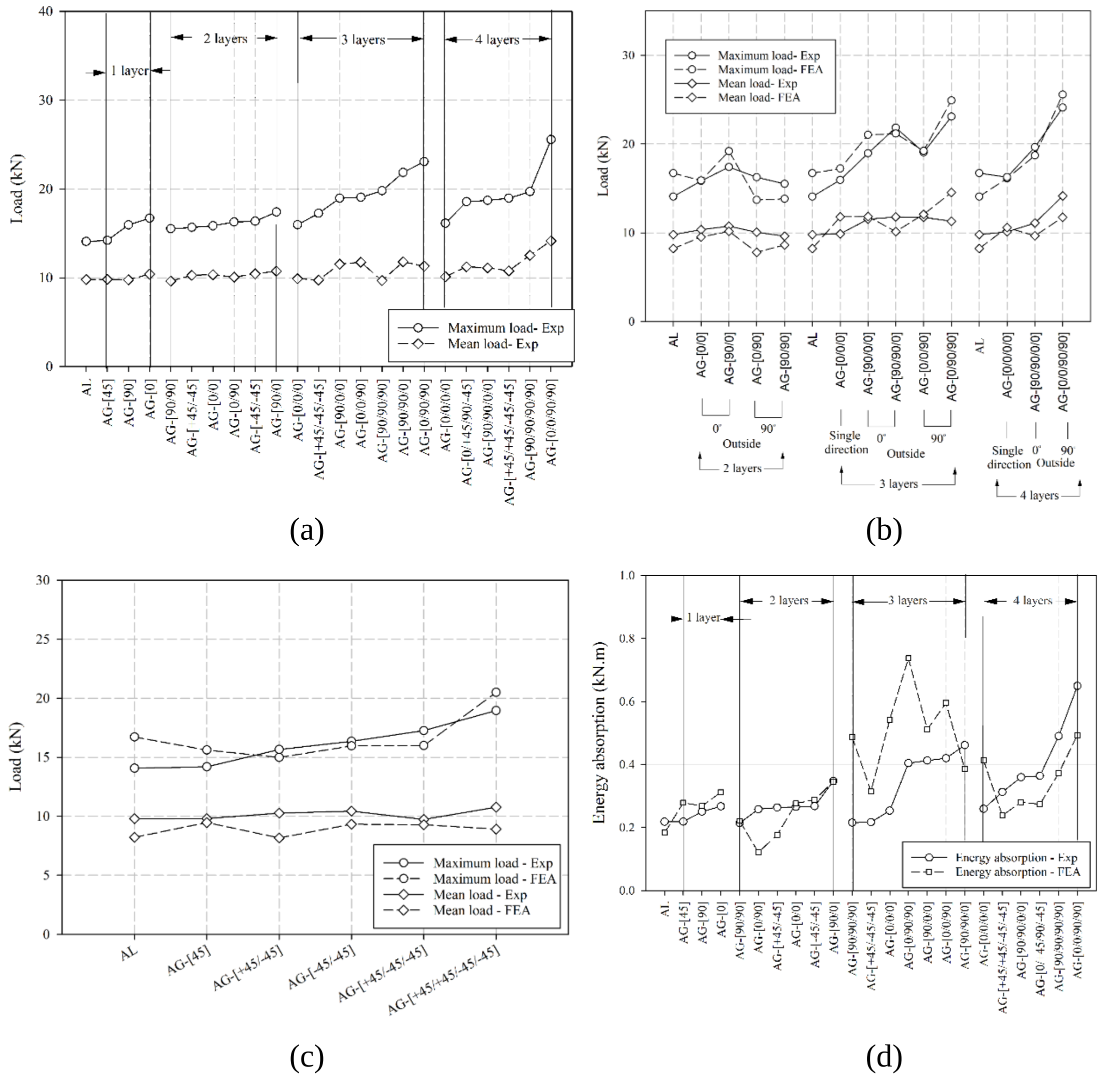

Figure 4.14 Mean and maximum loads of AL and hybrid tubes of D=30.48 mm, (a) results of all experimental specimens (b) results from specimens with 0 and 90 degree (c) results from specimens with 45 degree (d) energy absorption

4.3.4 Influence of stacking sequence

From the result in Figure 4.14 (b) and from the discussion earlier, it can be noticed that the sequence of fiber angle does have effect on crashworthiness of hybrid tubes. The values of P_{max} and P_{mean} are observed to be higher for tubes with fiber of 0 degree as inner layers and 90 degree as outer layers such as [0/90/90] or [0/0/90/90 as example. This is because the failure mechanism as explained earlier. It is also interesting to make a comparison between tubes of [90/90/0/0] and [0/0/90/90]. As can be seen that the [90/90/0/0] tube provide not very high value of loads because the inner-fiber of 90 degree failed in Fiber breaking while the outer-fiber of 0 degree failed in Laminar bending and spring out from specimen. In this circumstance, the outer fiber cannot support and keep the whole fiber together, so higher value of loads cannot be expected. This mechanism is in contrast with the [0/0/90/90] tube, which the inner 0 degree fiber failed in Local buckling and the outer 90 degree help to support them before breaking. Therefore, the [0/0/90/90] tube provides maximum value of mean loads. The comparison between experiment and FEA model found to be in the same trend, although the value of loads may be quite different in some cases.

4.3.5 Energy absorption capacity

The energy absorption of specimens are plotted in Figure 4.14 (d). It is noticed that the energy absorption of naked AL tube and hybrid tube with 1 layer are not much different. However, it is going higher for 3 and 4 layers hybrid tube. The result reveals that [90/90/0] and [0/0/90/90] tubes trend to absorb higher energy than other tube because of mode of collapse as well as the influence of layer number.

4.4 Observation results of hybrid tube with diameter of 38.10 mm

The specimen is aluminum tube wrapped with GFRP having diameter of 38.10 mm, thickness of 1.2 mm and 100 mm long. The GFRP is E-glass/Polyester resin with 1, 2, 3 and 4 layers wrapped with different angles and sequences as showed in Table 1.2, Chapter 1.

4.4.1 Load response of the specimen

The response of the specimens can be presented in form of load-time curves as showed in Figure 4.15. As can be seen that the load-time curve is fluctuating in a wavy-shape, corresponding to the formation of failure lobes. It is observed that the curves of hybrid tubes are generally higher than the curve of aluminum tube. This implies that AL/GFRP hybrid tube can absorb higher energy than naked AL tube. However, the collapse process of hybrid tube is a bit shorter than that of AL tube. It is also noticed that, the fiber orientation angle and stacking sequence of fiber layers also affect to the characteristic of curves.

The comparison of results from FEA and experiment are showed in Figure 4.16 - 4.19. It is observed that those results are in the same trend and agree well. The failure modes from FEA are also similar to the experiment.

4.4.2 Mechanism and mode of collapse of the specimen

The collapse mechanism of this specimens will be investigated and explained in this section according to the FEA and experimental results showed in Figure 4.16-4.17. The naked AL tube is found to failed in Diamond mode with 4-folds. This is in similar modes for both experiment and FEA model. Considering the hybrid tube with 1-layer fiber, the AL tube failed in Concertina and Diamond mode. The in 5 rings of Concertina mode occurs in hybrid tube of 0 degree, while the Diamond mode occurs for hybrid tube with 90 degree. Considering the fiber layers of this hybrid tube, it fails in 2 modes, Laminar buckling and Fiber breaking mode. The Laminar buckling is found for 0degree fiber, while the Fiber breaking is found in 90 and 45 degree fiber. Figure 4.16 illustrates those mode of collapse.

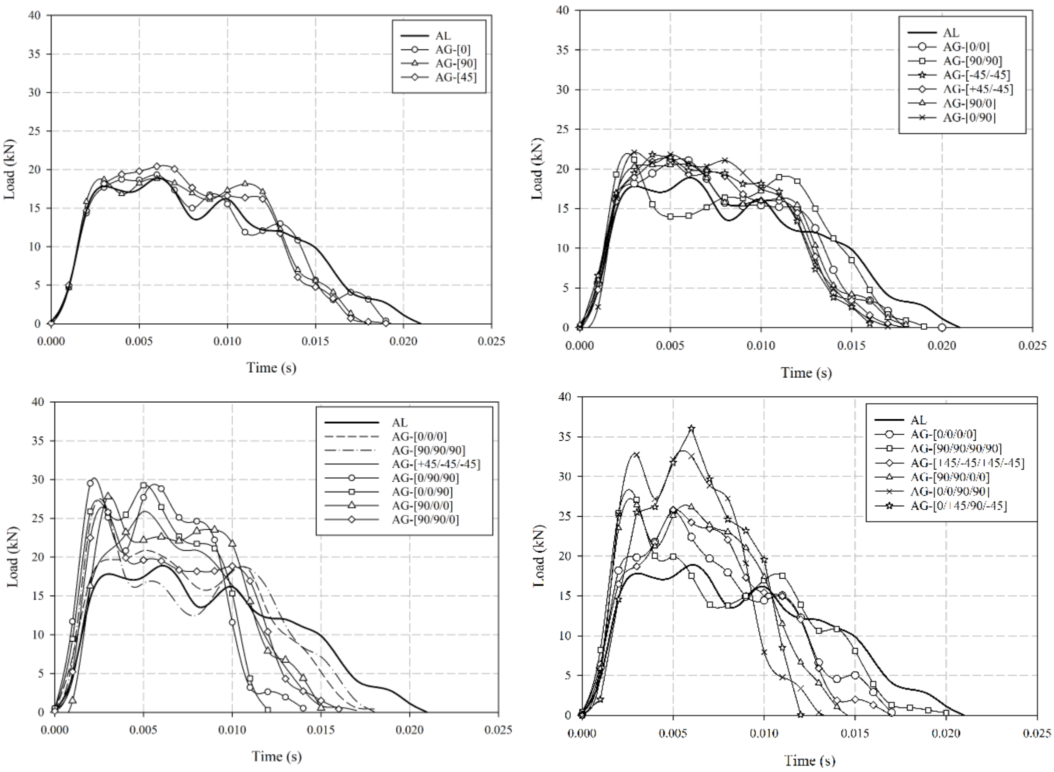

Figure 4.15 Load-time curves of naked AL tube and hybrid tubes of D=38.10 mm, with GFRP of 1, 2, 3 and 4 layers under impact

The hybrid tube with 2-layer fiber, the AL tube failed in Diamond and Mixed mode. The Diamond mode occurs for tubes which have fiber of 45 or 90 degree taking part. The Mixed mode is found for 0 degree tubes with 2 rings of Concertina and 2 fold of Diamond mode. The failure mode of GFRP layers, it fails in Laminar buckling for pure 0 degree fiber. The Fiber breaking is found for tube with fiber of 90 or 45 degree. The Local buckling is found in tubes of [0/90] while the Laminar bending is found for [90/0] tube. Illustration of collapse mode is in Figure. 4.17.

For hybrid tube with 3 GFRP layers, The AL tube is failed in Concertina and Diamond. The Concertina mode occurs for 0 degree fiber, while the Diamond mode is found in tubes with combination of 45 and 90 degree fibers. Considering the fiber layer, it fails in Laminar buckling for [0/0/0] tube. The Fiber breaking is found for [+45/-45/-45] in which some of the broken pieces of fiber is inserted in between AL folds. The Local buckling is found in [0/0/90] and [0/90/90] tubes which 0 degree fiber is in the inner layer. The Laminar bending is found in [90/0/0] and [90/90/0] tubes which the 0 degree fiber in outside. The mode of collapse of these tubes are in Figure 4.18.

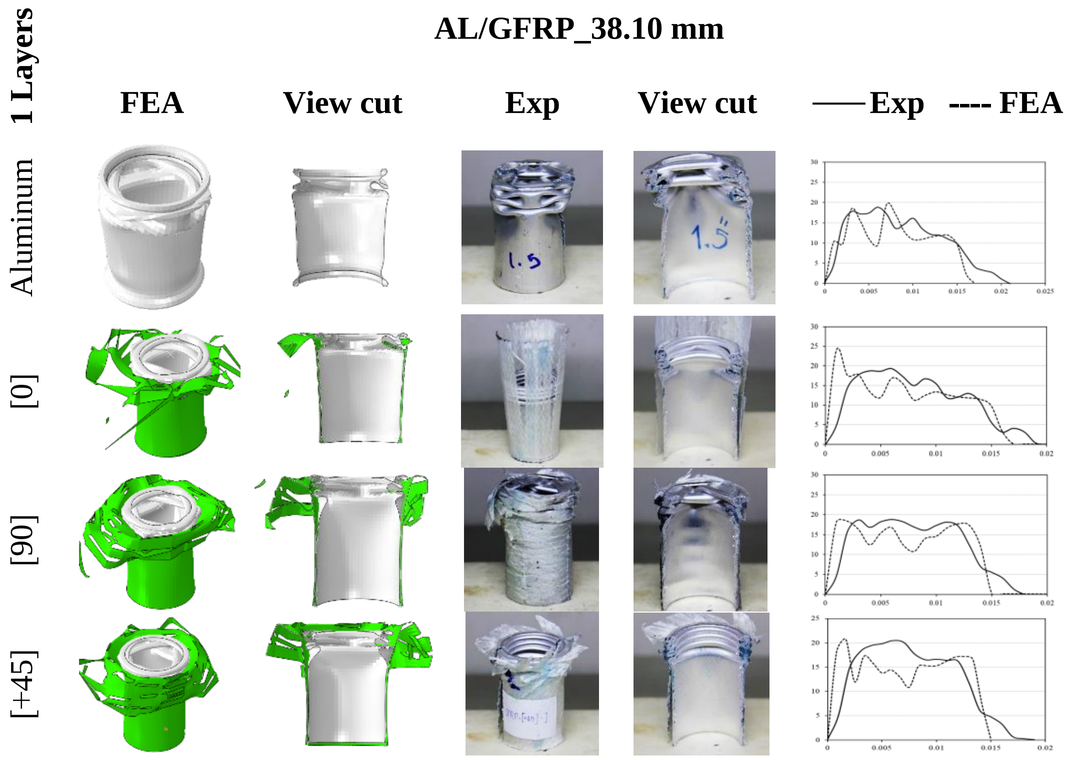

Figure 4.16 Failure mode of 38.10 mm diameter hybrid tube with 1 layer of GFRP

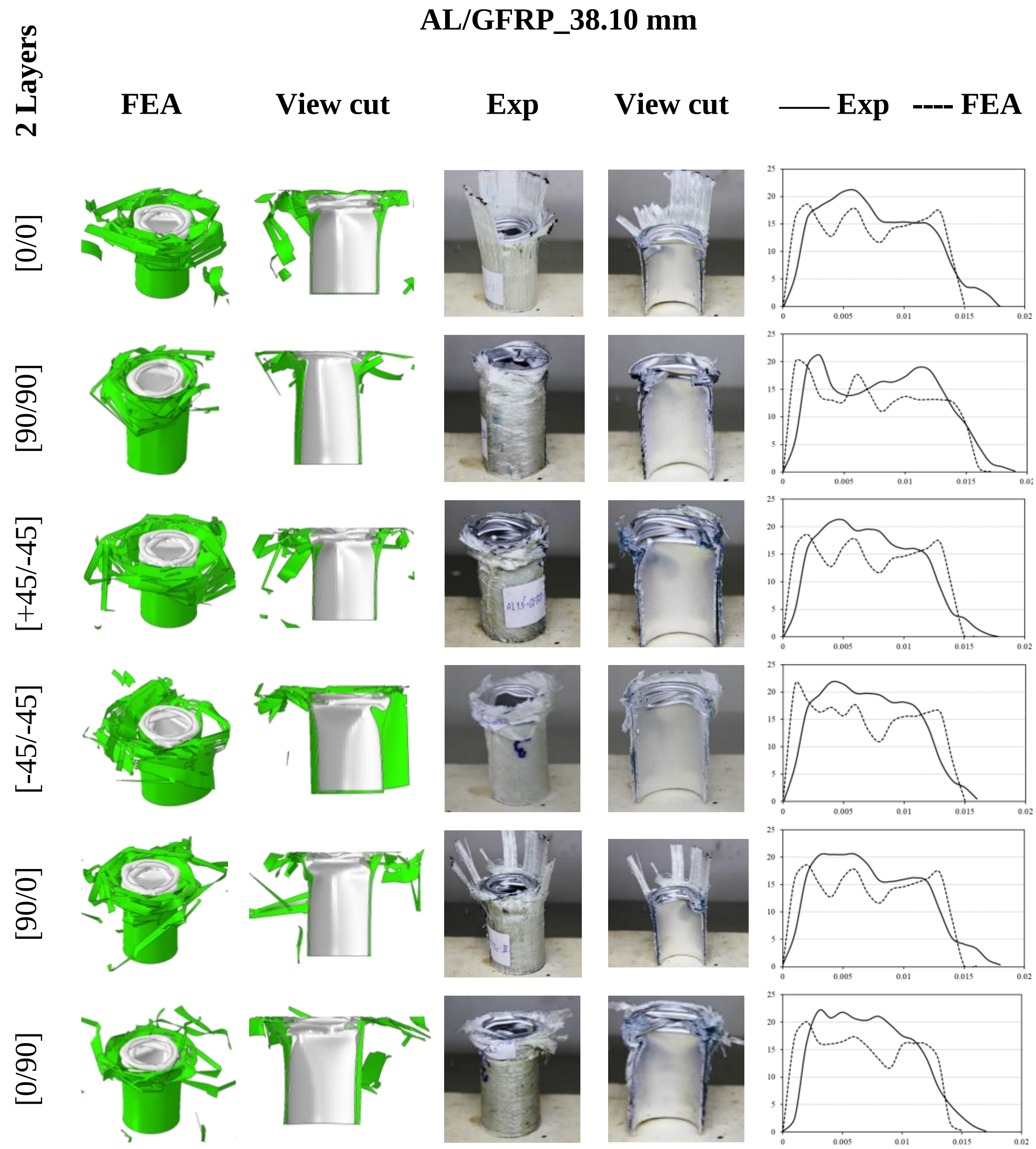

Figure 4.17 Failure mode of 38.10 mm diameter hybrid tube with 2 layers of GFRP

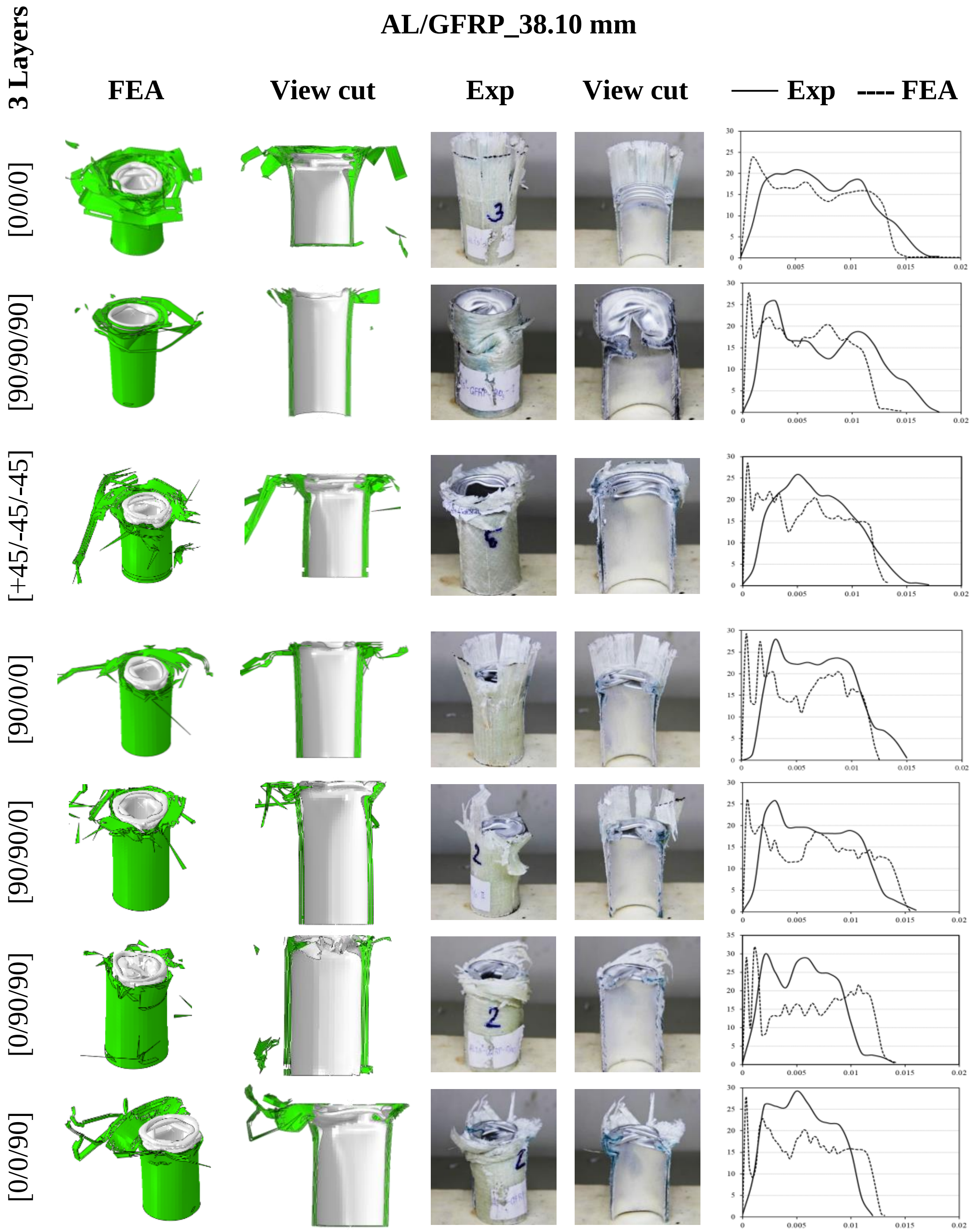

Figure 4.18 Failure mode of 38.10 mm diameter hybrid tube with 3 layers of GFRP

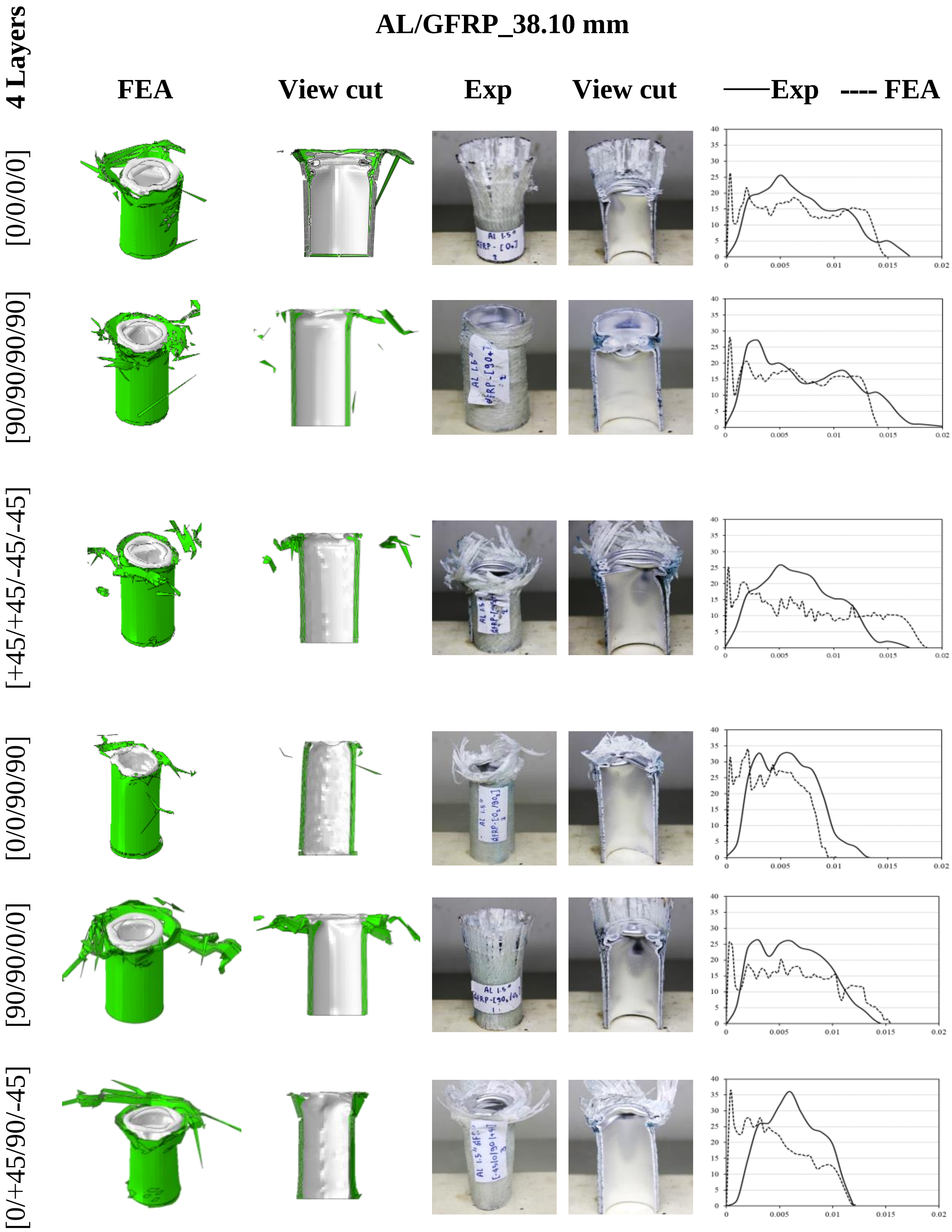

Figure 4.19 Failure mode of 38.10 mm diameter hybrid tube with 4 layers of GFRP

For hybrid tube with 4 GFRP layers, The AL tube is failed in Diamond for tubes of [90/90/0/0] and [0/0/90/90]. Considering the fiber parts, the Laminar buckling is found for [0/0/0/0] while the Fiber breaking is occurs in [+45/+45/-45/-45] tube. In case of [0/0/90/90] tube, it fails in 2 modes which are Local buckling occurs in 0 degree of fiber in 1^{st} and 2^{nd} layers, while the Fiber breaking occurs in the 3^{rd} and 4^{th} fiber layers with 90 degree. In case of [90/90/0/0] tube, the Fiber breaking is found for 90 degree fiber of 1^{st} and 2^{nd} layers and inserted in between AL folds, while the 3^{rd} and 4^{th} fiber of 0 degree are failed in Laminar bending. In case of [0/+45/90/-45], the 0 degree fiber fails in Local buckling followed by the fiber breaking in 2^{nd} – 4^{th} fiber layers. The Figure of failure modes are showed in Figure 4.19.

4.4.3 Maximum load and mean load

Figure 4.20 (a) shows maximum load of AL tube and hybrid tubes with 1, 2, 3 and 4 GFRP layers. It is observed that the [0/0/90] offer high value of maximum loads. This is due to the 2 inside layers of 0 degree help resist impact load and the outer layer of 90 degree help support them to stick with AL tube. The combination pattern of [0/+45/90/-45] tube also provide high value of maximum load compared to naked AL tube. Considering the mean load in Figure 4.20 (a), it is observed that the value of mean load is increasing as the number of layers increases. Similar to prior discussion, hybrid tube with 1 GFRP layer does not have significant increment in mean load. For hybrid tube with 2, 3 and 4 layer, the mean load increases significantly when the fiber angles are changing layer by layer such as [0/90]. It is also noticed from Figure 4.14 (c) that the fiber of 45 degree does not provide significant improvement for maximum or mean load.

4.4.4 Influence of stacking sequence

From the result in Figure 4.20 (b) and from the discussion earlier, it can be noticed that the sequence of fiber angle does have effect on crashworthiness of hybrid tubes. In case of 2-layer fiber tube, the value of P_{max} and ค่า P_{mean} are high for tube with [0/90].

For 3- and 4-layer of hybrid tubes, it is found that by putting 90 degree of fiber in the outside layer help promoting P_{max} and P_{mean} more than tube wit 0 degree at outside. So, the combination of 0 degree and 90 degree in these pattern i.e. [0/90/90], [0/90/90/90] or [0/0/90/90] may be recommended. The mechanism of failure of these tubes has been explained and discussed earlier. The comparison of [90/90/0/0] tube and [0/0/90/90] tube can reveal the effect of stacking sequence obviously. The [0/0/90/90] tube, which 2-layer of 90 degree fiber is outside and 2-layer of 0 degree in inside, provides higher value of mean load and maximum load because the 0 degree fiber absorbs impact load and break while the 90 degree fiber try to strap and support them in place. As the result the majority of structure is still in shape while the broken pieces are pushed in between AL folds. In contrast, the [90/90/0/0] tube is failed in different manner. The 90 degree is failed in Fiber breaking and the 0 degree fiber, which is outside, is failed in Local bucking and fall off from the whole structure. As the result, the whole structure cannot be stay packed and cannot deliver higher mean load.

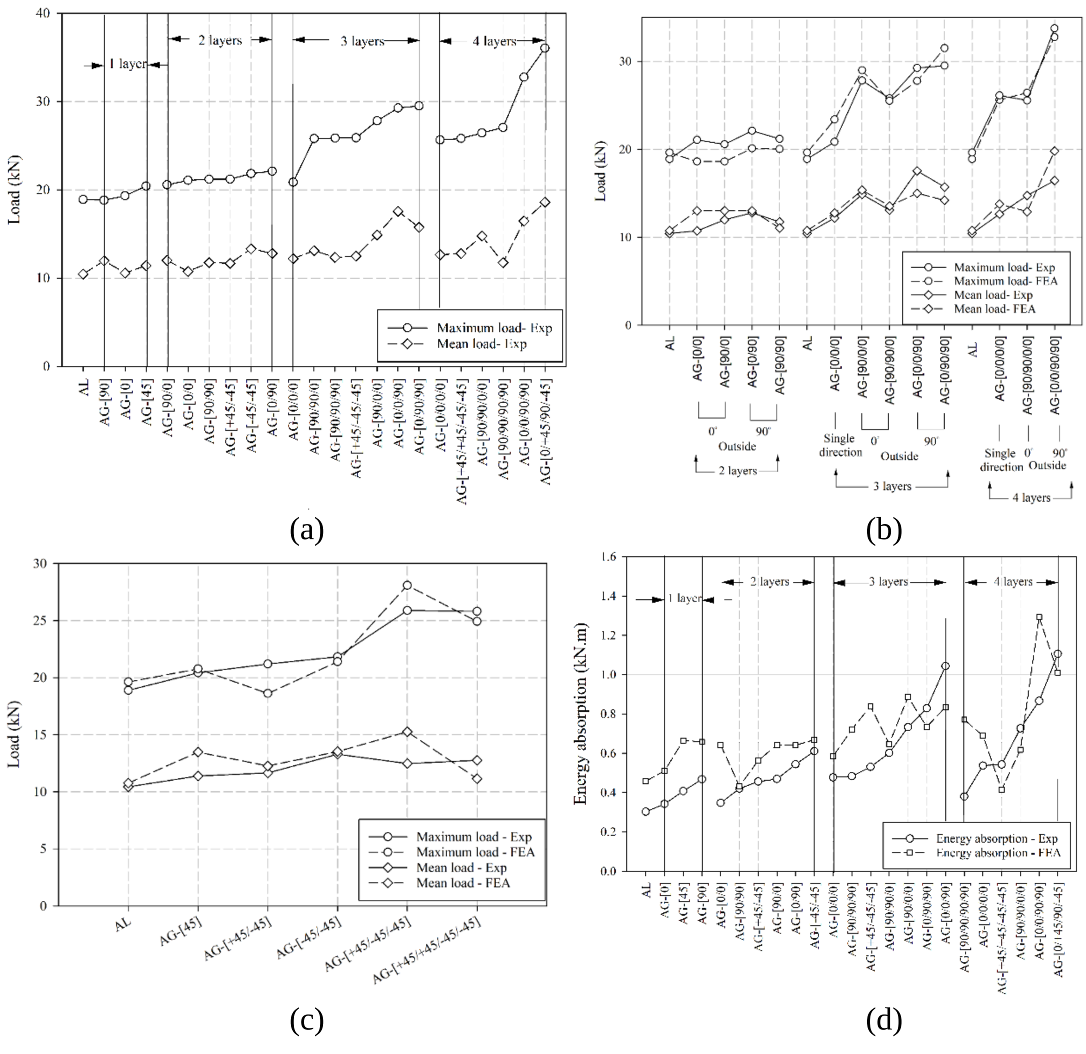

Figure 4.20 Mean and maximum loads of AL and hybrid tubes of D=38.10 mm, (a) results of all experimental specimens (b) results from specimens with 0 and 90 degree (c) results from specimens with 45 degree (d) energy absorption

In addition, the author would like to mention here that the values of P_{max} and P_{mean} achieved from experimental and FEA of these cases are agreed quite well. The discrepancy found is between 2.98% - 16.96% which are quite acceptable.

4.4.5 Energy absorption capacity

The energy absorption of specimens are plotted in Figure 4.20 (d). It is noticed that the energy absorption of naked AL tube and hybrid tube with 1 layer are increased not very much. However, it is going higher for 3 and 4 layers hybrid tube. The result reveals that for the 2-layer tube, the [-45/-45] absorb highest energy. While the hybrid tube of 3 and 4 layer, the [0/0/90], [0/0/90/90] and [0/+45/90/-45] provide high value of energy absorption.

4.5 Observation results of hybrid tube with diameter of 45.72 mm

The specimen is aluminum tube wrapped with GFRP having diameter of 45.72 mm, thickness of 1.2 mm and 100 mm long. The GFRP is E-glass/Polyester resin with 1, 2, 3 and 4 layers wrapped with different angles and sequences as showed in Table 1.2, Chapter 1.

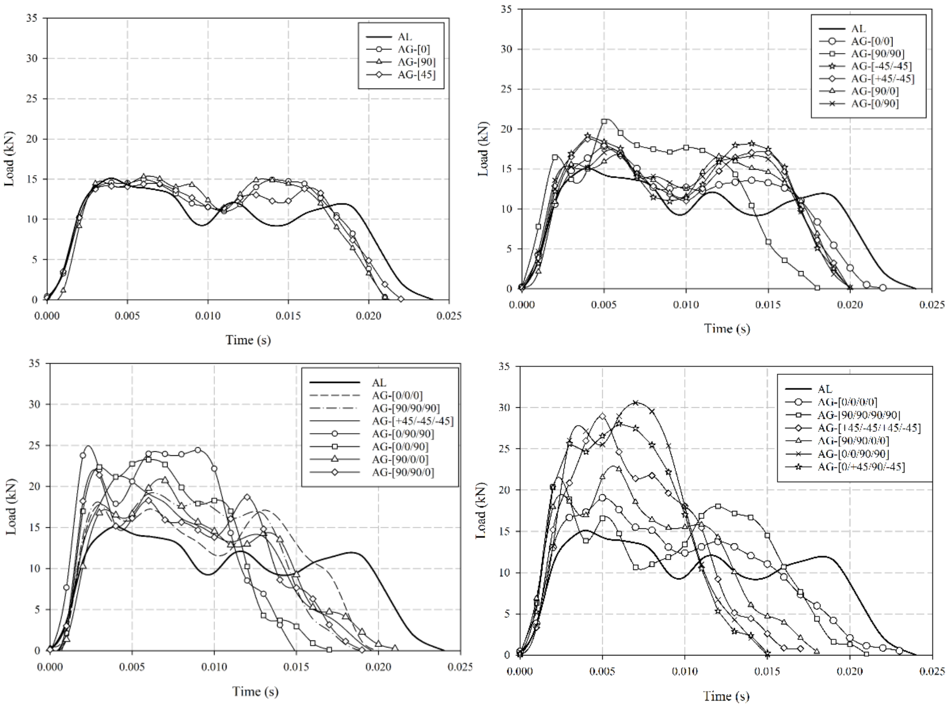

Figure 4.21 Load-time curves of naked AL tube and hybrid tubes of D=45.72 mm, with GFRP of 1, 2, 3 and 4 layers under impact

4.5.1 Load response of the specimen

The response of the specimens can be presented in form of load-time curves as showed in Figure 4.21. As can be seen that the load-time curve is fluctuating in a wavy-shape, corresponding to the formation of failure lobes. It is observed that the curves of hybrid tubes are generally higher than the curve of aluminum tube. This implies that AL/GFRP hybrid tube can absorb higher energy than naked AL tube. However, the collapse process of hybrid tube is a bit shorter than that of AL tube. It is also noticed that, the fiber orientation angle and stacking sequence of fiber layers also affect to the characteristic of curves.

4.5.2 Mechanism and mode of collapse of the specimen

The comparison of results from FEA and experiment are showed in Figure 4.22 - 4.25. It is observed that those results are in the same trend and agree well. The failure modes from FEA are also similar to the experiment.

Mode of collapse of 1-layer GFRP tube are Mixed mode and Diamond mode. The Mixed mode occurs for 0 degree and 45 degree fiber tubes. The Diamond mode occurs for 90 degree fiber tube. The GFRP layer is failed in Laminar bucking for 0 degree fiber, while the Fiber breaking is found in 45 and 90 degree fiber.

In case of hybrid tube with 2 layers, the AL tube fails in Mixed mode and Diamond mode. The Mixed mode is found for pure 0 degree fiber and the Diamond mode found in the combination of 0 and 90 degree fiber. For the fiber layers, it is found that the [90/0] fails in Fiber breaking and laminar bending in the 1st and 2nd layer respectively. The Local buckling is found for [0/90] in which the fiber can insert in between the AL folds. The modes of collapse from FEA and experiment are agreed quite well and they are showed in Figure. 4.23.

For hybrid tube with 3 layers, the AL part is failed in diamond mode with large size of lobe. This is due to the insertion of broken fiber in between the lobe. The mode of collapse of fiber is found in 3 modes, i.e. Fiber breaking, Local bucking and Laminar bending. The fiber breaking occurs for tube which is consisted of 45 and 90 degree fiber. The Local bucking normally happen at 1st and 2nd layers which is in 0 degree. The Laminar bending occurs for the 0 degree fiber in 2nd and 3rd layers. The FEA result of modes agreed well with the experiment and are showed in Figure 4.24.

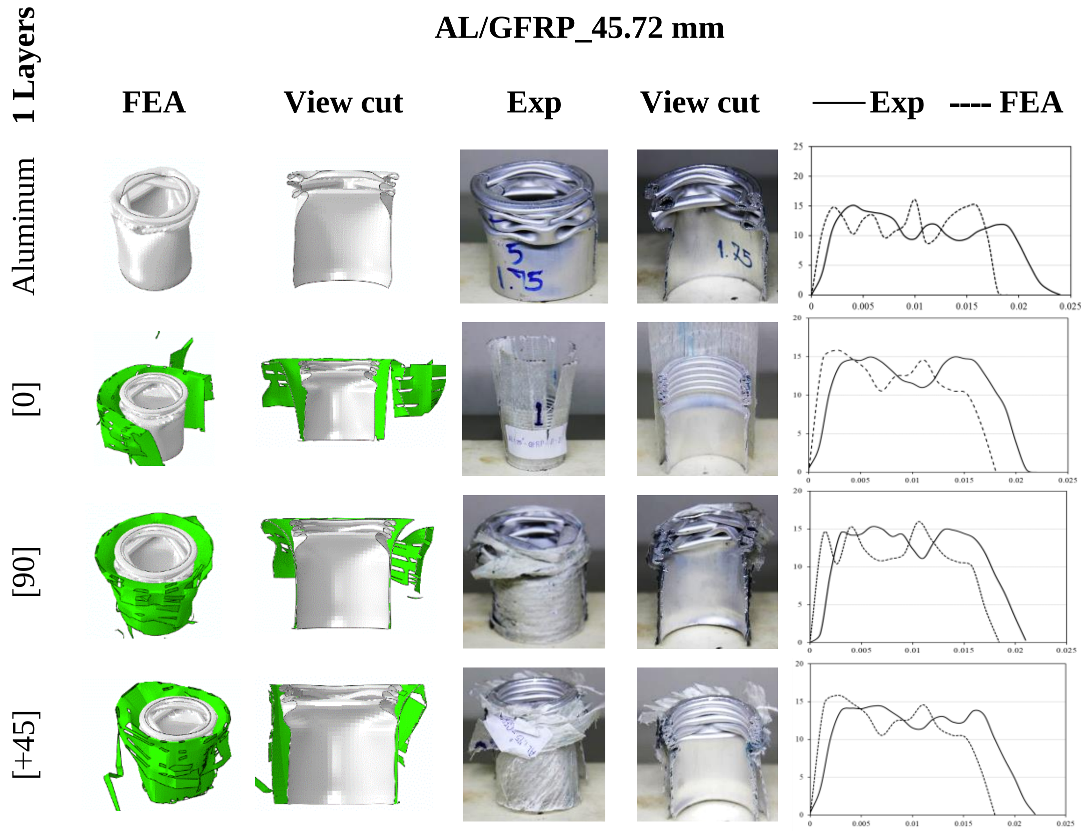

Figure 4.22 Failure mode of 45.72 mm diameter hybrid tube with 1 layer of GFRP

The failure mode of hybrid tube with 4 layers are explained here. AL tubes are failed in Diamond mode for [90/90/0/0] and [0/0/90/90]. Considering the fiber parts, the fiber of [0/0/0/0] fails in Laminar buckling, while the Fiber breaking is observed for [+45/+45/-45/-45]. The tube with [0/0/90/90] fails in Local buckling for 0 degree of 1st and 2nd layers while the Fiber breaking is found in 3rd and 4th layers which are in 90 degree. Tube of [90/90/0/0] fails in Fiber breaking in 90 degree fiber layers and Laminar bending in 0 degree fibers. In case of [0/+45/90/-45], the 0 degree fiber fails in Local buckling followed by fiber breaking in 2nd – 4th layers. Figure 4.25 illustrates mode of collapse of these tubes.

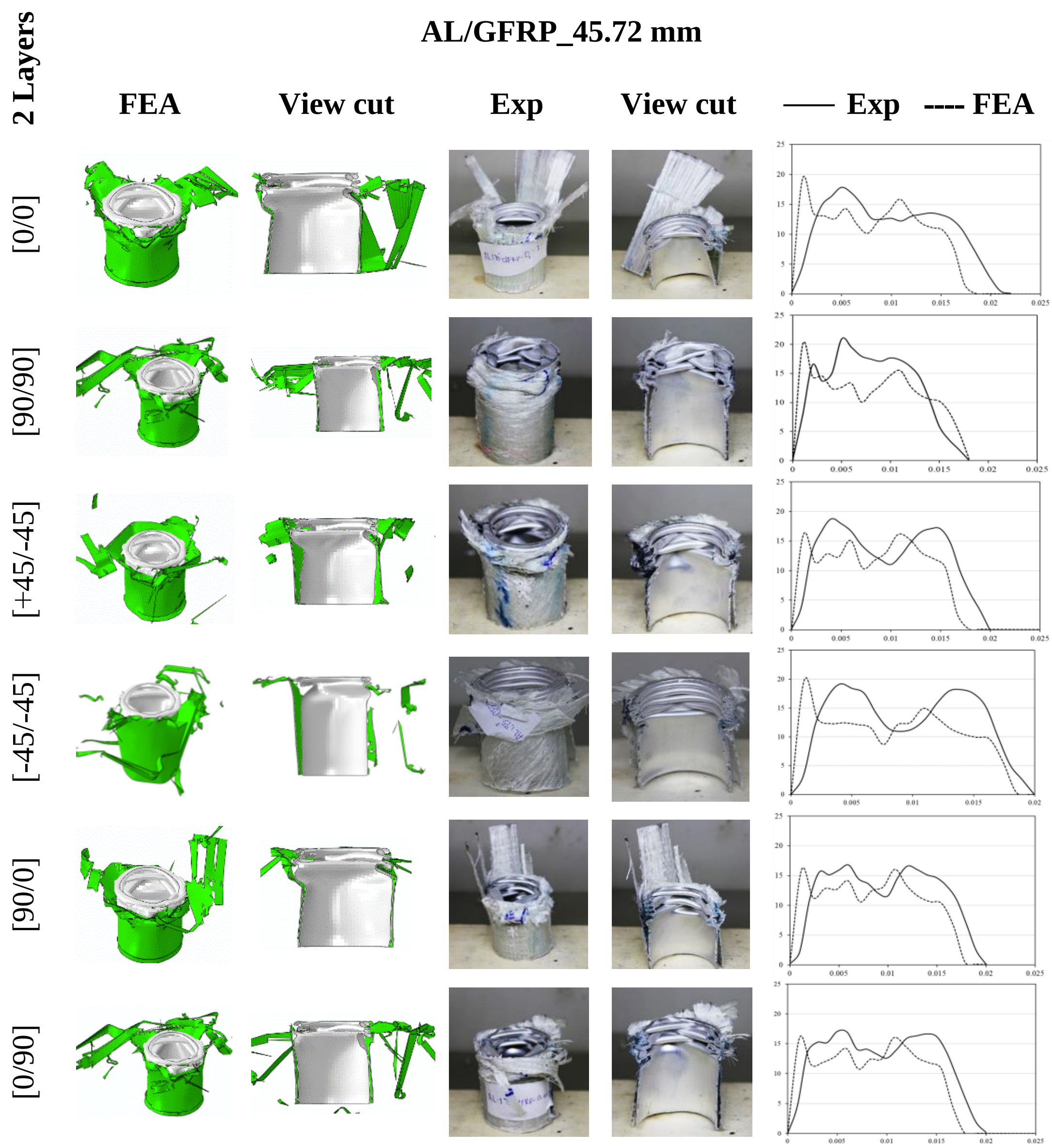

Figure 4.23 Failure mode of 45.72 mm diameter hybrid tube with 2 layers of GFRP

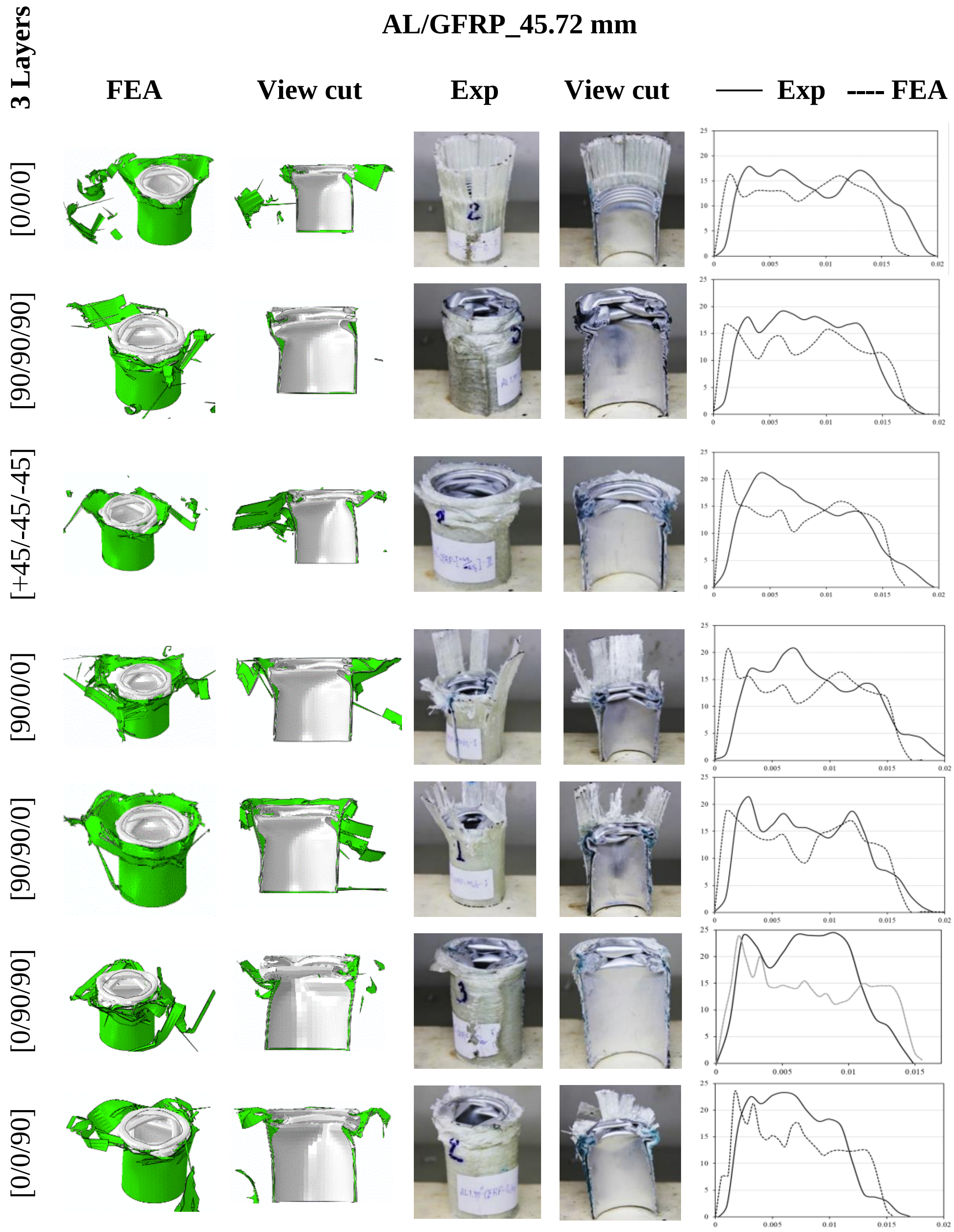

Figure 4.24 Failure mode of 45.72 mm diameter hybrid tube with 3 layers of GFRP

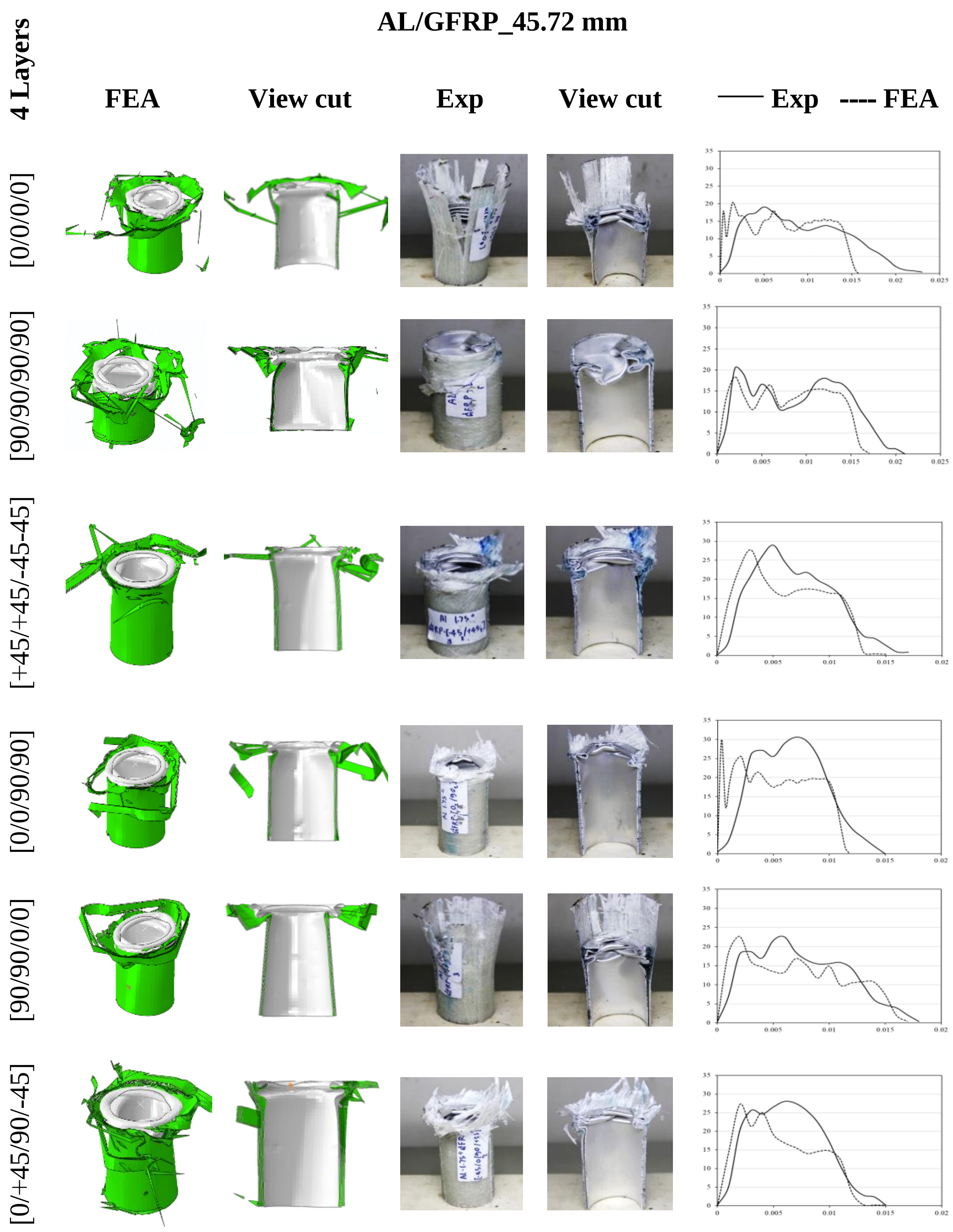

Figure 4.25 Failure mode of 45.72 mm diameter hybrid tube with 4 layers of GFRP

4.5.3 Maximum load and mean load

Figure 4.26 (a) shows maximum load of AL tube and hybrid tubes with 1, 2, 3 and 4 GFRP layers. It is observed that maximum load and mean load of 1 layer hybrid are not much different from naked tube. However, the maximum load and mean load of 2, 3 and 4 layers tubes are increasing significantly as number of layer increases. It is observed that the [0/0/90] and [0/90/90] tube provide high value of maximum load and mean load. The reason is similar to the earlier discussion.

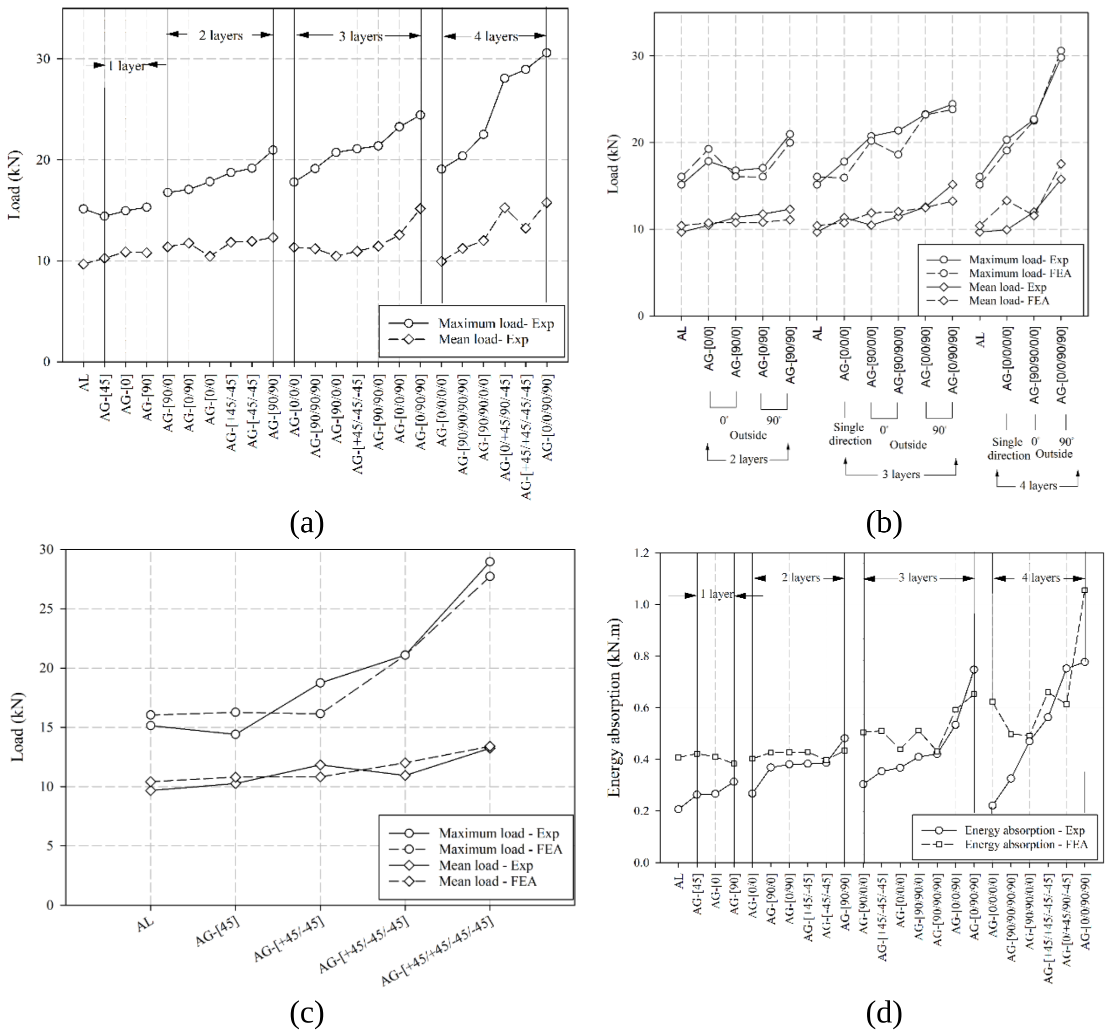

Figure 4.26 Mean and maximum loads of AL and hybrid tubes of D=45.72 mm, (a) results of all experimental specimens (b) results from specimens with 0 and 90 degree (c) results from specimens with 45 degree (d) energy absorption

Focusing on mean load in Figure 4.26 (b), it is increasing as the increment of fiber number. It should be noted that the mean load of hybrid tube with 1 layer in increased only about 1.6% which is considered not significant. For tubes with 2-, 3- and 4-layer, it is also observed that hybrid tubes with 0 degree fiber inside combined with 90 degree outside offer higher value of mean load. This is similar to the previous results and discussions.

4.4.5 Influence of stacking sequence

It is better to noticed here that the 45 degree fiber does not provide influence to P_{mean} significantly, no matter 1, 2, 3 or 4 layers, as can be seen from Figure 4.26 (c). However, it does have influence on P_{max} and value of P_{max} is increasing as number of layers increases. However, the influence of 0 degree and 90 degree are still higher, and shall be focused.

Considering tubes with 0 degree and 90 degree fiber, it is observed that the combination of 0 and 90 degree is better that using single angle alone. The same result is also noticed that by putting 90 degree for outside layers together with 0 degree fiber for inside layer usually give higher value of mean load and maximum load. So, the patterns of [0/90/90], [0/0/90] and [0/0/90/90] are preferable. The pattern of opposite sequence i.e. [90/0/0], [90/90/0] or [90/90/0/0] provide comparative low value of mean load and maximum load, as can be observed in Figure 4.26 (b). In addition, the comparison between FEA model and experiment gives the discrepancy between 2.5%-13.53% and considered well agreement.

4.4.6 Energy absorption capacity

The energy absorption of specimens are plotted in Figure 4.26 (d). It is noticed that the energy absorption of naked AL tube and hybrid tube with 1- and 2-layer are increased not very much. However, the 3- and 4-layer hybrid tube have significant increment in energy absorption compared to naked AL tube. The energy absorption of tube with combination fiber angles trends to be higher than that of single fiber angle. It is observed that these tubes i.e. [0/90/90], [0/0/90] and [0/0/90/90] provide very high energy absorption especially the last pattern is best. In this case, it is interesting to see that the [0/+45/90/-45] also giver high energy absorption.

CHAPTER 5
CONCLUSIONS AND RECOMMENDATIONS

5.1 Conclusions

This research investigated the behavior of hybrid AL/GFRP tubes under axial impact. Mode of collapse and collapse mechanism of GFRP fiber as well as some crashworthiness parameters are investigated in detail. The conclusions may be made as follow.

5.1.1 Mode of collapse of AL tube found in this study are Concertina mode, Diamond mode and Mixed mode. The formation of each mode is affected by dimension of tube, fiber angle of GFRP, stacking sequence and number of layers.

5.1.2 Mode of collapse of fiber can be classified in 4 modes which are Lamina buckling, Fiber breaking, Local buckling and Laminar bending

The laminar buckling mode, it fails by the outer fiber is buckled, bended outward and totally separated from aluminum tube. The fiber breaking mode, in this mode, the fiber is broken in pieces, some are inserted between the folds of aluminum while some are torn out from the aluminum tube. The local buckling mode, the fiber is buckling in a limited area adjacent to the impact hammer and inserted in between the folds. The laminar bending mode, fiber adjacent to the impact hammer is broken and bended outward from AL tube.

5.1.3 By wrapping of GFRP on AL tube, so called hybrid tube, can enhance the crashworthy of the tube. However, the 1-layer hybrid tube is not recommended since the influence of GFRP layer is too small and cannot improve crashworthiness capacity of AL tube significantly. The influence of GFRP is obviously seen for 2-, 3- and especially for 4-layer of GFRP.

5.1.4 The crashworthiness behavior of hybrid tube is directly affected by number of fiber layers, fiber angle and the stacking sequence of fiber layers.

5.1.5 In general, the maximum load, mean load and energy absorption of hybrid tube are getting higher as number of fiber layer is increasing.

5.1.6 Fiber angle of 45 degree does not provide much effect on the crashworthiness capacity of hybrid tube, while the 0 and 90 degree do influence on the capacity significantly.

5.1.7 Hybrid tubes with single fiber angle such as [0/0], [0/0/0], [0/0/0/0], [90/90], [90/90/90] and [90/90/90/90] provide certain improvement on the crashworthy of tubes but less than that of tube with a combination of fiber angle.

5.1.8 By putting 0-degree fiber for inner layers together with putting 90-degree fiber for outer layers of hybrid tubes i.e. [0/0/90], [0/90/90] and [0/0/90/90], can enhance the crashworthiness capacity of structure most. The maximum load, mean load as well as the energy absorption of those hybrid tubes are increased most. This is explained by the collapse mechanism of the 0-degree fiber which is failed in Local bucking, while the 90-degree fiber which is in the outer layer helps support and bundle the 0-degree layer to stick with AL tube. This mechanism keeps the whole structure together before total collapse as well as help pushing the broken pieces of fiber in between AL folds.

5.2 Recommendations

5.2.1 Other fiber angles may be further investigated such as 15, 30, 60 and 75 degree as well as the stacking sequence of those.

5.2.2 The study on other kinds of fiber and resin may be carried out such as carbon fiber as example.

5.2.3 It would be great if the velocity and displacement of dropped hammer can be measured because the exact value of stroke as well as the energy absorption of specimens will be obtained.

5.2.4 The FEA modeled may be improved by focusing on Cohesive behavior such as Traction separation Mode I, Mode II and Mode III for example.

REFERENCES

REFERENCES

[1] Kil-Sung. Lee and et al. “Crushing behavior of light mass structural member”, **Transactions of nonferrous metals society of china.** 19: 276-279; September, 2009.

[2] Kil-Sung. Lee and et al. “Collapse behavior evaluation of hybrid thin-walled member by stacking condition”, **Transactions of nonferrous metals society of china.** 21: 135-140; March, 2011.

[3] M. Costas, J. Diaz and et al. “Static and dynamic axial crushing analysis of car frontal impact hybrid absorbers”, **International journal of impact engineering.** 62: 166-181; December, 2013.

[4] M. Kathiresan and K. Manisekar. “Axial crush behaviors and energy absorption characteristics of aluminum and E-glass/epoxy over-wrapped aluminum conical frusta under low velocity impact loading”, **Composite structures.** 136: 86-100; February, 2016.

[5] Hongyong Jiang and et al. “Numerical investigation on links between the stacking sequence and energy absorption characteristics of fabric and unidirectional composite sinusoidal plate”, **Composite structures.** 171: 382-402; July, 2017.

[6] M. Y. Huang, Yuh- Shiou Tai and H. T. Hu. “Numerical study on hybrid tubes subjected to static and dynamic loading”, **Applied composite materials.** 19: 1-19; February, 2012.

[7] Hee Chul Kim, Dong Kil Shin and Jung Ju Lee. “Characteristics of aluminum/CFRP short square hollow section beam under transverse quasi-static loading”, **Composites part B.** 51: 345-358; August, 2013.

[8] D.K. Shin, H.C. Kim and J.J. Lee. “Numerical analysis of the damage behavior of an aluminum/CFRP hybrid beam under three-point bending”, **Composites Part B**. 56: 397-407; January, 2014.

[9] Qiang Liu and et al. “Lateral crushing and bending responses of CFRP square tube filled with aluminum honeycomb”, **Composites part B.** 118: 104-115; June, 2017.

REFERENCES (CONTINUED)

[10] S. Solaimurugan and R. Velmurugan. "Influence of fiber orientation and stacking sequence on petalling of glass/polyester composite cylindrical shells under axial compression", **International journal of solids and structures.** 44 No. 21: 6999-7020; October, 2007.

[11] M. M. Shokrieh, H. Tozandehjani and M. J. Omidi. "Effect of fiber orientation and cross section of composite tubes on their energy absorption ability axial dynamic loading", **Mechanics of composite materials.** 45 No. 6: 567-576; November, 2009.

[12] Dayong Hu and et al. "Effect of fiber orientation on energy absorption characteristics of glass cloth/epoxy composite tubes under axial quasi-static and impact crushing condition", **Composite part A.** 90: 489-501; November, 2016.

[13] M. Mirzaei and et al. "Experimental and analytical assessment of axial crushing of circular hybrid tubes under quasi-static load", **Composite structures.** 94: 1959-1966; May, 2012.

[14] วิริยะ ทองเรือง. **วิศวกรรมพอลิเมอร์.** สงขลา: หน่วยเทคโนโลยีการศึกษา คณะวิศวกรรมศาสตร์ มหาวิทยาลัยสงขลานครินทร์, 2554.

[15] Thinvongpituk, C. **The behavior of non-constant thickness conical shells under axial loading.** Doctor's Thesis: University of Manchester Institute of Science and Technology (UMIST), 2002.

[16] Onsalung, N. **The study on energy absorption of foam – filled tube subjected to impact.** Doctor's Thesis: Ubon ratchathani University, 2013.

[17] Vladimir S. Sokolinsky, Kyle C. Indermuehle and Juan A. Hurtado. "Numerical simulation of the crushing process of a corrugated composite plate'', **Composites: Part A.** 42: 1119–1126; September, 2011.

[18] F. Aymerich, F. Dore and P. Priolo. "Simulation of multiple delaminations in impacted cross-ply laminates using a finite element model based on cohesive interface elements", **Composites Science and Technology.** 69: 1699-1709; September, 2009.

REFERENCES (CONTINUED)

[19] Jikui Zhang and Xiang Zhang. "Simulating low-velocity impact induced delamination in composites by a quasi-static load model with surface-based cohesive contact", **Composite Structures.** 125: 51-57; July, 2015.

[20] Shengqing Zhu and Gin Boay Chai. "Low-velocity impact response of fibre-metal laminates-Experimental and finite element analysis", **Composites Science and Technology**. 72: 1793-1802; October, 2012.

[21] Jaehong Lee and et al. "Experimental characterization of pultruded GFRP bridge deck for light-weight vehicles", **Composite Structures.** 80 Issue 1: 141-151; September, 2007.

[22] M.Golzar and M.Poorzeinolabedin. "Prototype fabrication of a composite automobile body based on integrated structure", **International Journal Manufacturing Technology.** 49 Issue 9-12: 1037-1045; August, 2010.

[23] S.M.R. Khalili, M. Soroush A. Davar and O. Rahmani. "Finite element modeling of low-velocity impact on laminated composite platesand cylindrical shells", **Composite Structures.** 93 No. 5: 1363-1375; April, 2011.

[24] Chien-Hua Huang and Ya-Jung Lee. "Experiments and simulation of the static contact crush of composite laminated plates", **Composite Structures.** 61 Issue 3: 265-270; August, 2003.

[25] Giovanni Belingardi, Alem Tekalign Beyene and Ermias Gebrekidan Koricho. "Geometrical optimization of bumper beam profile made of pultruded composite by numerical simulation'', **Composite Structures**. 102: 217-225; August, 2013.

[26] Carla J. McGregor, Reza Vaziri, Anoush Poursartip and Xinran Xiao. "Simulation of progressive damage development in braided composite tubes under axial compression", **Composites: Part A.** 38: 2247-2259; November, 2007.

[27] Deepak Siromani, Jonathan Awerbuch and Tein-Min Tan. "Finite element modeling of the crushing behavior of thin-walled CFRP tubes under axial compression", **Composites: Part B.** 64: 50-58; August, 2014.

REFERENCES (CONTINUED)

[28] Jovan Obradovic , Simonetta Boria and Giovanni Belingardi. “Lightweight design and crash analysis of composite frontal impact energy absorbing structures”, **Composite Structures.** 94: 423-430, January, 2012.

[29] Carla McGregor , Reza Vaziri and Xinran Xiao. “Finite element modelling of the progressive crushing of braided composite tubes under axial impact”, **International Journal of Impact Engineering.** 37: 662-672; June, 2010.

[30] Matthew David and Alastair F. Johnson. “Effect of strain rate on the failure mechanisms and energy absorption in polymer composite elements under axial loading”, **Composite Structures**. 122: 430-439; April, 2015.

[31] M.W. Joosten, S. Dutton, D. Kelly and R. Thomson. “Experimental and numerical investigation of the crushing response of an open section composite energy absorbing element”, **Composite Structures.** 93: 682-689; January, 2011.

[32] Paolo Feraboli and et al. “Crush energy absorption of composite channel section specimens”, **Composites: Part A.** 40 Issue 8: 1248-1256; August, 2009.

[33] Louis N.S. Chiu et al. “Finite element modelling of composite structures under crushing load”, **Composite Structures.** 131: 215-228; 2015.

[34] Haili Zhou and et al. “Finite element analyses on transvers impact behaviors of 3-D circular braided composite tube with different braiding angles”, **Composite Part A.** 79: 52-62; December, 2015.

[35] B.P. Bussadori, K. Schuffenhauer and A. Scattina. “Modelling of CFRP crushing structures in explicit crash analysis”, **Composites Part B.** 60: 725-735; April, 2014.

[36] D. Kakogiannis and et al. “Response of pultruded composite tubes subjected to dynamic and impulsive axial loading”, **Composites Part B.** 55: 537-547; December, 2013.

[37] S. Boria, J. Obradovic and G. Belingardi. “Experimental and numerical investigations of the impact behavior of composite frontal crash structures”, **Composites Part B.** 79: 20-27; September, 2015.

REFERENCES (CONTINUED)

[38] A. Esnaola and et al. "Effect of fiber volume fraction on energy absorption capabilities of E-glass/polyester automotive crash structures", **Composites Part B.** 85: 1-7; February, 2016.

APPENDIX

LIST OF PUBLICATIONS

The publications are submitted for the degree of Doctor of Philosophy in Mechanical Engineering. The following articles on the work presented in the thesis have been published:

International conference

[1] Junchuan, V. and Thinvongpituk, C., "Effect of Fiber Orientation and Stacking Sequence of AL/GFRP Hybrid Tube under Axial Impact", **The World Congress on Engineering 2016**. 1050-1054; June 29 - July 1, 2016, London, U.K.

International conference

Proceedings of the World Congress on Engineering 2016 Vol II
WCE 2016, June 29 - July 1, 2016, London, U.K.

Effect of Fiber Orientation and Stacking Sequence of AL/GFRP Hybrid Tube under Axial Impact

Junchuan, V. and Thinvongpituk, C.

***Abstract*—This research was aimed to study the effect fiber orientation and stacking sequence on the energy absorption capacity of hybrid tube subjected to axial impact. The specimens were composite cylindrical AL/GFRP tubes. They were manufactured using circular aluminum tubes and wrapped with 2 and 4 layers of E-glass/polyester. The orientations of E-glass/polyester layers were $[0_2]$, $[90_2]$ and [0/90], [90/0] for 2 layers and $[0_4]$, $[90_4]$, $[0_2/90_2]$, $[90_2/0_2]$ for 4 layers. They were tested under free fall impact using Vertical Impact Testing Machine with a speed of 6.67 m/s. The results implied that hybrid tube with $[0_2/90_2]$ of GFRP can resist highest impact load while the $[0_4]$ tube absorbed highest impact energy. The mode of collapse of each tube was also discussed in this paper.**

***Index Terms*— energy absorption, hybrid tube, axial impact, composite tube.**

I. Introduction

Composite material is a high potential alternative materials. It is widely used in many industries such as spacecraft and automobile. This is because the strength per weight of composite material is high which is very useful for transportation. In addition, the property of composite material can be improved corresponding to direction of load. Therefore, composite material is selectively used in frontal section of automobile.

The automobile cockpit is generally made of metal, because metal is prominent in absorbing impact. However, metal is low strength per weight, fatigue and corrosive. Therefore, composite can be alternative for metals and attack intentions of researchers.

S. Solaimurugan et al. [1] studied the energy absorption of cylindrical composite tube subjected to impact. The specimens were composed of 4 and 6 layers of fiber glass. The fiber glass is woven roving (WRM) with 610 g/m^2 density and unidirection (UD) with density of 750 g/m^2. Isophthalic resin is used as binder. The specimens were manufactured by hand layup technique in a sequence of [WRM/(UD)$_m$/WRM] for 4 and 6 layers. The D/t ratio of specimens are 15 and 25. The end angle of each was cut to be 30 degree. The specimens were tested with a speed of 2 mm/min. The results revealed that the energy absorption capacity of tube is increasing as the number of layer increased. P. Feraboli et al. [2] studied on the crashworthiness of rectangular composite tubes subjected to impact. The specimens were 5 different sections but thickness, composition, manufacturing process and testing method were similar. The material used for making specimens were T700 / 2510 carbon fiber/epoxy prepreg, fabricated in $[0/90]_{4s}$ by vacuum technique. They were tested with a speed of 50.8 mm/min. The results revealed that tubes with higher number of angle offer higher energy absorption capacity. M. M. Shokrieh et al. [3] investigated the effect of manufacturing process of glass/polyester tubes focusing on vacuum and non-vacuum process. The result suggested that the vacuum process provides tube with twice in energy absorption compare to the non-vacuum process. In addition, the circular tube can absorption higher energy than square tube. H. C. Kim et al. [4] investigated the characteristics of hybrid aluminum tube subjected to quasi-static load. The specimens were Al 6063-T5 wrapped with CFRP. Three patterns of fiber orientation were $[0]_4$, $[90]_4$, $[0/90]_2$, $[45/\text{-}45]_2$, [0/45/90/-45] / $[0]_8$, $[90]_8$, $[0/90]_4$, $[45/\text{-}45]_4$, $[0/45/90/\text{-}45]_2$ and $[0]_{12}$, $[90]_{12}$, $[0/90]_6$, $[45/\text{-}45]_6$, $[0/45/90/\text{-}45]_3$. It found that the tube with $[0/45/90/\text{-}45]_3$ is the most efficient in term of energy absorption. M. Costas et al. [5] conducted a study on crashworthiness parameters of hybrid tubes under impact and quasi-static load. Five different types of specimens were used i.e. empty tube, hybrid tube with fiber glass, hybrid tube with CFRP, tube filled with polyethylene foam, tube filled with cork. The quasi-static experiment was carried out with speed of 1 mm/s while the impact was conducted by free falling of 350 kg weight from 2.5 m tower. The result suggested that hybrid tube with fiber glass absorbed higher energy than others. M. Y. Huang et al. [6] conducted a numerical study on energy absorption capacity of hybrid tube under quasi-static and impact test. The specimens were steel tubes wrapped with carbon fiber and focused parameters are thickness, type of load and ply angle. Those ply angles were $[+0/\text{-}0]_3$, $[+15/\text{-}15]_3$, $[+30/\text{-}30]_3$, $[+45/\text{-}45]_3$, $[+60/\text{-}60]_3$, $[+75/\text{-}75]_3$ and $[+90/\text{-}90]_3$. It was found that the energy absorption of hybrid tube is improved compared to empty one. M. Mizaei et al. [7] also studied on aluminum tube hybrid with GFRP under quasi-static axial load. The thickness and sequence of ply angle were investigated. Diamond mode of collapse was normally found and specimens of [60/-45/0/90] was excellent in energy absorption. M. Kathiresan et al. [8] investigated the behavior of aluminum cone wrapped with fiber glass under impact using FEA. The study suggested that cones with low angle offer higher energy absorption. In addition, the cones with

Junchuan, V. is with *Department of Mechanical Engineering, Faculty of Engineering, Ubon Ratchathani University* (corresponding author to provide phone: +6645-353309; fax: +6645-353308; e-mail: unicorn_ton@hotmail.com).

Thinvongpituk, C. is with *Department of Mechanical Engineering, Faculty of Engineering, Ubon Ratchathani University* (corresponding author to provide phone: +6645-353309; fax: +6645-353308; e-mail: chawalit@rocketmail.com).

fiber glass were higher in energy absorption by about 15% compared to empty cone. Effect of apex angle and impact velocity were also discussed. R. Kalhor et al. [9] investigated square 304 stainless tube wrapped with S glass / Heuply Prepreg steels. The effect of ply angle and thickness were studied. The specimen was tested at a speed of 6 mm/min using MTS 810 testing machine. The result showed that hybrid tube can change collapse mode from split mode to be axisymmetric mode or mix mode and absorb higher energy. In addition, the fluctuation of load was also reduced throughout the collapse process.

This study is aimed to investigate the crush characteristic of AL/GFRP hybrid tube under axial impact. The study is focused on the effect of ply angle and stacking sequence of GFRP layers on crashworthiness of tube. Modes of collapse and energy absorption are discussed.

II. EXPERIMENT

A. Specimen

The specimens were made from aluminum tube wrapped with E glass unidirectional mat and Isophthalic polyester resin. Orientation angle and number of layers were $[0]_2$, $[90]_2$, $[0/90]$, $[90/0]$, $[0]_4$, $[90]_4$, $[0_2/90_2]$ และ $[90_2/0_2]$. The specimens were manufactured using vacuum process in order to reduce to effect of bubble. The specimens were 44.4 mm diameter, 1.2 mm thickness and 100 mm long. Figure 1 (a) illustrates the stacking sequence of aluminum tube and AL/GFRP. Figure 1 (b) shows direction of ply angle, 0 degree is measured along tube axial while 90 degree is tangent to the tube surface.

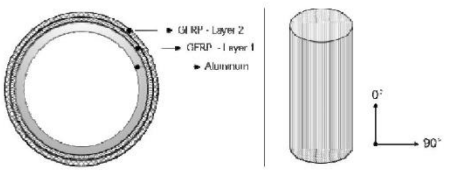

(a) (b)
Fig. 1. (a) Stacking sequence AL/GFRP (b) direction of GFRP

B. Specimens fabrication

Aluminum tube of 44.4 mm diameter and 500 mm long was prepared. The E glass unidirectional mat was cut in an assigned angle to have 450 mm width and 500 mm long. The aluminum tube was cleaned with acetone solution and wrapped with E glass mats to have designed orientations and layers. The specimen was contained in a sealed vacuum bag. The vacuum pump was used to evacuate air from bag. Polyester resin was mixed with hardener, put in the container and let it flow all over the specimens. The specimen was left for 24 hours, took the mold off and cut in a desired size. Figure 2 shows equipments and setting up in the specimen manufacturing process.

Fig. 2. Vacuum process setting up

III. IMPACT TEST

The impact testing was carried out using Vertical Impact Testing Machine, as showed in Figure 3. The machine is a 3 m height tower and consists of a 20-60 kg hammer which can be free fallen to impact to target specimen. The bottom of machine is an anvil with load cell embedded. The load cell is connected to data logger to record reaction force. The load and time of impact were then process for analysis. In this study, 45 kg hammer was dropped from 2.33 m and impact speed was 6.67 m/s. High speed camera was also used to record the collapse development throughout the process.

Fig. 3. Vertical impact testing machine

Proceedings of the World Congress on Engineering 2016 Vol II
WCE 2016, June 29 - July 1, 2016, London, U.K.

IV. COLLAPSE BEHAVIOR OF SPECIMENS

A. Characteristic of load displacement curve

As the specimen was impacted, it failed in a certain form of collapse modes. In the collapse process, the reaction force and displacement of structure were formed corresponding to the collapse mode. Therefore, the collapse mode and load-displacement curve are worth to be investigated. Figure 4-6 show some examples of failure history of specimens. Figures 7 and 8 illustrate load history curves, which total displacement and duration of impact can be observed.

The collapse process of aluminum tube is showed in Figure 4. It is observed that the specimen is failed from the top end and progressed to the bottom in a series of lobes. The total displacement is 61 mm and impact time was 0.024 sec.

Figure 5 shows the collapse process of AL/GFRP-[0_2] tube, which is collapsed for 69 mm within 0.025 sec. The collapse process of AL/GFRP-[0_4] tube is showed in Figure 6, the total displacement is 76 mm and impact time is 0.026 sec.

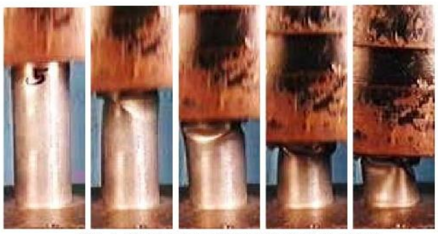

Fig. 4. Progressive collapse of naked aluminum

Fig. 5. Progressive collapse of AL/GFRP - 2 Layers and [0_2]

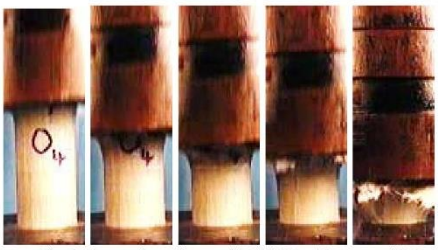

Fig. 6. Progressive collapse of AL/GFRP - 4 Layers and [0_4]

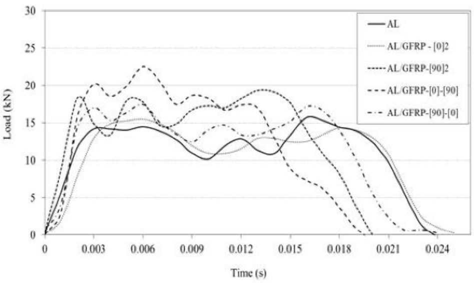

Fig. 7. Load-time curve of AL and AL/GFRP-2 layer tubes

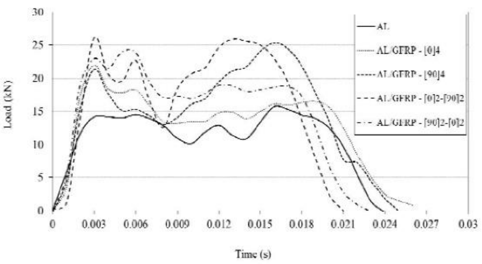

Fig. 8. Load-time curve of AL and AL/GFRP-4 layer tube

B. Mode of collapse

This study found that AL and AL/GFRP tubes fail in 5 modes, which are Diamond mode, Lamina bucking, Fiber breaking, Local bucking and Laminar bending. The details of these modes are discussed as followed.

Figure 9 is the collapse mode of AL tube which is called diamond mode. This mode consists of a number of lobes stacking on each other.

Figure 10 (a) shows the collapse mode of AL/GFRP- [0_2] tube. It is observed that the AL tube is failed in diamond mode while the GFRP which is oriented in 0 degree for 2 layers, is failed by bending in horizontal direction. This is called Lamina bucking mode. In this mode, the GFRP sheet is buckling and spring out of the AL tube. The final mode is showed in Figure 12 (a).

The final collapse of AL/GFRP- [90_2] is showed in Figure 10 (b). The aluminum tube is also failed in diamond mode while the GFRP is failed in Fiber breaking. This mode, the fiber is broken and inserted in between two adjacent lobes of aluminum wall.

Figure 10 (c) is the collapse mode of AL/GFRP- [0/90] tube, the AL tube is also failed in diamond mode, while the 1^{st} layer of fiber, lied in 0 degree, is failed in Local bucking. The 2^{nd} layer, lied in 90 degree, is failed in Fiber breaking and helps maintaining the 1^{st} layer in position, as showed in Figure 12 (c).

Figure 10 (d) is the final mode of AL/GFRP- [90/0] tube. Again, the aluminum tube is failed in diamond mode while the 1^{st} layer of fiber, 90 degree orientation, is failed in Fiber breaking. The 2^{nd} layers of fiber, 0 degree orientation, is failed in Laminar bending as showed in Figure 12 (d).

Figure 11 (a) shows final collapse of AL/GFRP- [0_4]. The aluminum tube is failed in diamond mode. The fiber, 0 degree orientation for 4 layers, is failed in Lamina bucking mode as showed in Figure 13 (a).

ISBN: 978-988-14048-0-0
ISSN: 2078-0958 (Print); ISSN: 2078-0966 (Online)

Figure 11 (b) is the collapse mode of AL/GFRP- $[90_4]$ tube. Aluminum tube is also failed in diamond mode while the fiber layers are failed in Fiber breaking and inserted between two lobes as showed in Figure 13 (b).

Figure 11 (c) shows the failure mode of AL/GFRP- $[0_2/90_2]$ tube. It is found that the AL tube is failed in diamond mode. The first two layers of fiber, 0 degree orientation, are buckling in Local bucking mode and inserted into lobes of aluminum tube. The 3rd and 4th layers of fiber which are 90 degree orientation, failed in Fiber breaking. The fibers are broken, some are inserted between lobes while some are spring out off aluminum tube, as showed in Figure 13 (c).

The collapse mode of AL/GFRP- $[90_2/0_2]$ is showed in Figure 11 (c). Aluminum tube is failed in diamond mode, while the 1st and 2nd layers of fiber, lied in 90 degree, are failed in Fiber breaking and inserted between the wall of collapse tube. The 3rd and 4th layers of fiber, 0 degree orientation, are failed in Laminar bending and spring out of the aluminum tube. Figure 13 (d) illustrates the failure mode of this case.

Fig. 9. Final mode of AL tube.

(a) (b) (c) (d)
Fig. 10. Mode of collapse of AL/GFRP tubes (a) $[0_2]$, (b) $[90_2]$, (c) [0/90] and (d) [90/0].

(a) (b) (c) (d)
Fig. 11. Mode of collapse of AL/GFRP tubes (a) $[0_4]$, (b) $[90_4]$, (c) $[0_2/90_2]$ and (d) $[90_2/0_2]$.

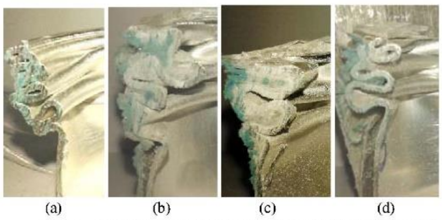

(a) (b) (c) (d)
Fig. 12. Sectioned of collapsed wall of AL/GFRP tubes (a) $[0_2]$, (b) $[90_2]$, (c) [0/90] and (d) [90/0].

TABLE I
ENERGY ABSORPTION OF IMPACT TEST

Specimen	Maximum load (kN)	Average load (kN)	Energy absorption (kN.m)
AL	15.719	10.819	17.991
Al-GFRP 2 PLY			
$[0_2]$	15.470	10.740	14.040
$[90_2]$	19.327	13.493	9.121
[0/90]	22.538	12.643	7.291
[90/0]	17.476	11.162	12.569
Al-GFRP 4 PLY			
$[0_4]$	21.992	12.439	13.258
$[90_4]$	25.286	14.341	12.690
$[0_2/90_2]$	26.060	16.423	9.430
$[90_2/0_2]$	23.895	14.814	11.468

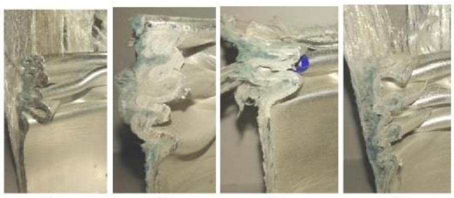

(a) (b) (c) (d)
Fig. 13. Sectioned of collapsed wall of AL/GFRP tubes (a) $[0_4]$, (b) $[90_4]$, (c) $[0_2/90_2]$ and (d) $[90_2/0_2]$

V. ENERGY ABSORPTION BEHAVIOR

A. Maximum and Average Load

The maximum load, average load and energy absorption of specimens under impact are showed in table 1. From table 1, considering on AL tubes with 2 layers GFRP, the maximum loads of [0/90], $[90_2]$, [90/0], AL and $[0_2]$ are 22.53, 19.32, 17.47 15.71 and 15.47 kN respectively. Considering on the average load, it is found that the hybrid tube of AL/GFRP- $[90_2]$ gives 13.49 kN while the hybrid tubes of [0/90], [90/0], AL and $[0_2]$ give 12.64, 11.16, 10.81 and 10.74 kN of average load respectively. The comparison between AL tube and AL/GFRP tubes suggests that the hybrid tube with $[0_2]$, $[90_2]$, [0/90] and [90/0] give different of average load as -0.65, +19.86, +14.47 and +3.13 % respectively.

In case of the AL tube and hybrid AL/GFRP tube of 4 layers, the result revealed that the maximum load of tube with AL/GFRP-$[0_2/90_2]$, $[90_4]$, $[90_2/0_2]$, $[0_4]$ and naked AL are 26.06, 25.28, 23.89, 21.99 and 15.71 kN, respectively. In addition, it is found that the AL/GFRP tube with $[0_2/90_2]$, $[90_2/0_2]$, $[90_4]$, $[0_4]$ and AL tube give the average loads of 16.42, 14.81, 14.34, 12.43 and 10.81 kN, respectively. The comparative result between AL and AL/GFRP tube, it is found that the hybrid tube with $[0_4]$, $[90_4]$, $[0_2/90_2]$ and $[90_2/0_2]$ give higher average value than AL tube by 13.03, 24.61, 34.16 and 27.00 %, respectively. It is obviously seen that hybrid tubes with orientation of [0/90] and $[0_2/90_2]$ give highest value of maximum load. This is because the 0 degree fiber is inserted into the collapsed lobes of aluminum tube and enhances the load resistance capacity of tube.

B. Energy absorption

The energy absorptions of specimens are showed in Table 1. It is found that AL tube absorbs energy of 17.99 kN.m. The hybrid AL/GFRP tube of 2 layers with $[0_2]$ absorbs 14.04 kN.m, while the hybrid tubes of [90/0], $[90_2]$ and [0/90]

ISBN: 978-988-14048-0-0
ISSN: 2078-0958 (Print); ISSN: 2078-0966 (Online)

absorb 12.56, 9.12 and 7.29 kN.m of impact energy, respectively. This is implied that hybrid tubes with $[0_2]$ absorb higher energy than that of [90/0], $[90_2]$ and [0/90] by 11.701, 53.94 and 92.59 % respectively.
Considering hybrid AL/GFRP tube of 4 fiber layers, it reveals that tube with $[0_4]$ absorbs highest impact energy at 13.25 kN.m. This is higher than that of hybrid tube with $[90_4]$, $[90_2/0_2]$ and $[0_2/90_2]$ by 4.41, 16.22 and 40.50 %, respectively. In addition, the hybrid tube with $[0]_4$ absorbs highest energy compared to other orientations.

VI. Conclusion

This study investigates the influence of ply angle and stacking sequence of GFRP wrapped on aluminum tube, focusing on its energy absorption capacity. The crashworthiness and mode of collapse are observed and discussed. It is found that the aluminum tube was normally failed in diamond mode. Considering the fiber layer, in case of $[0_2/90_2]$, the 0 degree orientation fiber is buckled and inserted into the gabs between folds of aluminum tube. In addition, it is also found that the 90 degree orientation fiber ties up the $[0_2]$ in the position.

The mean loads achieved from hybrid AL with 2 GFRP layers compared to naked aluminum tube are -0.65, +19.86, +14.47 and +3.13% for $[0_2]$, $[90_2]$, [0/90] and [90/0], respectively. In case of hybrid AL with 4 GFRP layers, the mean load are increasing by 13.03, 24.61, 34.16, and 27.00% for fiber orientation of $[0_4]$, $[90_4]$, $[0_2/90_2]$ and $[90_2/0_2]$, respectively.

The study also is found that hybrid tubes of 2 layers with $[0_2]$ absorb higher energy than [90/0], $[90_2]$ and [0/90] tube by 11.701, 53.94 and 92.59%. In case of $[0_4]$, it absorbs more energy than $[90_4]$, $[90_2/0_2]$ and $[0_2/90_2]$ hybrid tubes by 4.41, 16.22 and 40.50%, respectively.

Acknowledgment

Authors wish to thank Department of Mechanical Engineering, Faculty of Engineering, Ubon Ratchathani University, for supporting all test rigs.

References

[1] S. Solaimurugan, R. Velmurugan. "Influence of fiber orientation and stacking sequence on petalling of glass/polyester composite cylindrical shells under axial compression", International Journal of Solids and Structures. 44 (21): 6999–7020, 2007.
[2] P. Feraboli, B. Wade, F. Deleo, M. Rassaian "Crush energy absorption of composite channel section specimens", Composites: Part A. 40 (8): 1248–1256, 2009.
[3] M. M. Shokrieh, H. Tozandehjani, M. J. Omidi "Effect of fiber orientation and cross section of composite tubes on their energy absorption ability axial dynamic loading", Mechanics of Composite Materials. 45 (6): 567-576, 2009.
[4] H. C. Kim, D. K. Shin, J. J. Lee "Characteristics of aluminum/CFRP short square hollow section beam under transverse quasi-static loading", Composites: Part B 51: 345–358, 2013.
[5] M. Costas, J. Diaz, L.E. Romera, S. Hernández, A. Tielas "Static and dynamic axial crushing analysis of car frontal impact hybrid absorbers", International Journal of Impact Engineering 62: 166-181, 2013.
[6] M. Y. Huang, Y. S. Tai, H. T. Hu "Numerical Study on Hybrid Tubes Subjected to Static and Dynamic Loading", Appl Compos Mater: 19:1–19, 2012.
[7] M. Mirzaei, M. Shakeri, M. Sadighi, H. Akbarshahi "Experimental and analytical assessment of axial crushing of circular hybrid tubes under quasi-static load", Composite Structures 94: 1959–1966, 2012.
[8] M. Kathiresan, K. Manisekar "Axial crush behaviors and energy absorption characteristics of aluminum and E-glass/epoxy over-wrapped aluminum conical frusta under low velocity impact loading", Composite Structures 136 86–100, 2016.
[9] R. Kalhor, S. W. Case "The effect of FRP thickness on energy absorption of metal-FRP square tubes subjected to axial compressive loading", Composite Structures 130 44–50, 2015.

VITAE

NAME	Visit Junchuan
EDUCATION	2010 - 2013, Master Degree (Mechanical Engineering), Department of Mechanical Engineering, Ubon Ratchathani University (UBU), Thailand.
	2006 - 2010, Bachelor Degree (Mechanical Engineering), Department of Mechanical Engineering, Ubon Ratchathani University (UBU), Thailand.
MAIL ADDRESS	27 Moo 14, Sriboonrung District, Nongbualamphu Province, Thailand, 39180.
	Email: Visit.ju.57@ubu.ac.th